フランコ　ノリ　の

“ノリノリ”

プレゼンテーション

Remember to thank the organizers for their invitation!

(before I forget):

I would like to thank
the organizers for putting
together this great event.

(this “haiku” is not from Basho)

Superconducting Qubits

Franco Nori RIKEN Advanced Science Institute and U. of Michigan

Main collaborators:

Y.-X. Liu, J.Q. You, S. Ashhab, C.P. Sun, K. Maruyama, A. Zagoskin, L.F. Wei, X. Hu, R. Johansson, J.S. Tsai, Y. Pashkin, T. Yamamoto, Y. Nakamura, and many others …..

Goal: Controlling an “artificial atom” in a solid-state device

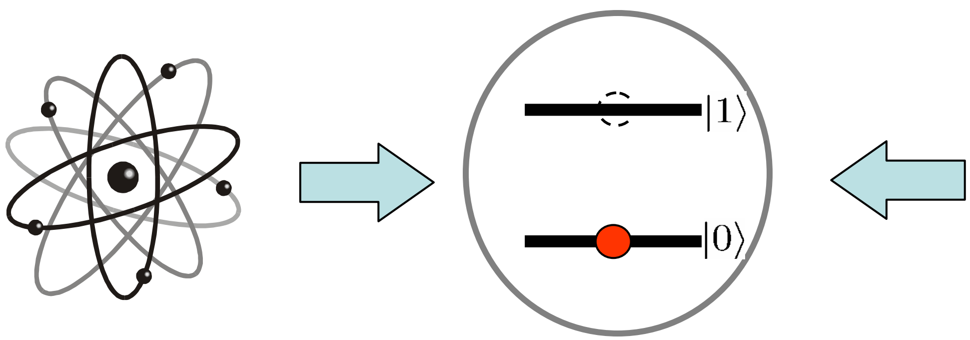

$$\alpha|0\rangle + \beta|1\rangle$$

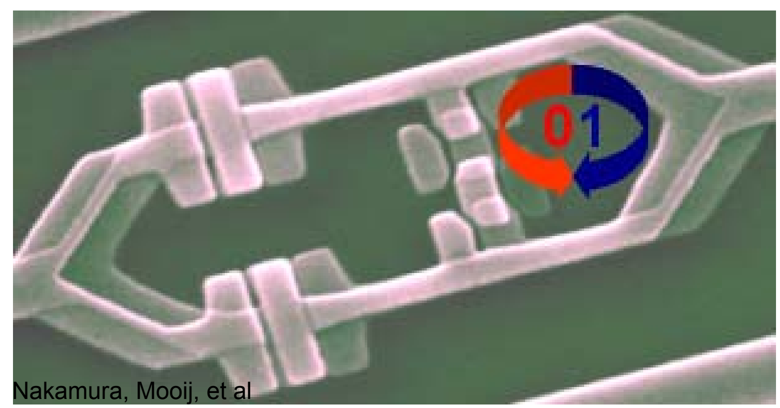

Qubit = Quantum two-level system

This talk:

First an overview of superconducting (SC) qubits

Afterwards, an overview of some (just very few) of the projects we are working on.

If somebody in the audience is interested in a specific topic, I will be glad to expand more on it, after the talk.

PDFs of our papers are available online at our web site.

Today's talk: controlling "artificial atoms" attached to wires.

Let us consider the following problem:

<u>How to attach wires to an atom</u>

Imagine that your sample becomes smaller and smaller ...

Eventually, you are left with an atom.

You still wish to use your voltmeters, current sources, etc.

Atoms are too small. Better to make larger "<u>artificial atoms</u>"!

Better summarize the talk in two sentences, in case some people fall asleep.

You and Nori, *Physics Today*, Nov. 2005

Superconducting Circuits and Quantum Information

Superconducting circuits can behave like atoms making transitions between two levels. Such circuits can test quantum mechanics at macroscopic scales and be used to conduct atomic-physics experiments on a silicon chip.

a PDF file with this pedagogical overview is available online at our web site.

Quantum Simulators

Both digital and analog

Also, Georgescu and Nori, for *Rev. Mod. Phys*.

You and Nori, *Nature*, in press (nine pages long review)

Atomic Physics and Quantum Optics using Superconducting Circuits.

.

REVIEW

doi:10.1038/nature10122

Atomic physics and quantum optics using superconducting circuits

J. Q. You[1,2] & Franco Nori[2,3]

Superconducting circuits based on Josephson junctions exhibit macroscopic quantum coherence and can behave like artificial atoms. Recent technological advances have made it possible to implement atomic-physics and quantum-optics experiments on a chip using these artificial atoms. This Review presents a brief overview of the progress achieved so far in this rapidly advancing field. We not only discuss phenomena analogous to those in atomic physics and quantum optics with natural atoms, but also highlight those not occurring in natural atoms. In addition, we summarize several prospective directions in this emerging interdisciplinary field.

To appear in Nature, June 30 (2011)

Most examples shown in the review are from our RIKEN group

Natural and artificial atoms

(**E** = externally applied electric field)

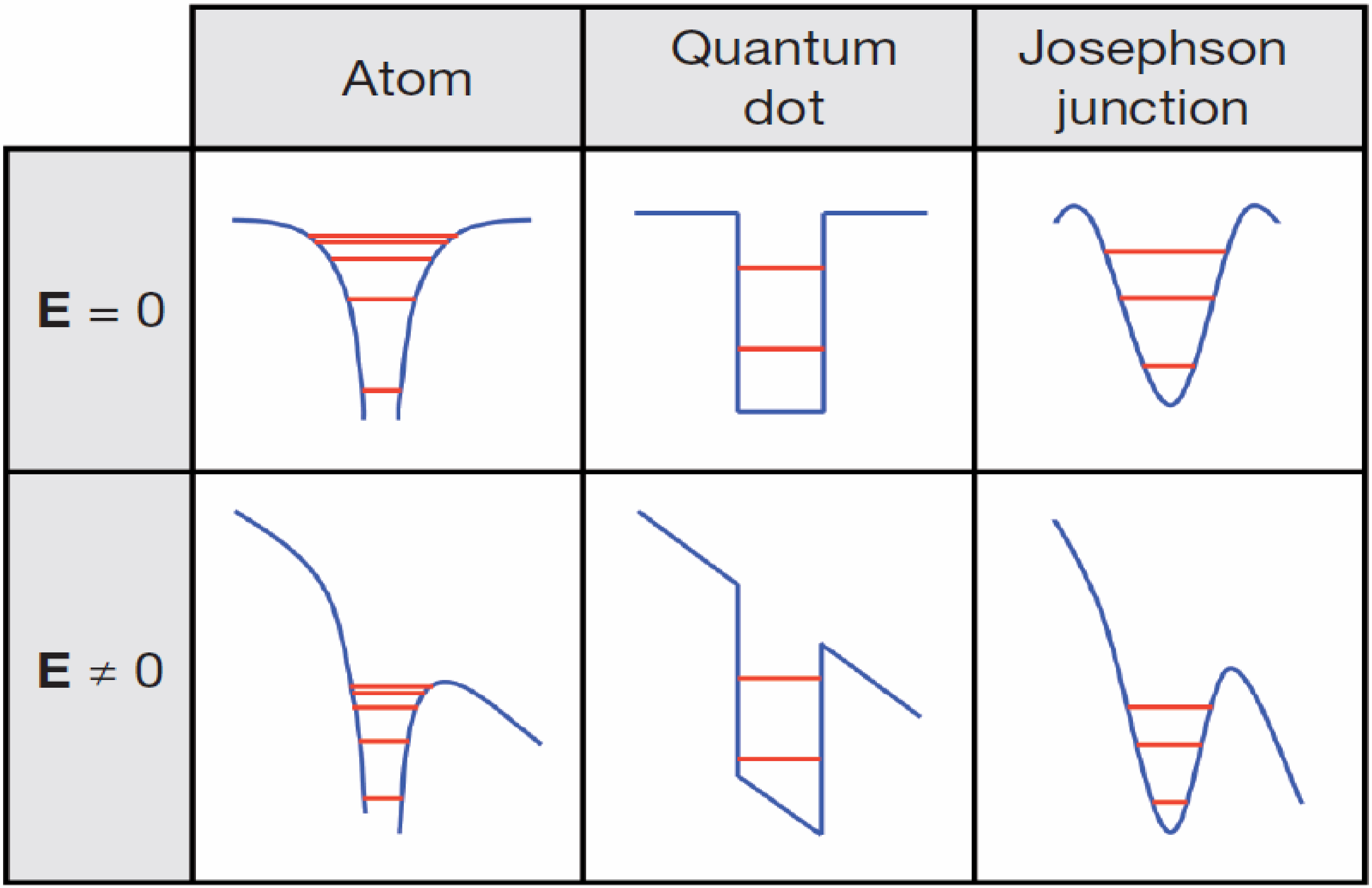

Natural and artificial atoms

	Neutral atoms	Trapped Ions	Supercond. qubit	Spins in semicond.
Energy gap	GHz (hyperfine), hundred THz (optical)	GHz (hyperfine), hundred THz (optical)	10-20 GHz	GHz, 30 THz
Tunable energy gap	no	no	yes	yes
Photon	Optical, MW	Optical, MW	MW	Optical, infrared
Vibrations	yes	yes	no	no
Tunable vibr. freq.	yes	yes	no	no
Dimension	~ 2 Å	~ 2 Å	~ μm	~ nm
Tunable dimension	no	no	yes	yes
Temperature	nK - μK	~ mK	~ mK	mK - K
Qubit interactions	Collisions, exchange	Coulomb	Capacitive, inductive	Coulomb, exchange
Cooling	Doppler, Sisyphus	Doppler, sideband	Sideband, Sisyphus	-
Cavity	Optical, MW	Optical, vib. modes	Transmission line	Optical

Table I. Comparison between natural and artificial atoms. (Buluta, Ashhab, Nori, Reports on Progress in Physics)

Very quick overview

(please fasten you seat belts!)

of several types of

superconducting quantum circuits

Charging energy of a capacitor

$$E_{charging} = Q^2 / (2C)$$

Charge qubit

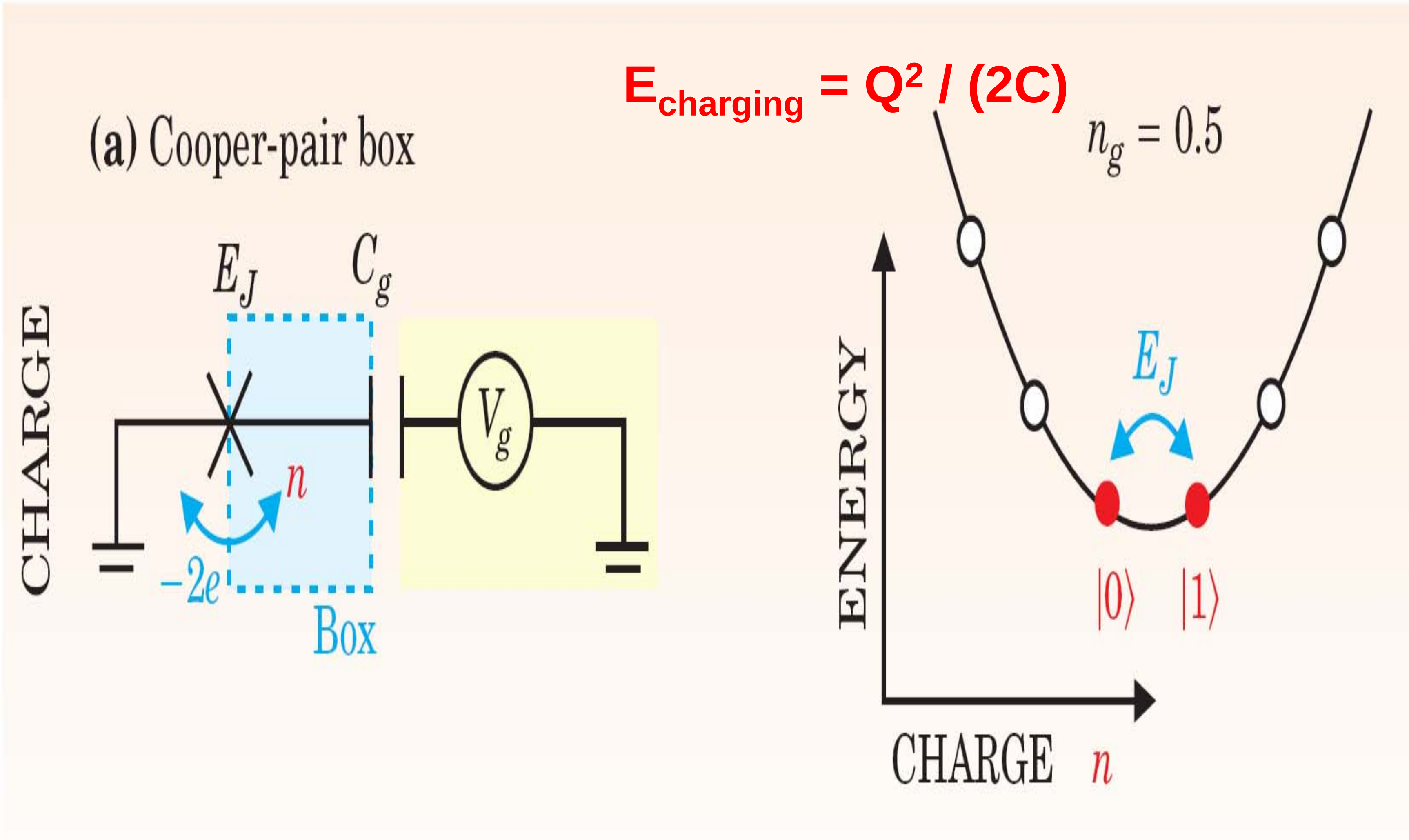

Figures from: You and Nori, *Physics Today* (November 2005)

Hamiltonian

The Cooper pair number *n* is the quantum mechanical conjugate of the phase φ

In the charge (or Cooper-pair-number) basis:

$$\hat{n} = \sum_{n=0} n \left| n \right\rangle \left\langle n \right| \ , \qquad \cos\varphi = \frac{1}{2} \sum \left(\left| n \right\rangle \left\langle n+1 \right| + \left| n+1 \right\rangle \left\langle n \right| \right)$$

In the charge basis, the Hamiltonian

$$H = 4E_c (n - C_g V_g / 2e)^2 - E_J \cos\varphi$$

can be written as

$$H = \sum 4E_c (n - n_g)^2 \left| n \right\rangle \left\langle n \right| - \frac{1}{2} \mathrm{E_J} \sum \left(\left| n+1 \right\rangle \left\langle n \right| + \left| n \right\rangle \left\langle n+1 \right| \right) ,$$

with the gate-induced charge $n_g = C_g V_g / 2e$

Hamiltonian

The Cooper pair number *n* is the quantum mechanical conjugate of the phase φ

In the charge (or Cooper-pair-number) basis:

$$\hat{n} = \sum_{n=0} n \left| n \right\rangle \left\langle n \right| \; , \qquad \cos\varphi = \frac{1}{2} \sum \left(\left| n \right\rangle \left\langle n+1 \right| + \left| n+1 \right\rangle \left\langle n \right| \right)$$

Thus, in the charge basis, the Hamiltonian

$$H = 4\,E_c (n - C_g V_g / 2e)^2 - E_J \cos\varphi$$

is replaced by

$$H = \sum 4 E_c (n - n_g)^2 \left| n \right\rangle \left\langle n \right| - \frac{1}{2} \mathrm{E}_\mathrm{J} \sum \left(\left| n+1 \right\rangle \left\langle n \right| + \left| n \right\rangle \left\langle n+1 \right| \right) ,$$

with the gate-induced charge $\quad n_g = C_g V_g / 2e$

Hamiltonian

The Cooper pair number *n* is the quantum mechanical conjugate of the phase φ

In the charge (or Cooper-pair-number) basis:

$$\hat{n} = \sum_{n=0} n|n\rangle\langle n| \ , \qquad \cos\varphi = \frac{1}{2}\sum\left(|n\rangle\langle n+1| + |n+1\rangle\langle n|\right)$$

Thus, in the charge basis, the Hamiltonian

$$H = 4E_c(n - C_g V_g/2e)^2 - E_J \cos\varphi$$

is replaced by

$$H = \sum 4E_c(n-n_g)^2 |n\rangle\langle n| - \frac{1}{2}\mathrm{E}_\mathrm{J}\sum\left(|n+1\rangle\langle n| + |n\rangle\langle n+1|\right),$$

with the gate-induced charge $n_g = C_g V_g / 2e$

Pauli operators

For two-level quantum systems used for qubits, two levels are denoted by |0> and |1>. In the basis {|0>, |1>}, the Pauli matrices are defined as

$$\mathbb{1} = \begin{pmatrix} 1 & 0 \\ 0 & 1 \end{pmatrix},\ \sigma_x = \begin{pmatrix} 0 & 1 \\ 1 & 0 \end{pmatrix},\ \sigma_y = \begin{pmatrix} 0 & -i \\ i & 0 \end{pmatrix},\ \text{and } \sigma_z = \begin{pmatrix} 1 & 0 \\ 0 & -1 \end{pmatrix}$$

The corresponding density matrix are

$$I = |0\rangle\langle 0| + |1\rangle\langle 1|, \qquad \sigma_x = |0\rangle\langle 1| + |1\rangle\langle 0|,$$
$$\sigma_y = -i|0\rangle\langle 1| + i|1\rangle\langle 0|,\ \sigma_z = |0\rangle\langle 0| - |1\rangle\langle 1|$$

Here, the matrix forms of |0> and |1> are:

$$|0\rangle = \begin{pmatrix} 1 \\ 0 \end{pmatrix}, \quad |1\rangle = \begin{pmatrix} 0 \\ 1 \end{pmatrix}$$

and also $\sigma_z|0> = |0>,\ \sigma_z|1> = -|1>$

a Voltage-driven box (charge qubit)

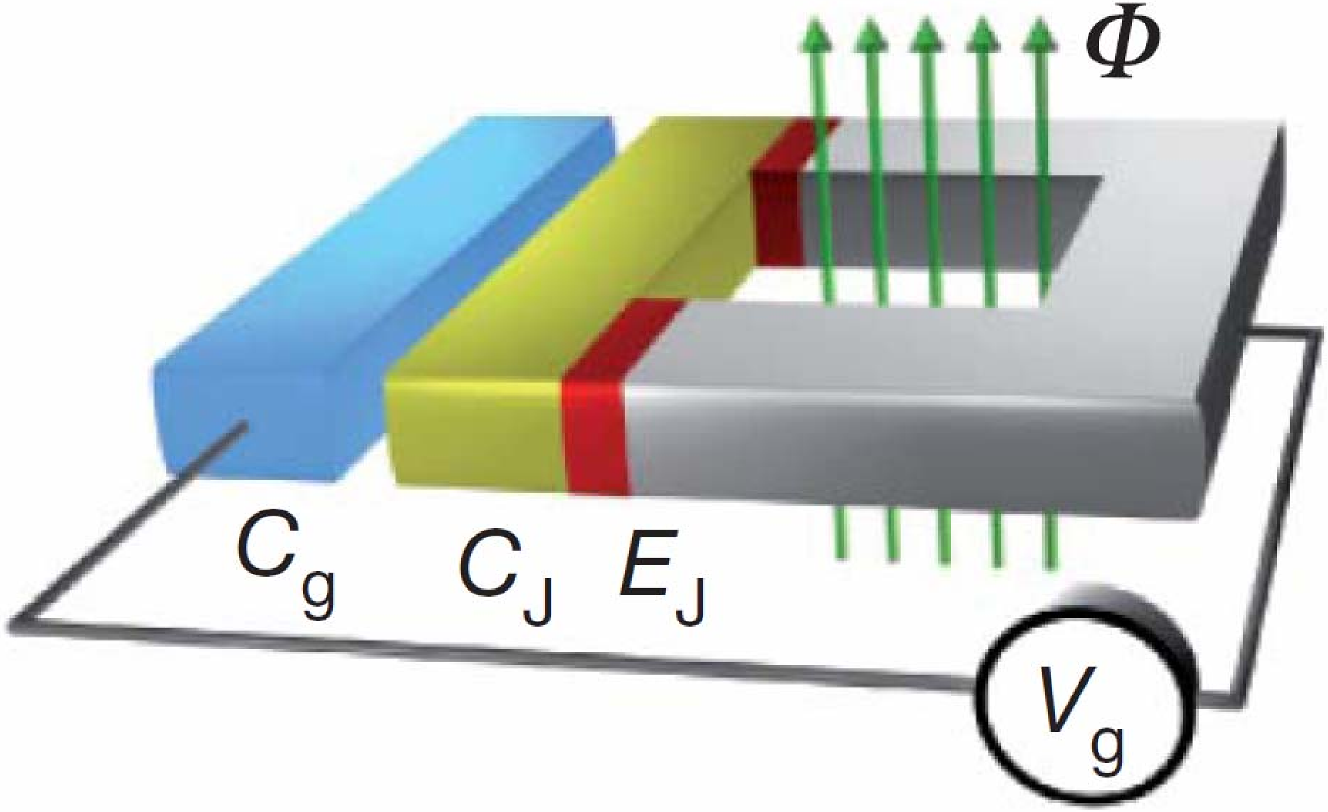

b Flux-driven loop (flux qubit)

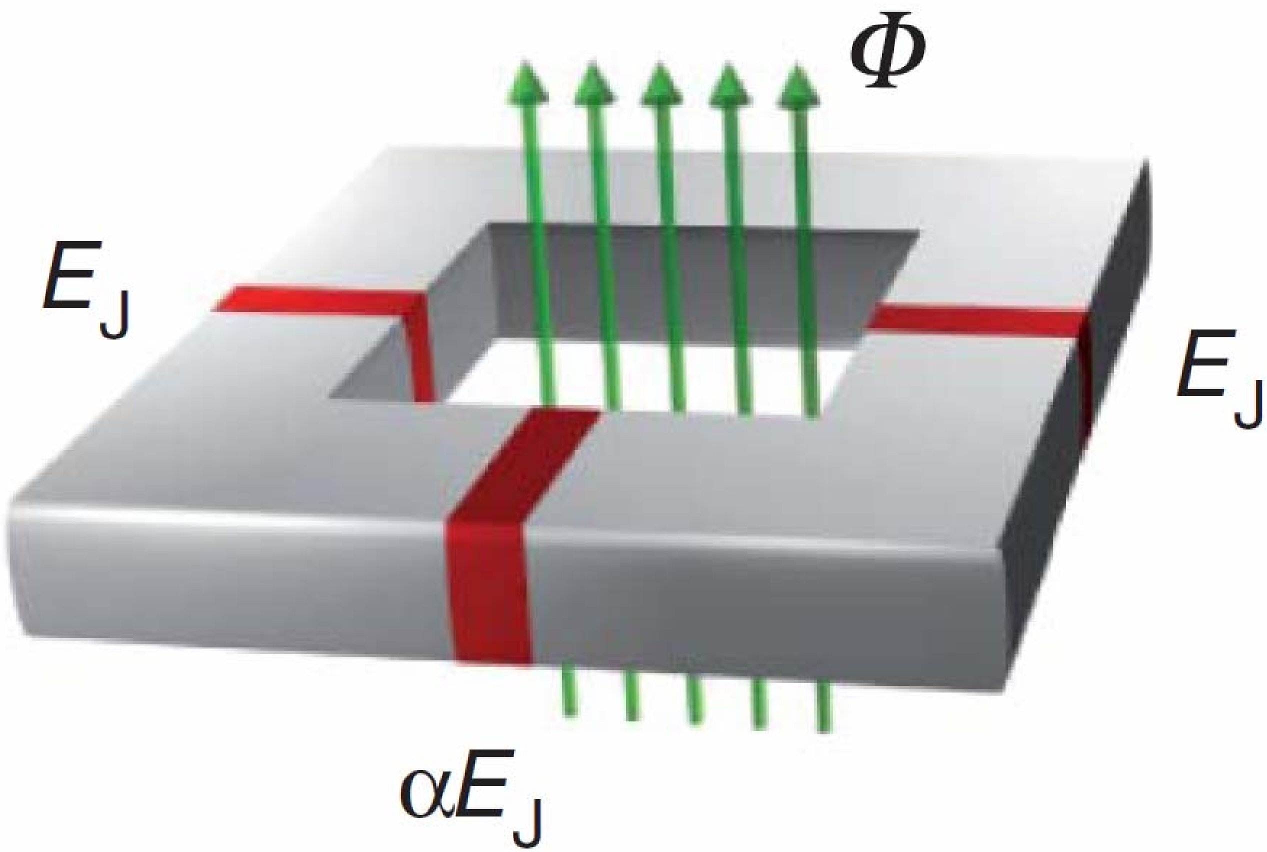

c Current-driven junction (phase qubit)

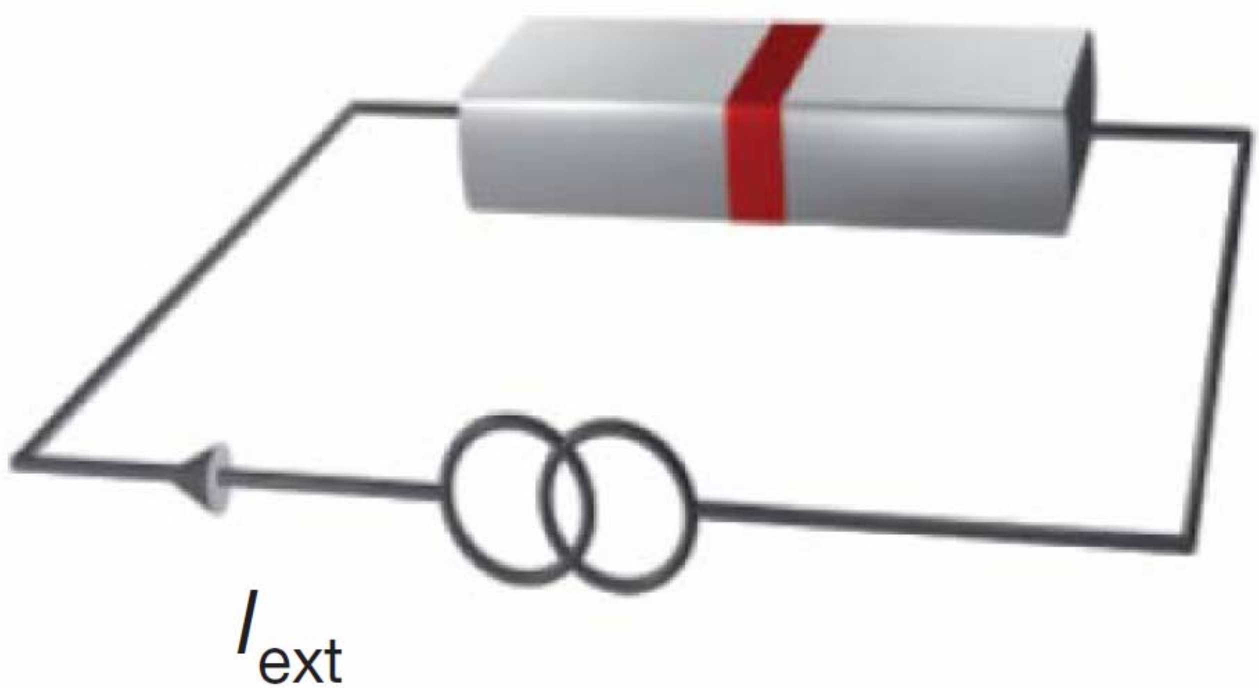

Charge qubit

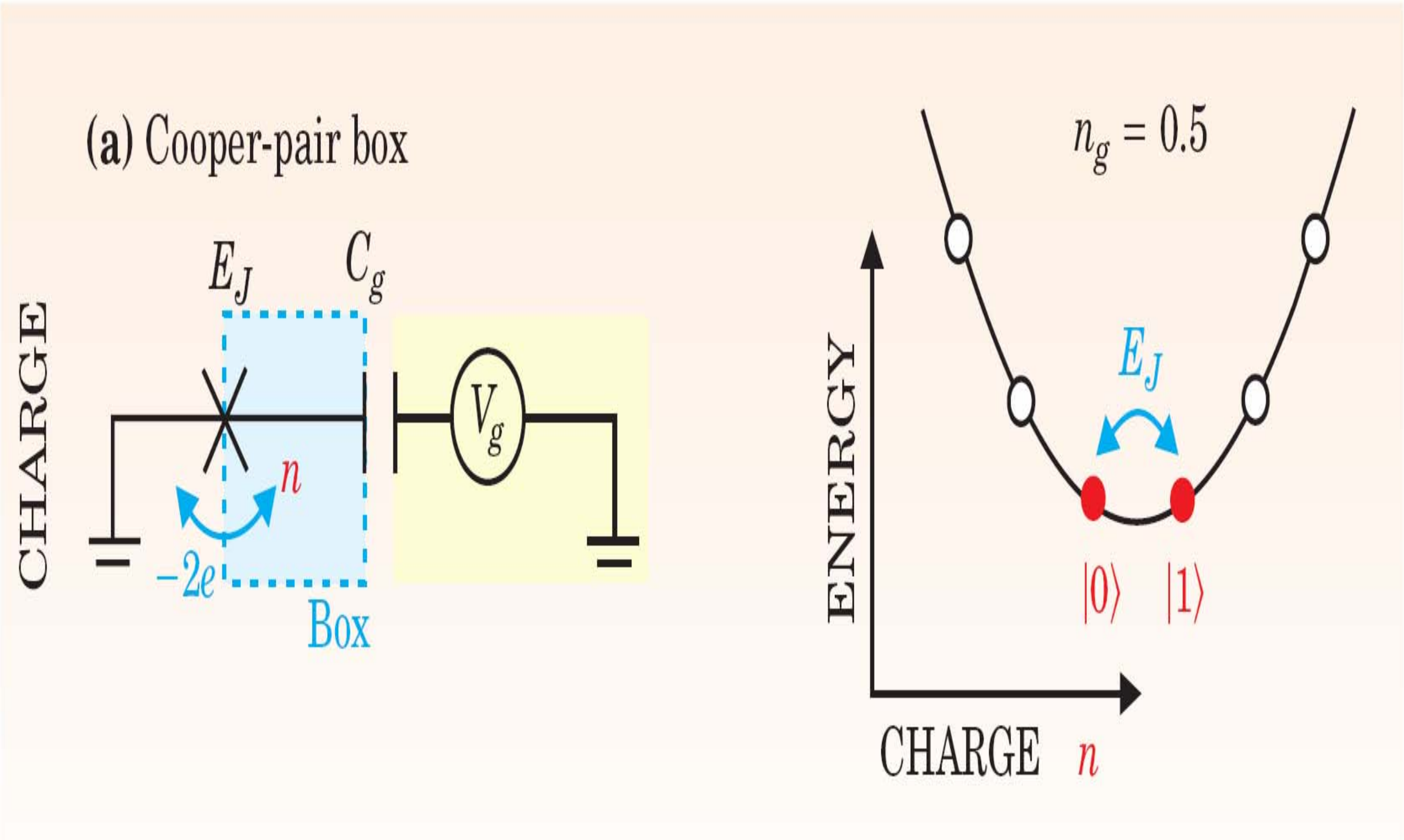

Figures from: You and Nori, *Physics Today* (November 2005)

Charge qubit

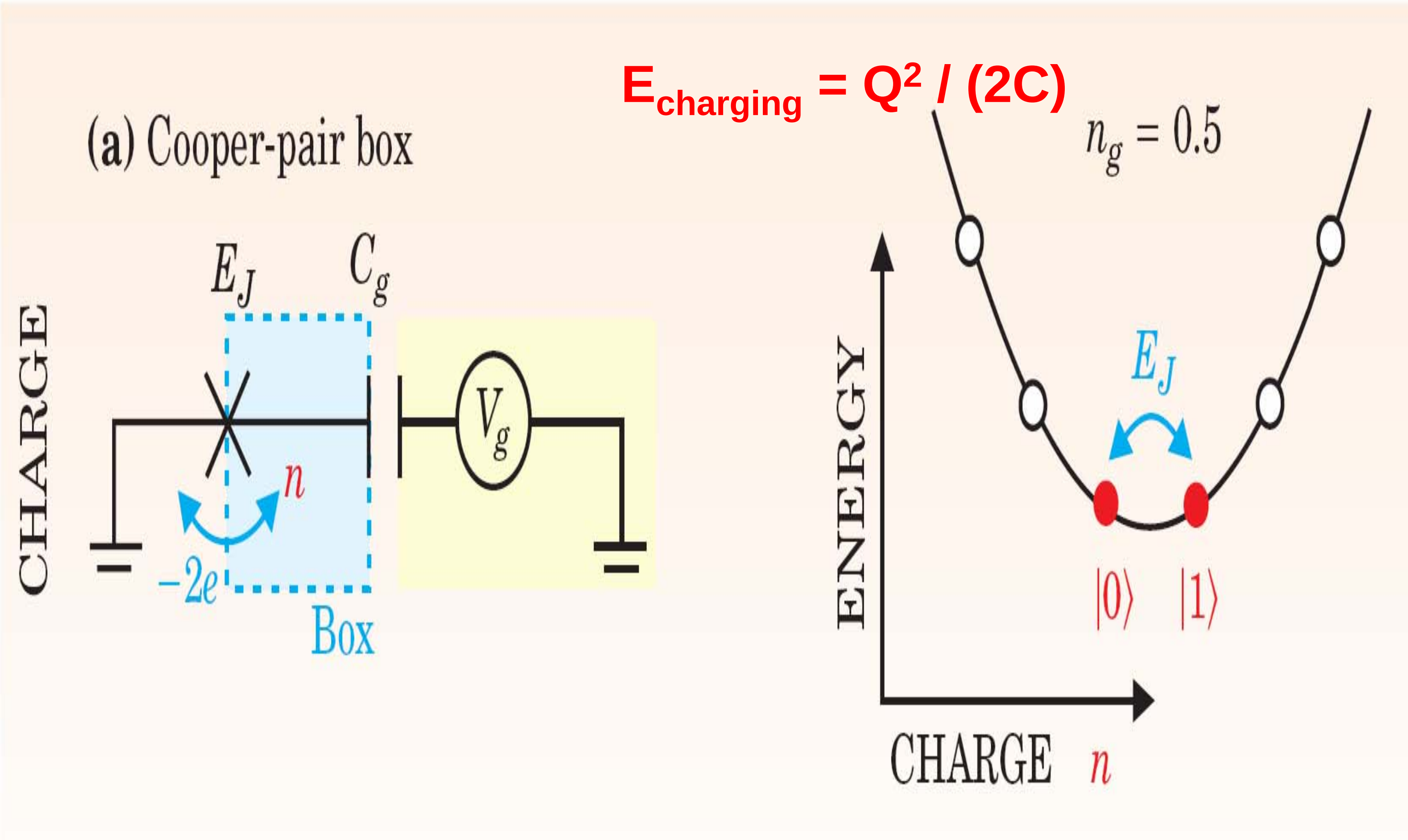

Figures from: You and Nori, *Physics Today* (November 2005)

Charge qubit

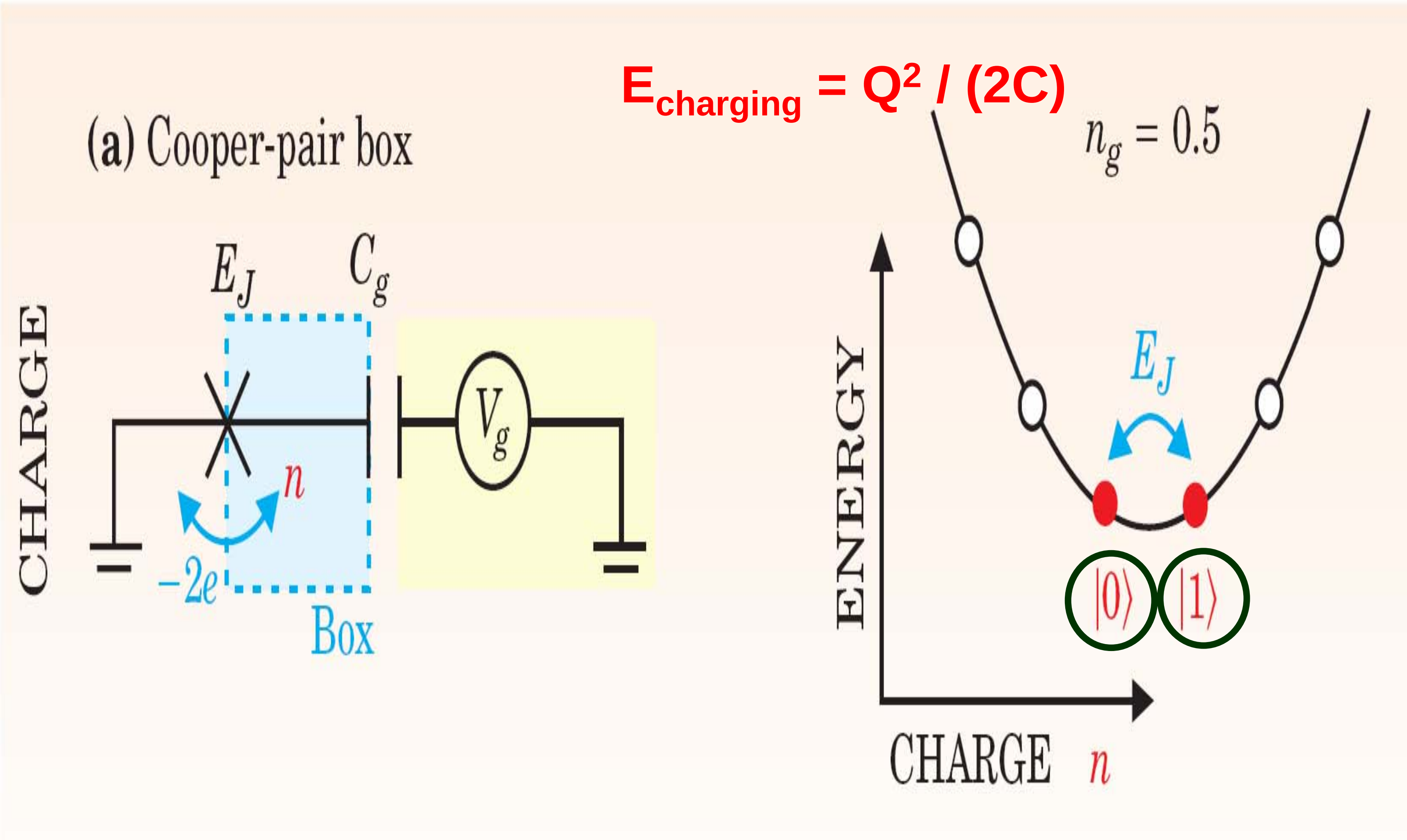

Figures from: You and Nori, *Physics Today* (November 2005)

Different types of superconducting qubits

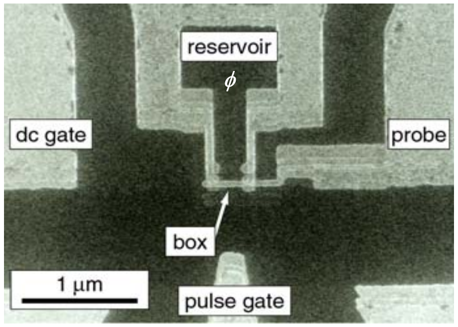

NEC-RIKEN

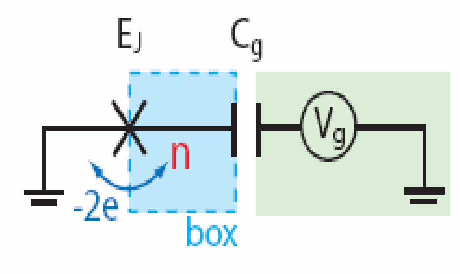

$E_C = 5\text{-}10\ E_J$

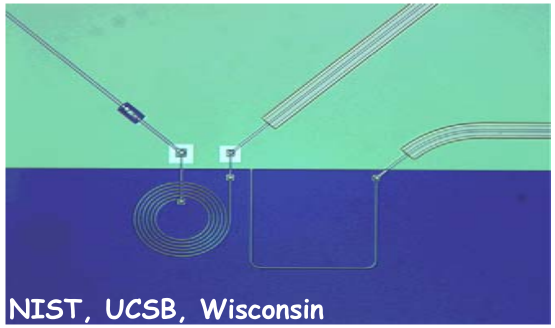

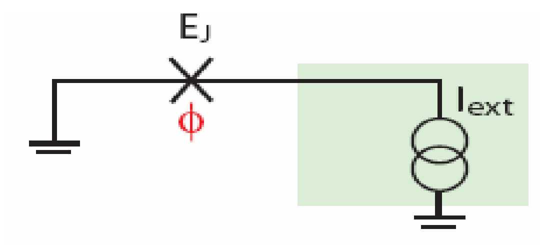

$E_J = 10^6\ E_C$

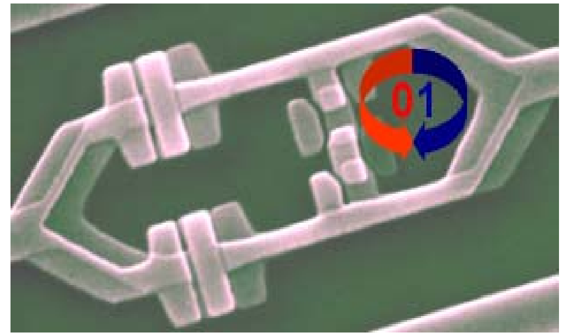

Delft

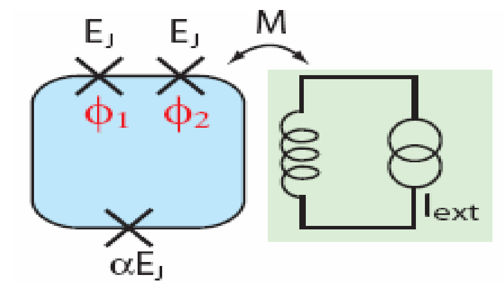

$E_J = 10\ E_C$

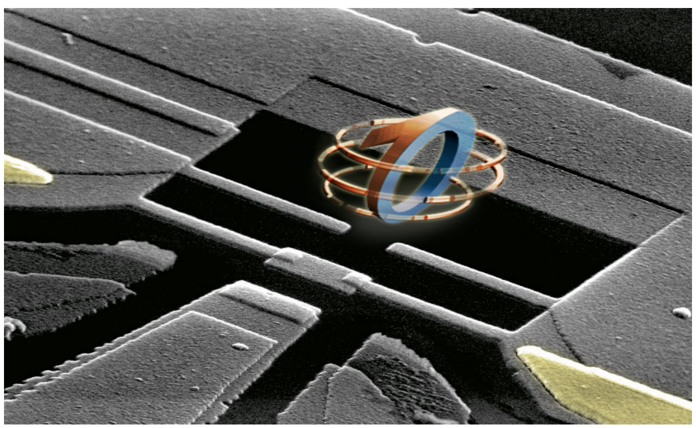

Saclay

$E_C \sim E_J$

Superconducting qubits

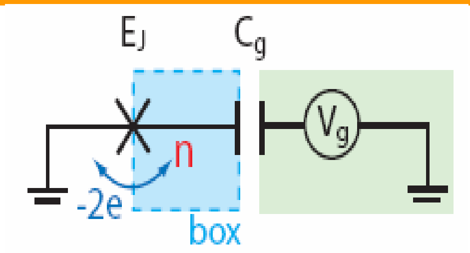

1999, NEC, T_1=2 ns, T_2=2 ns
2002, Saclay, T_1=1.8 μs T_2=0.5 μs
2005, Yale, T_1=7μs T_2=0.8 μs

$$H = 4E_c(n - C_g V_g / 2e)^2 - E_J \cos\varphi$$

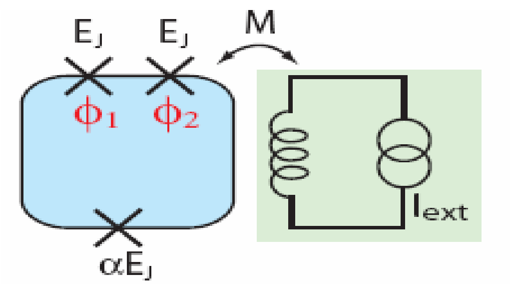

2003, Delft, T_1=900 ns, T_2=20 ns
2005, Delft, T_1=4 μs, T_2=3 μs

$$H = \frac{P_p^2}{2M_p} + \frac{P_m^2}{2M_m} + U(\varphi_p, \varphi_m, f)$$

$$U = 2E_J\left(1 - \cos\varphi_p \cos\varphi_m\right) + \alpha E_J\left[1 - \cos\left(2\varphi_m + 2\pi f\right)\right]$$

External current provide a bias magnetic flux

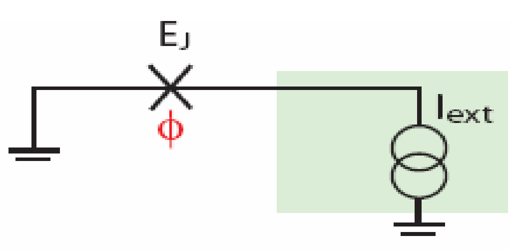

$$H = \frac{Q^2}{2C} - \frac{\Phi_0}{2\pi}\left(I_{\text{ext}}\varphi + I_c \cos\varphi\right)$$

The current source controls the potential well

UCSB, Wisconsin, Maryland, Kansas, T_2 ~ 0.1 μs

Josephson Qubits & Nonlinearity

- LC oscillator (linear): no qubit possible

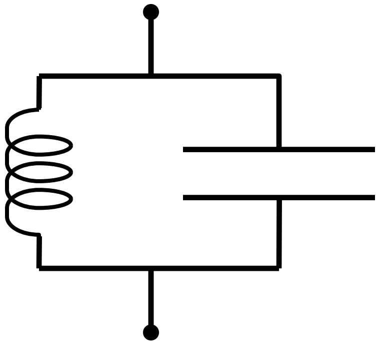

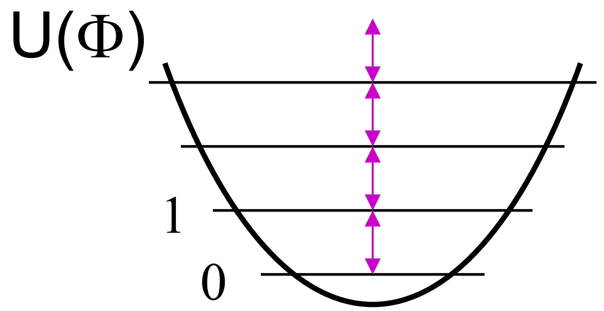

- Josephson junction: non-linear inductance with 1 photon (low loss)

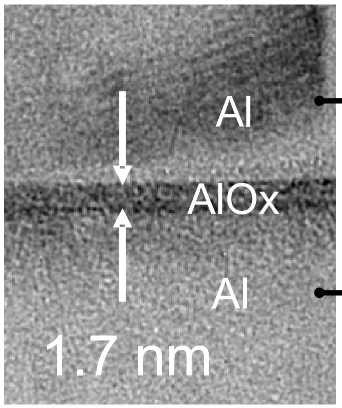

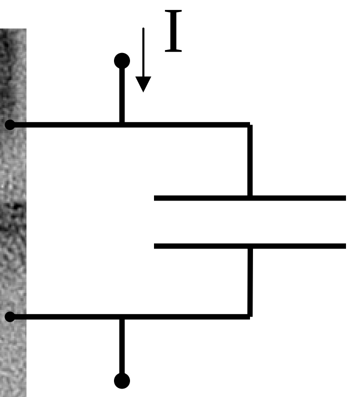

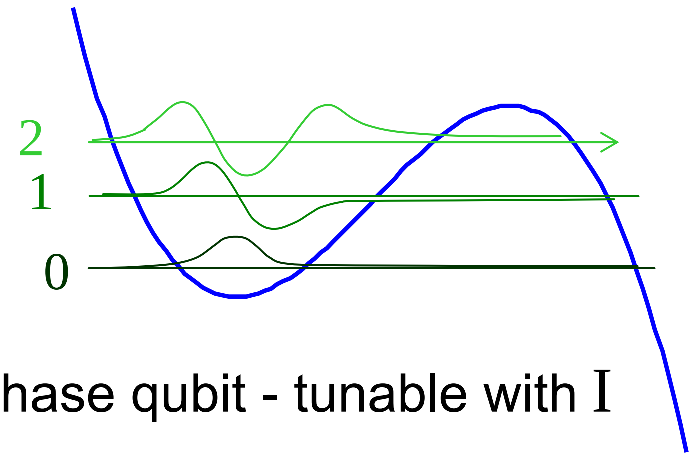

Phase qubit - tunable with I

F. Nori, *Quantum football,* Science **325**, 689 (2009).

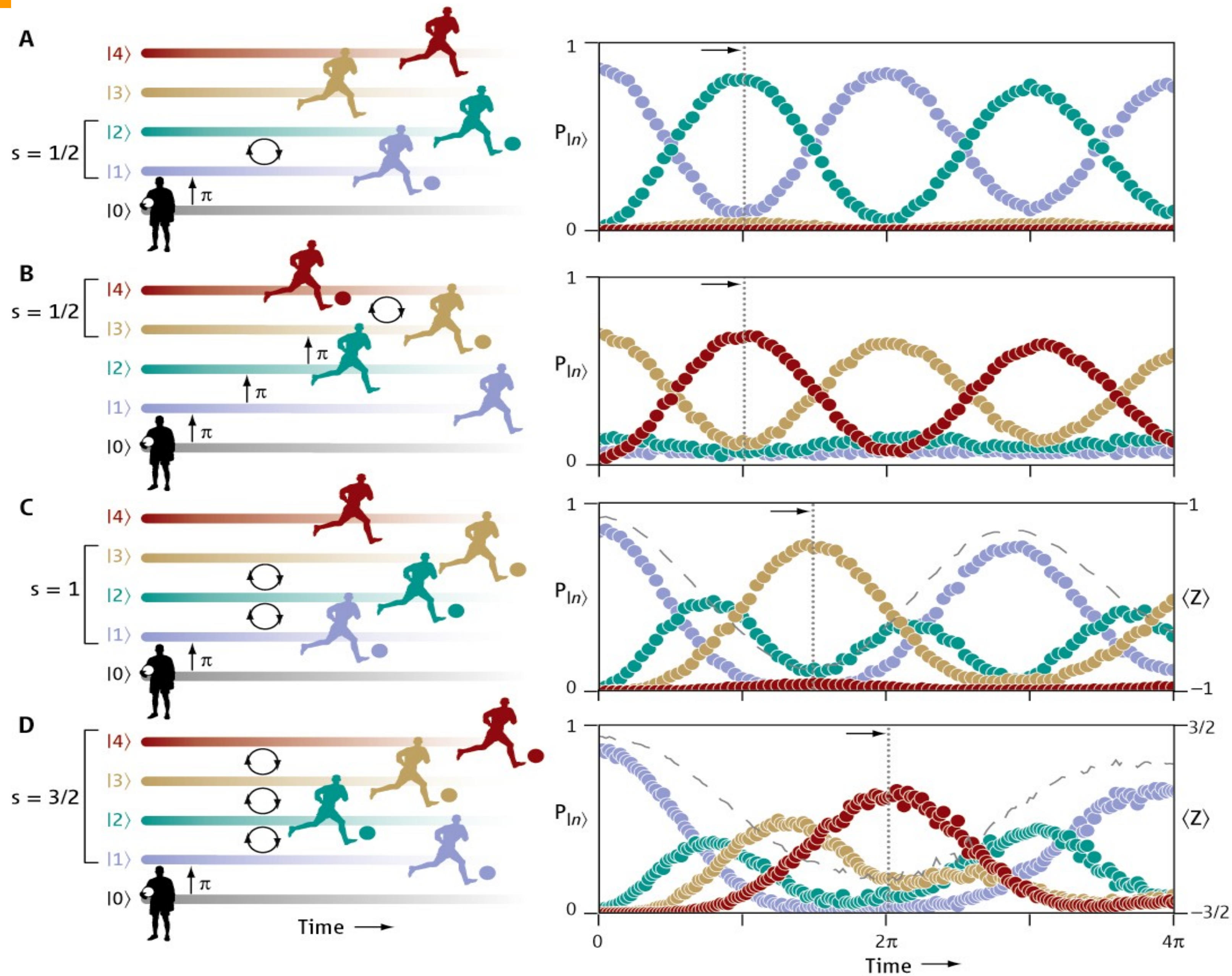

Buluta and Nori, *Science*, Oct. 2009

Quantum Simulators

Both digital and analog

Also, Georgescu and Nori, for *Rev. Mod. Phys*.

Superconducting circuits as artificial atoms

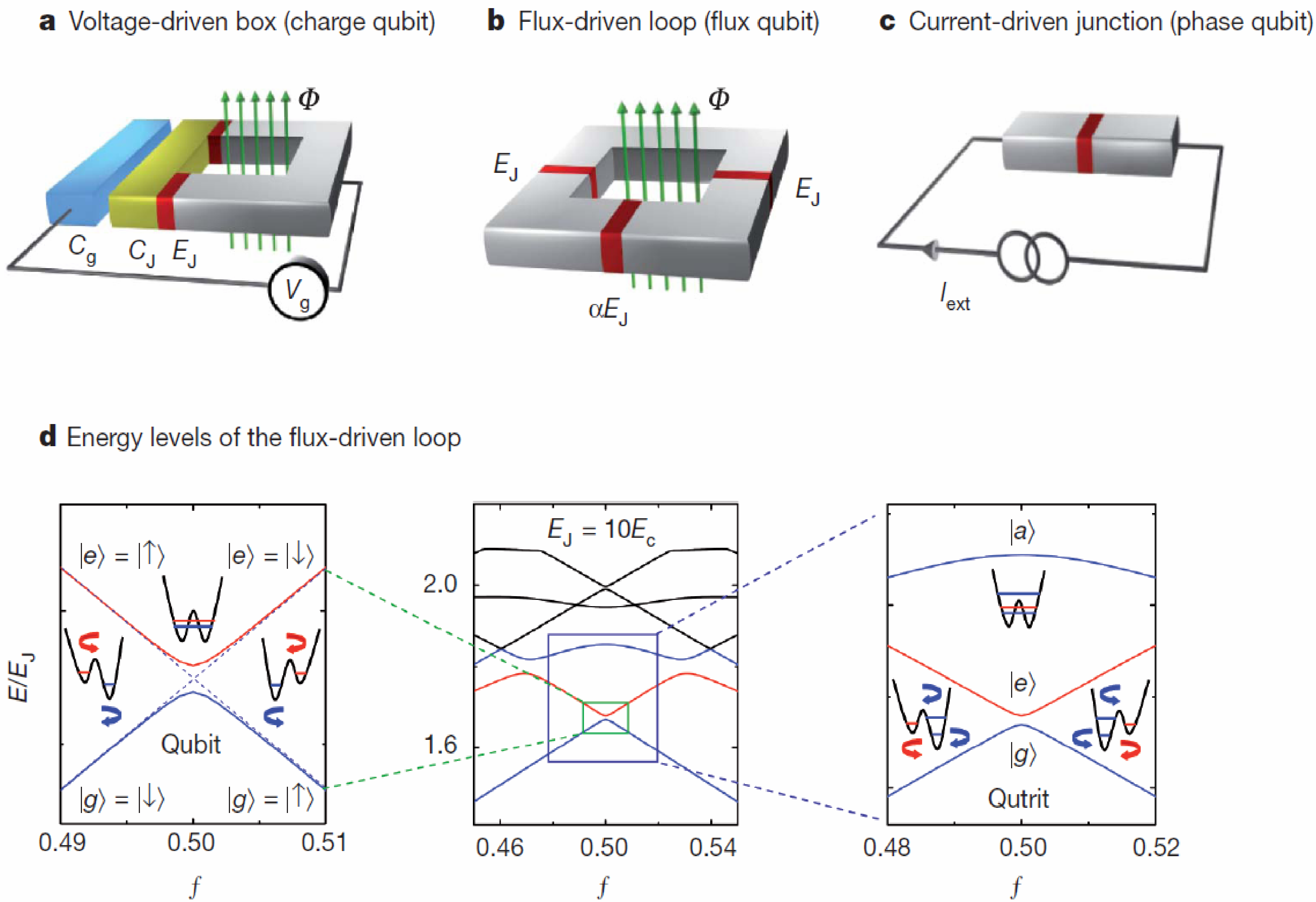

Goal

- Control of an artificial two-level system in a solid-state device

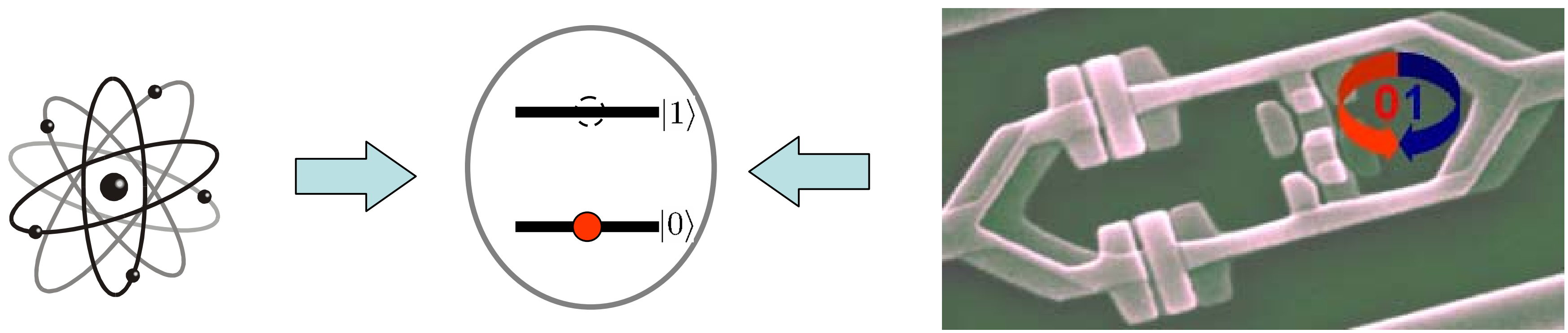

$$\alpha|0\rangle + \beta|1\rangle$$

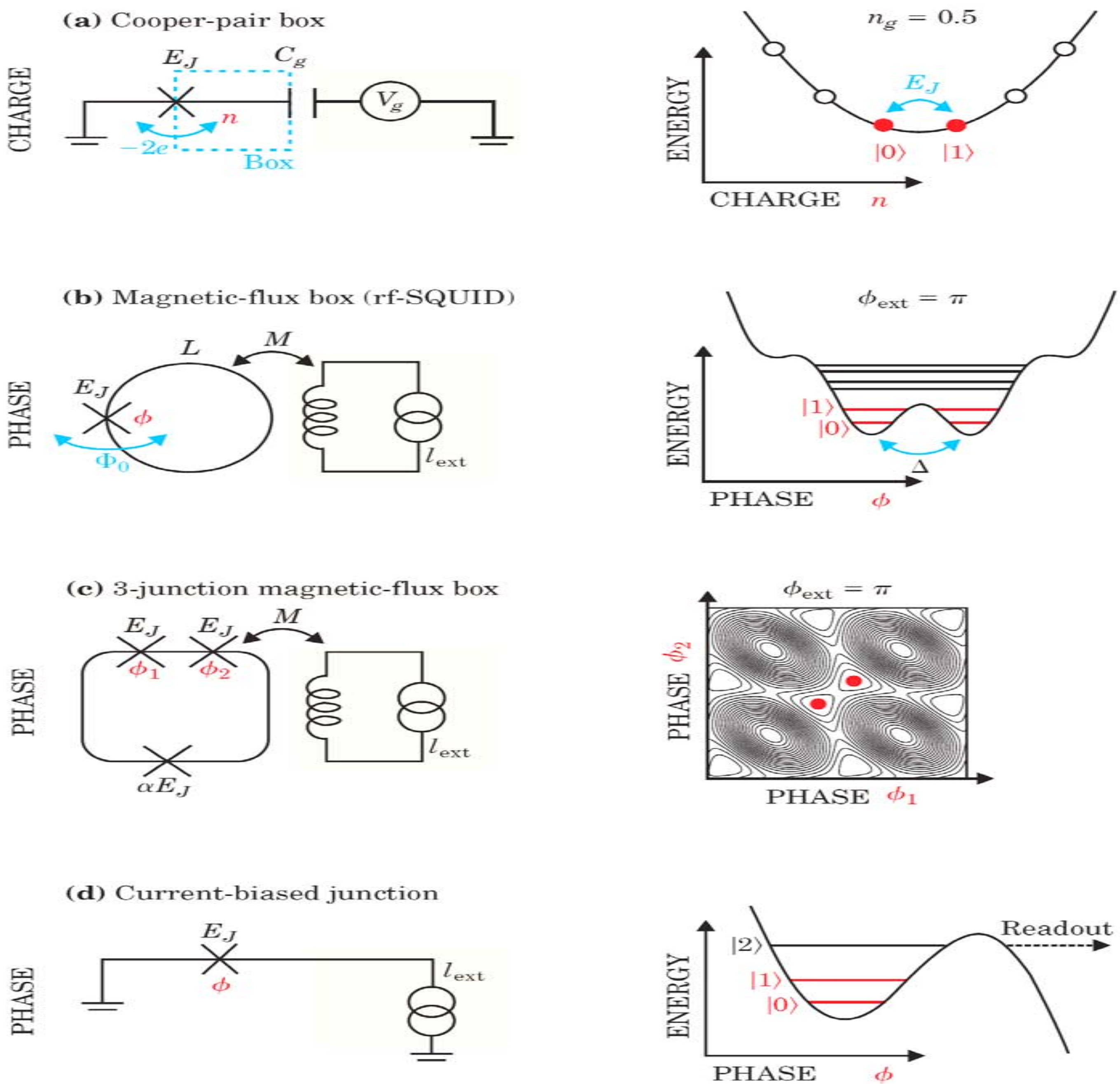

Figures from: You and Nori, *Physics Today* (November 2005)

a Voltage-driven box (charge qubit)

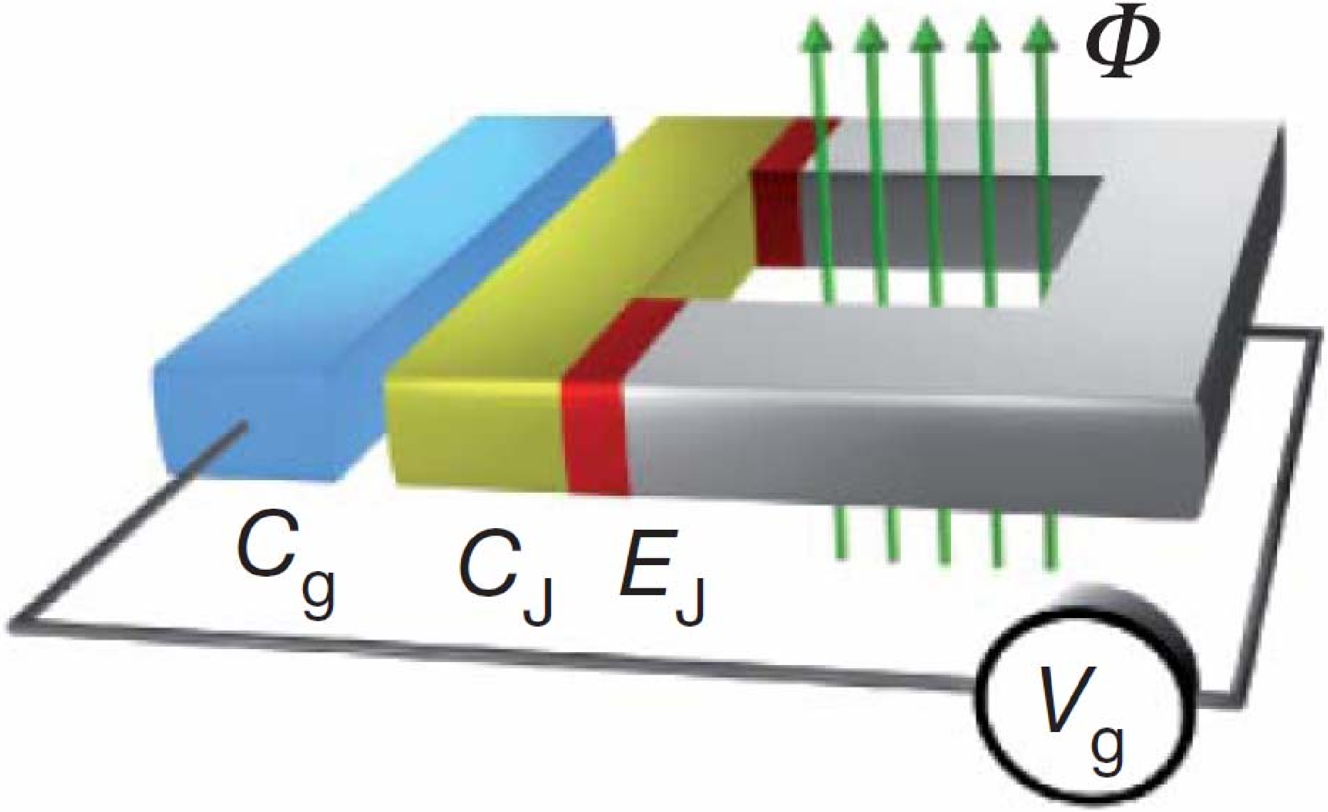

b Flux-driven loop (flux qubit)

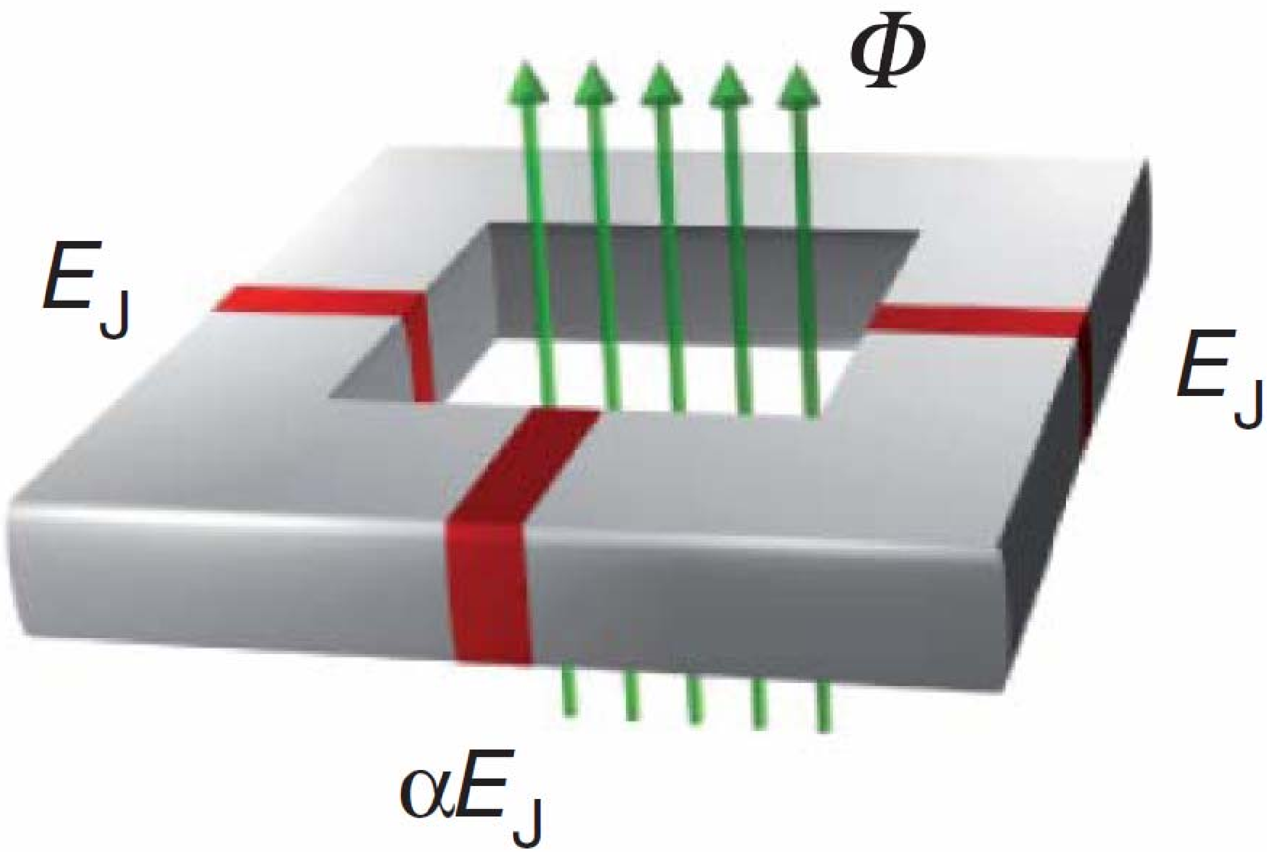

c Current-driven junction (phase qubit)

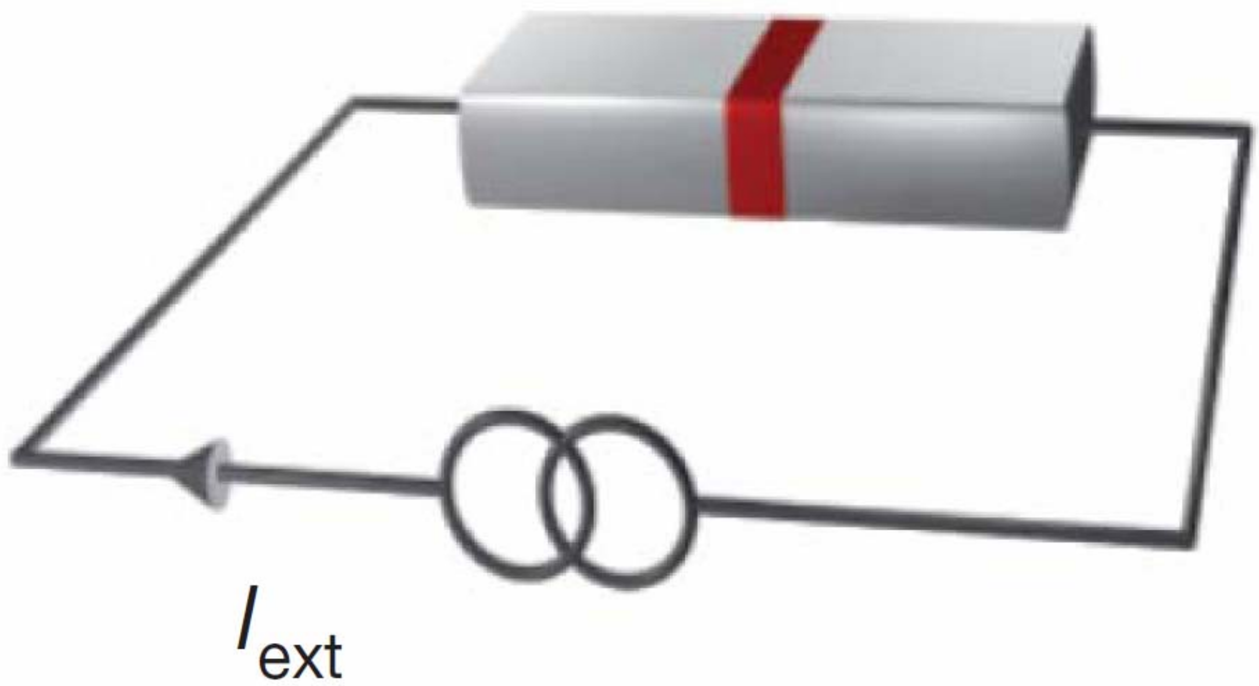

Comparison with atoms

Superconducting qubit	Atom
Josephson junction device	Atom
Current & voltage sources (& microwaves)	Light sources
Voltmeters and ampmeters	Detectors
T = 30 mK	T = 300 K
Electrodynamic environment	Cavity
Strong JJ-environment coupling	Weak atom-field coupling
Dissipation in environment	Photon losses

Comparison between SC qubits and trapped ions

Qubits	Trapped ions	Superconducting qubits
Quantized bosonic mode	Vibration mode	LC circuit
Classical fields	Lasers	Magnetic fluxes

Comparison between SC qubits and trapped ions

Trapped ions	Superconducting qubits
Moving qubits	Fixed qubits
Long coherence times (more isolated from env.)	Controllable coupling (coupling to env. --> more control)
High vacuum	Low temperatures

Approximate correspondence

Quantum Optics Atomic Physics	Quantum Supercond. circuits
Atoms, ions	Josephson junction
lasers	generators
optical fibers, beams	transmission lines, wires
mirrors	capacitors
Beam splitters	couplers
photodetectors	amplifiers

Micromaser

Carrier process: thermal excitation for micromaser

First red sideband excitation: the excited atoms enter the cavity, decay, and emit photons

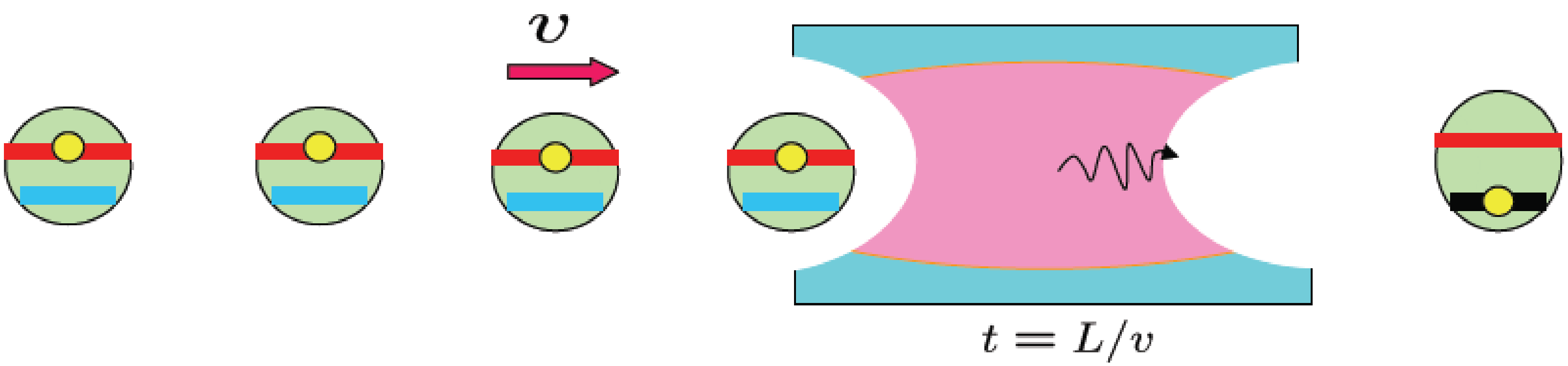

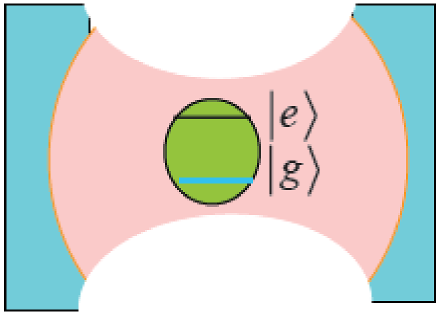

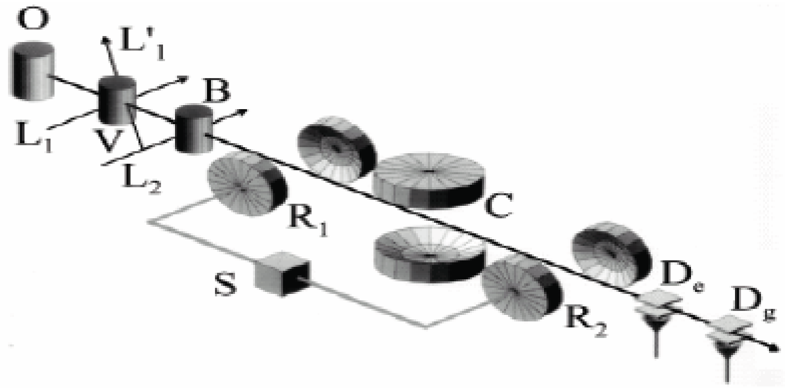

X. Maitre, et al., PRL 79, 769 (1997)

Comparison with a micromaser

	JJ qubit photon generator	Micromaser
Before	JJ qubit in its ground state then excited via $n_g = 1/2, \quad \Phi_C = \Phi_0$	Atom is thermally excited in oven
Interaction with microcavity	JJ qubit interacts with field via $n_g = 1, \quad \Phi_C = \Phi_0/2$	Flying atoms interact with the cavity field
After	Excited JJ qubit decays and emits photons	Excited atom leaves the cavity, decays to its ground state providing photons in the cavity.

Liu, Wei, Nori, *EPL* (2004); *PRA* (2005); *PRA* (2005)

Interaction between the JJ qubit and the cavity field

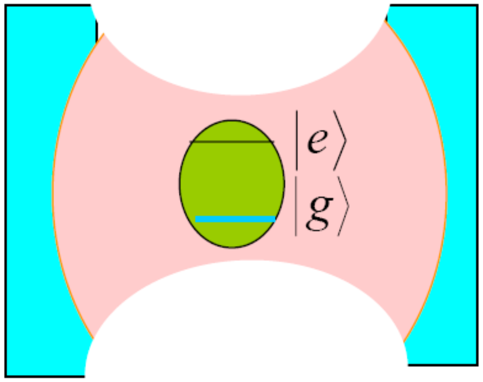

Liu, Wei, Nori,
EPL 67, 941 (2004);
PRA 71, 063820 (2005);
PRA 72, 033818 (2005)

$$H = \underbrace{\hbar\omega a^{\dagger}a}_{\text{cavity field}} \underbrace{-2E_C(1-2n_g)\sigma_z}_{\text{charging energy}} \underbrace{-E_J\cos\left[\frac{\pi}{\Phi_0}(\Phi_c + ga + g^* a^{\dagger})\right]\sigma_x}_{\text{interaction term}}$$

with $g = i\int_S u(r)\cdot ds$ and $\hbar\omega = 2E_C$

(1) The interaction between the cavity field and the SQUID is controlled by the gate charge n_g and the dc applied flux Φ_C.
(2) S is the area of the SQUID.
(3) $u(r)$ is a mode function of a single-mode cavity field.

Cavity QED on a chip

How to create superpositions of photon states

$\alpha_1|0\rangle + \alpha_2|1\rangle$ with $\alpha_1 = \cos(\Omega_1 t_1)$ and $\alpha_2 = e^{-i\theta}\sin(\Omega_1 t_1)$

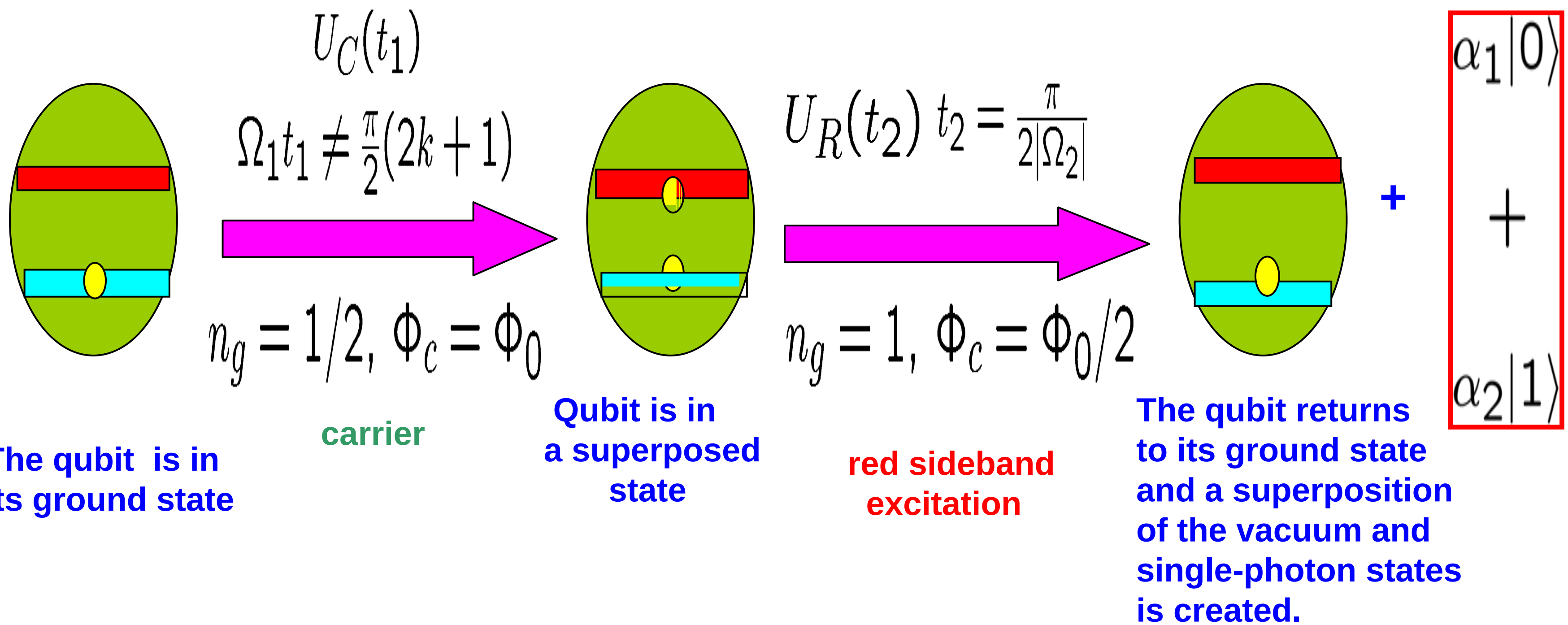

When the red sideband excitation satisfies the condition $t_2 = \pi/2|\Omega_2|$, it creates a superposition of the vacuum and single photon states.

Liu, Wei, Nori, *EPL* (2004); *PRA* (2005); *PRA* (2005)

Coupling superconducting qubits

(i.e., two artificial "atoms"
forming a "molecule")

Qubits can be ***coupled***

either <u>directly</u>

or

<u>indirectly,</u> using a data bus

(i.e., an “intermediary”)

Let us now very quickly
(fasten your seat belts!)
see a few experimental
examples of qubits
coupled directly

Capacitively coupled charge qubits

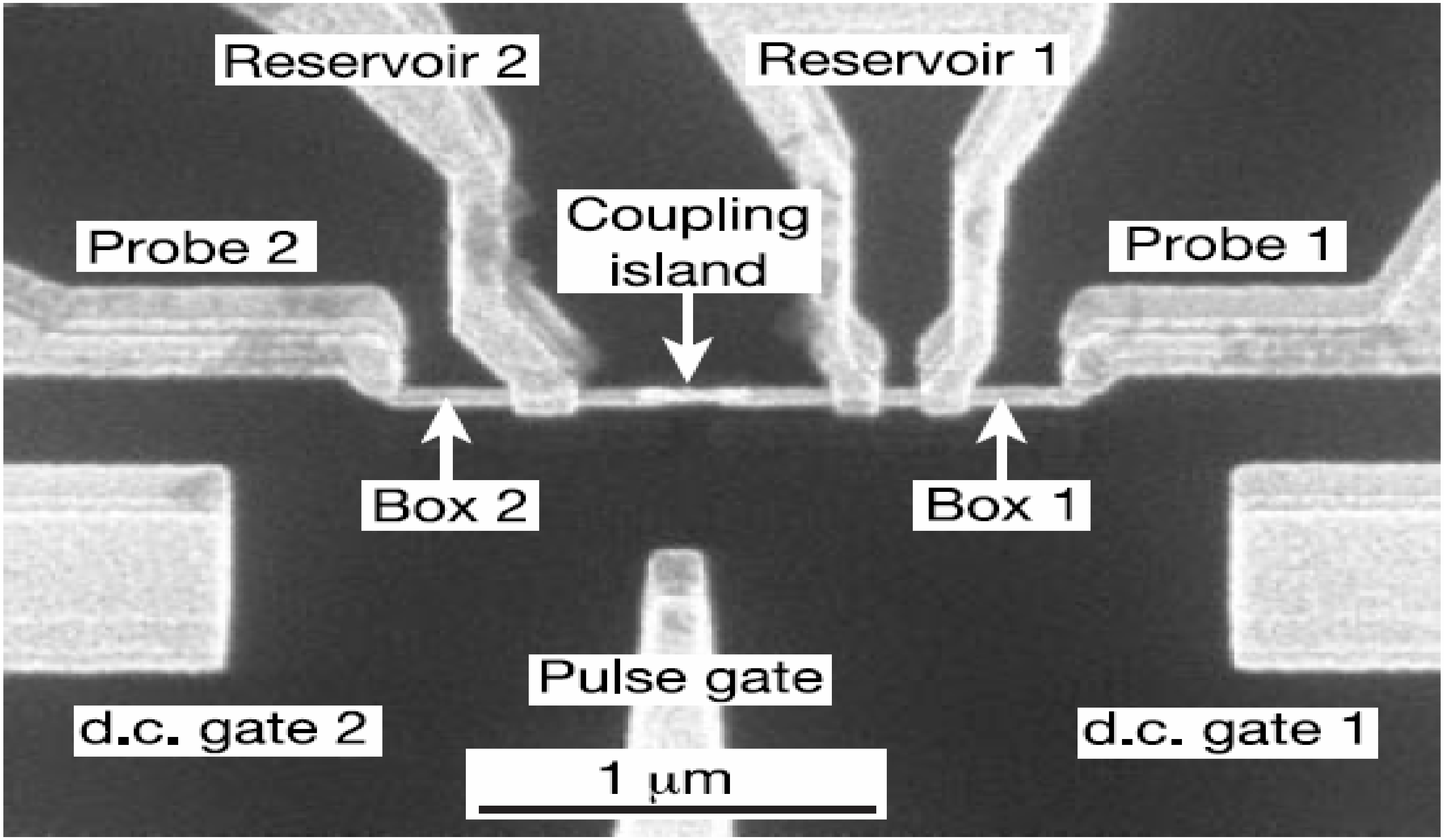

NEC-RIKEN

Entanglement; conditional logic gates

Inductively coupled flux qubits

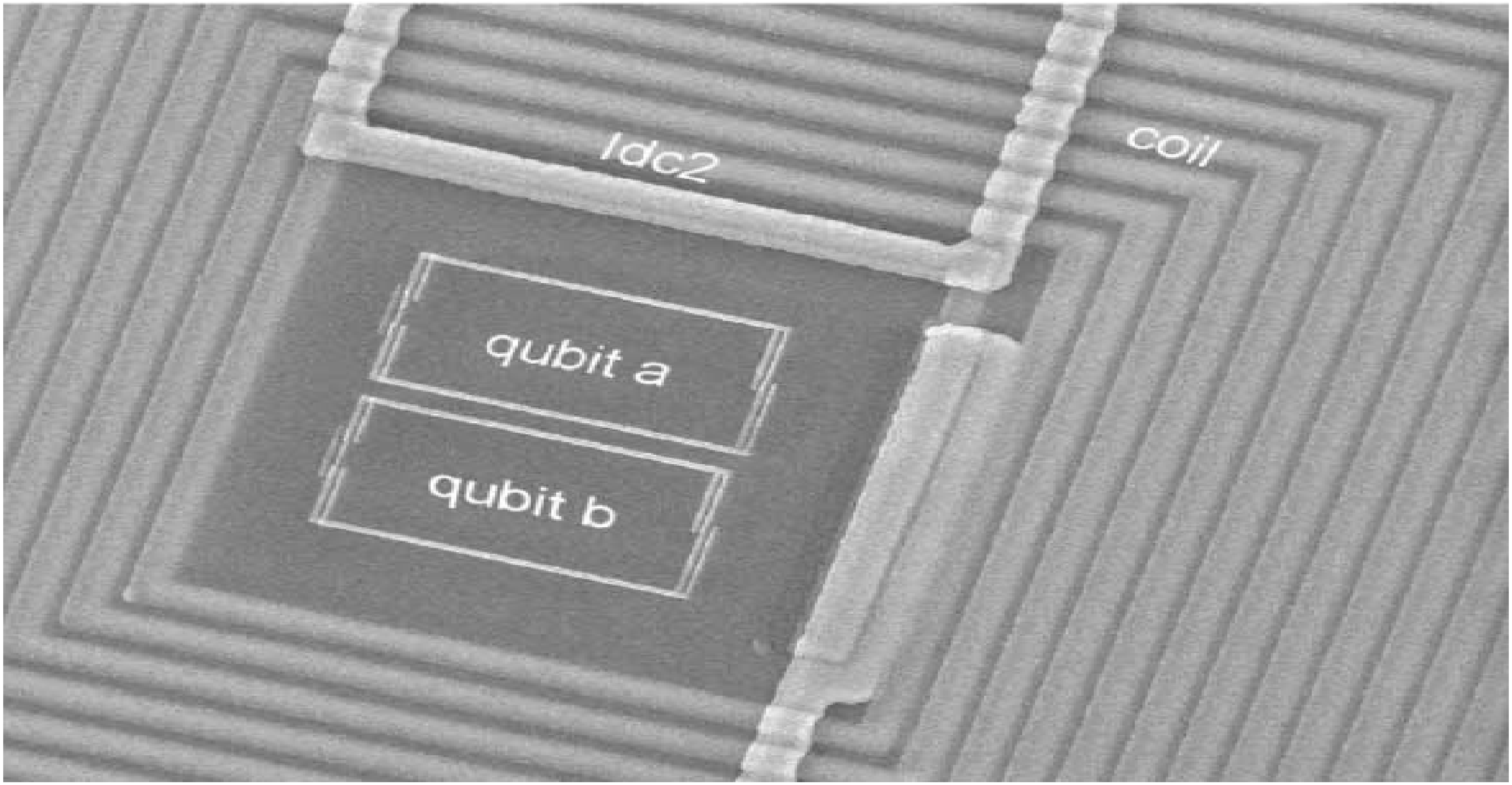

A. Izmalkov et al., PRL 93, 037003 (2004) . Jena group

Entangled flux qubit states

Inductively coupled flux qubits

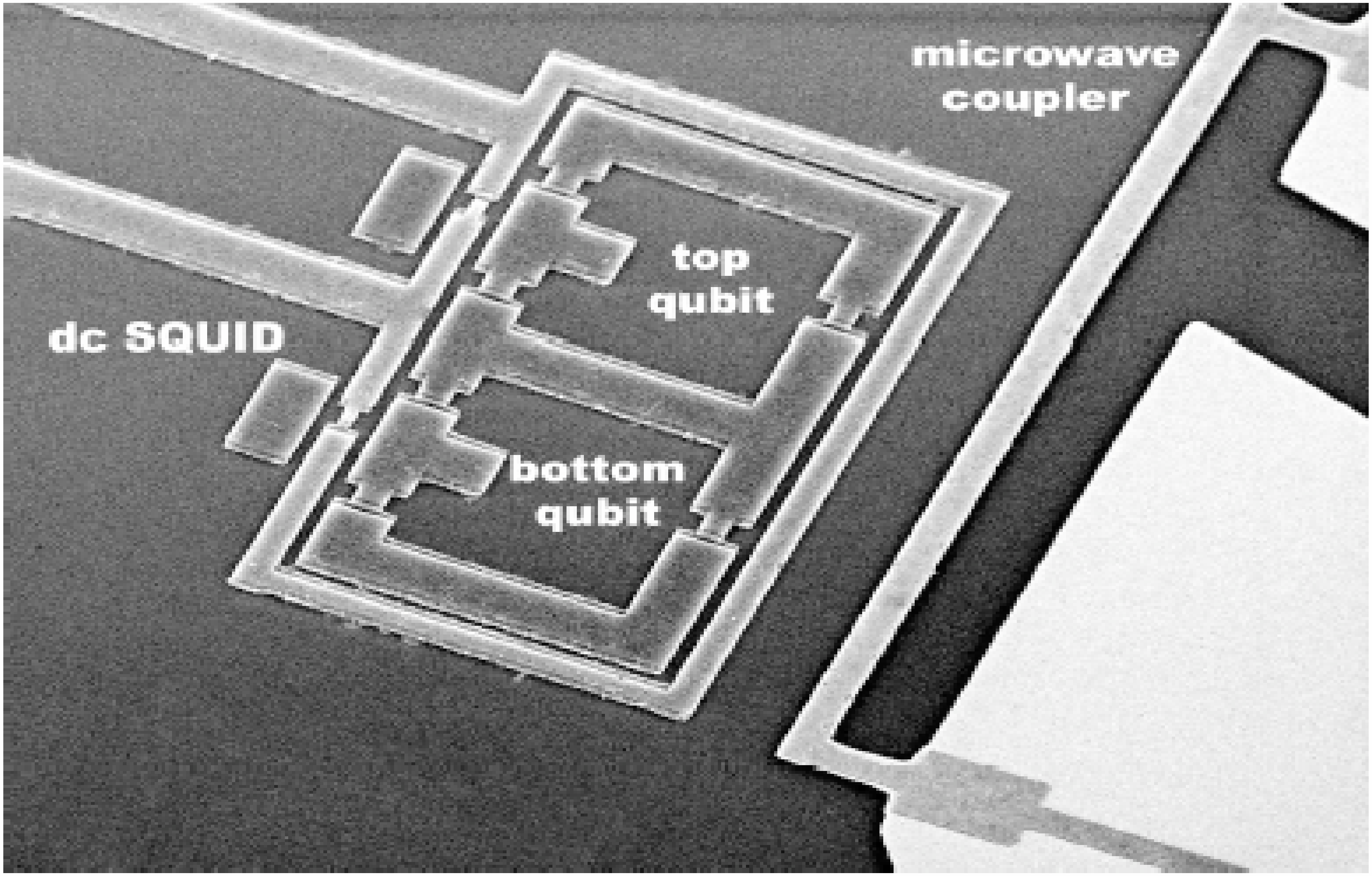

J.B. Majer et al., *PRL* 94, 090501 (2005). Delft group

Inductively coupled flux qubits

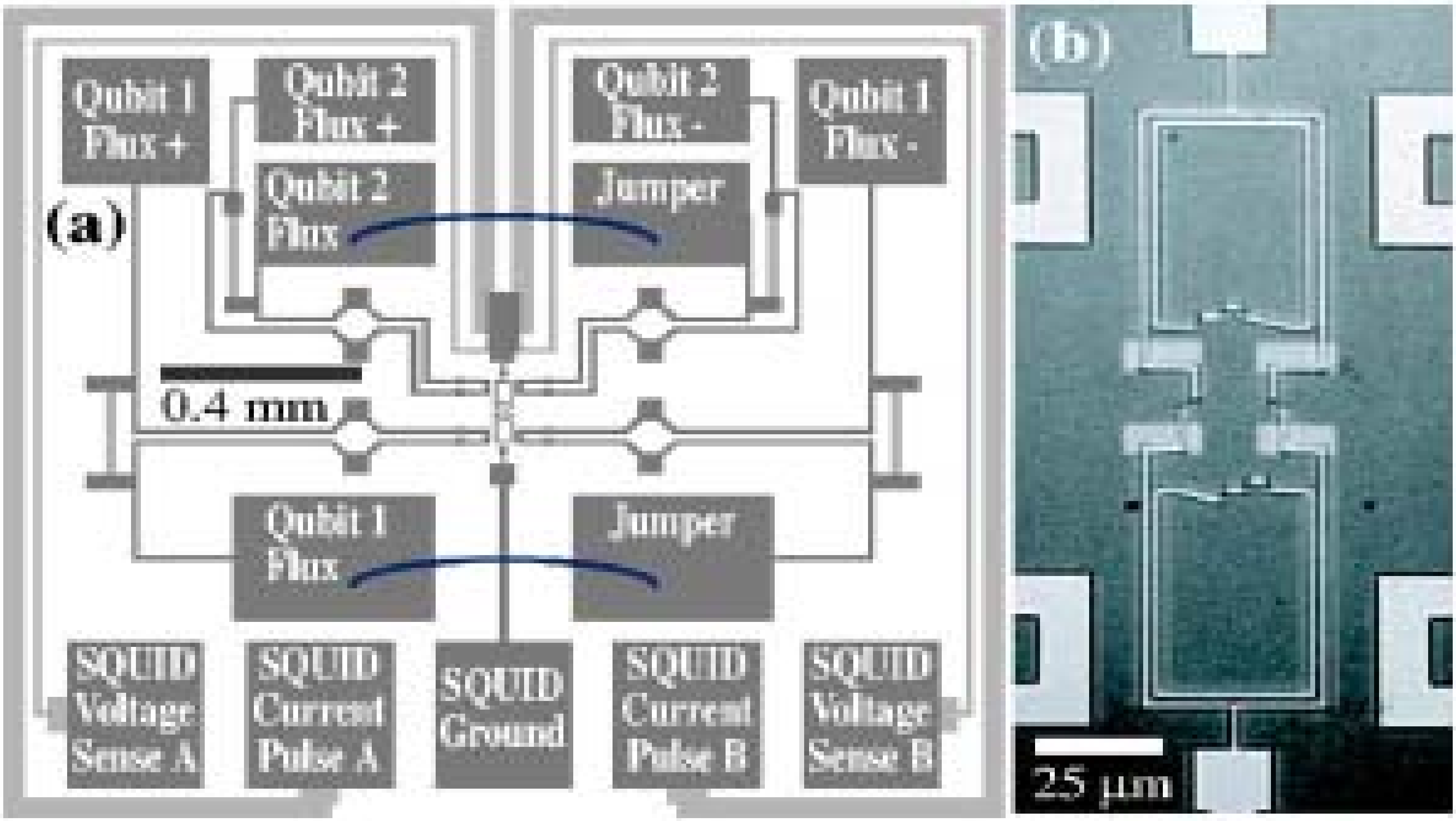

J. Clarke's group, Phys. Rev. B 72, 060506 (2005)

Capacitively coupled phase qubits

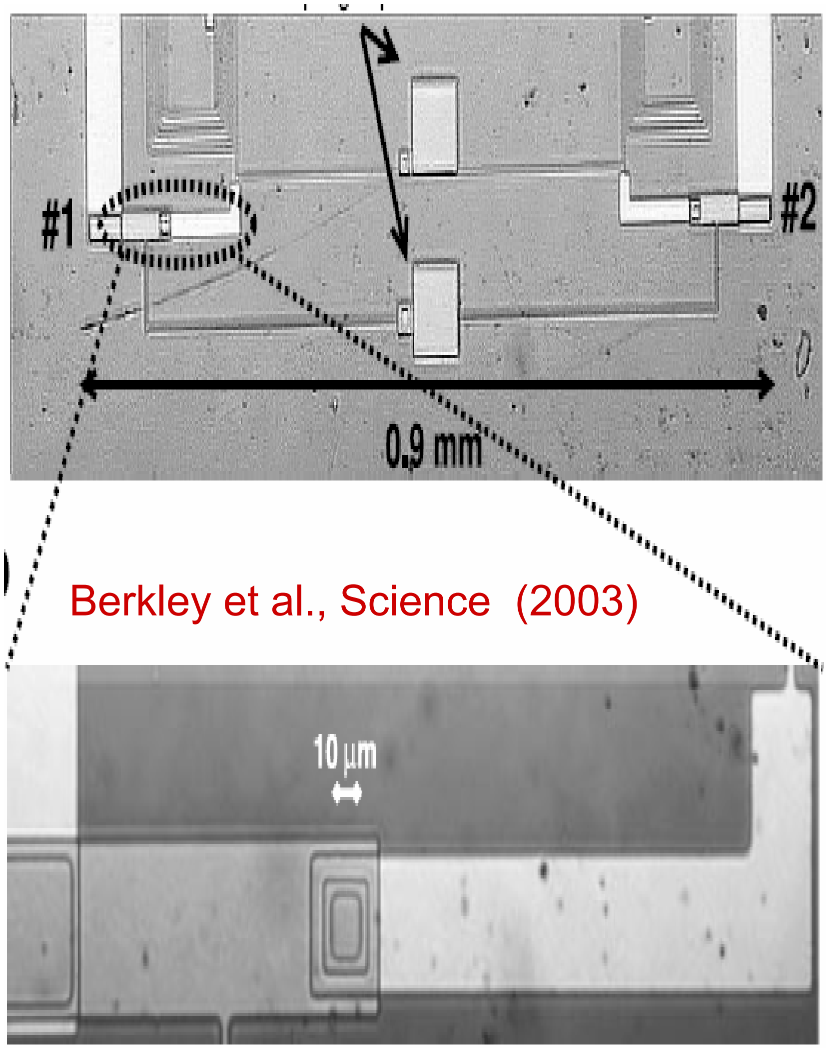

Berkley et al., Science (2003)

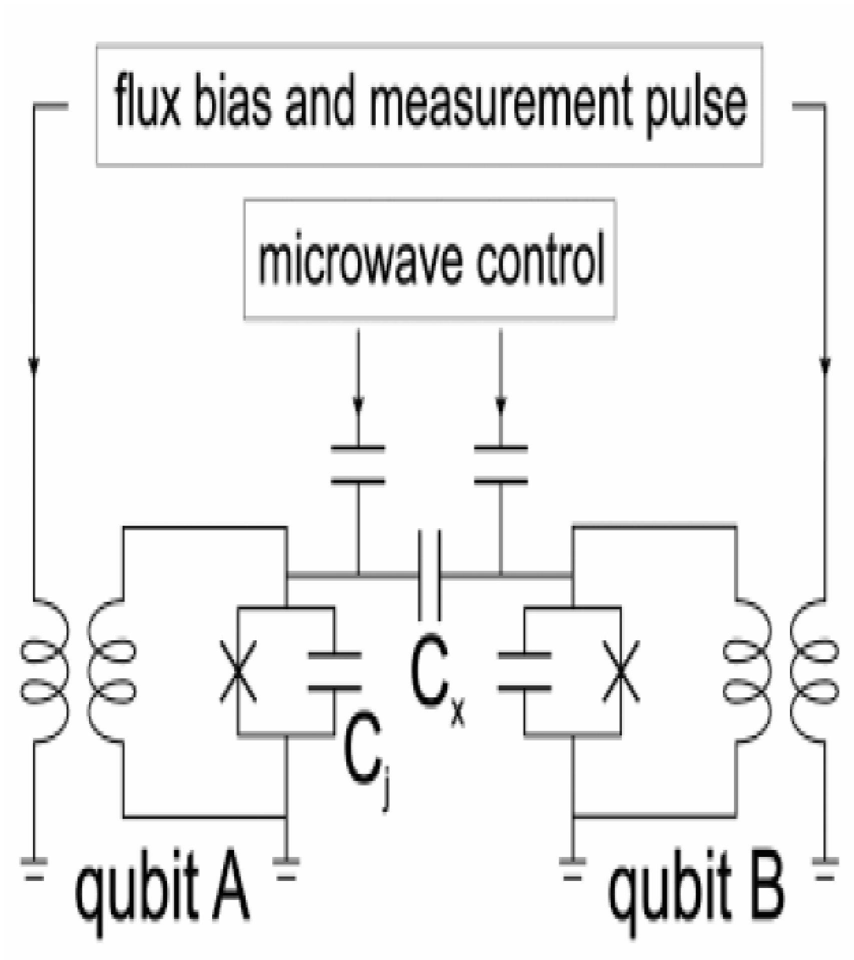

McDermott et al., Science (2005)

Entangled phase qubit states

Qubits can be

coupled *indirectly*

Coupling qubits using an LC data bus

LC-circuit-mediated interaction between qubits

Level quantization of a superconducting LC circuit has been observed.

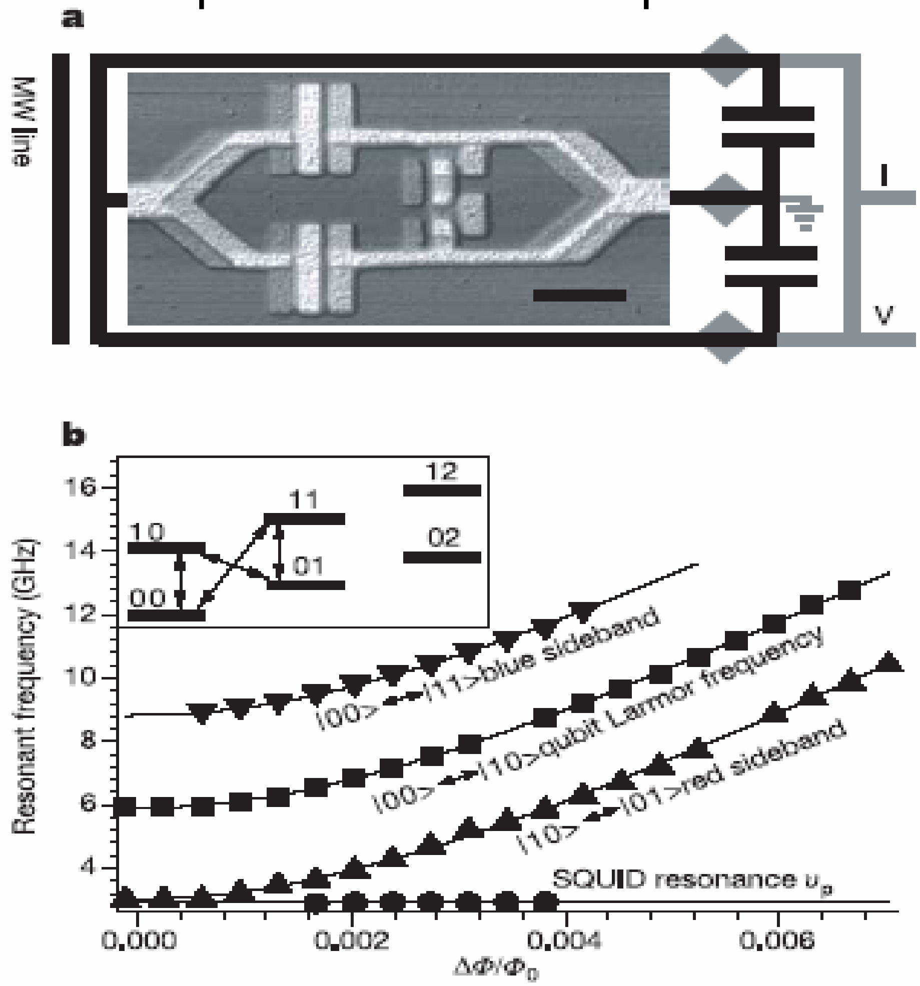

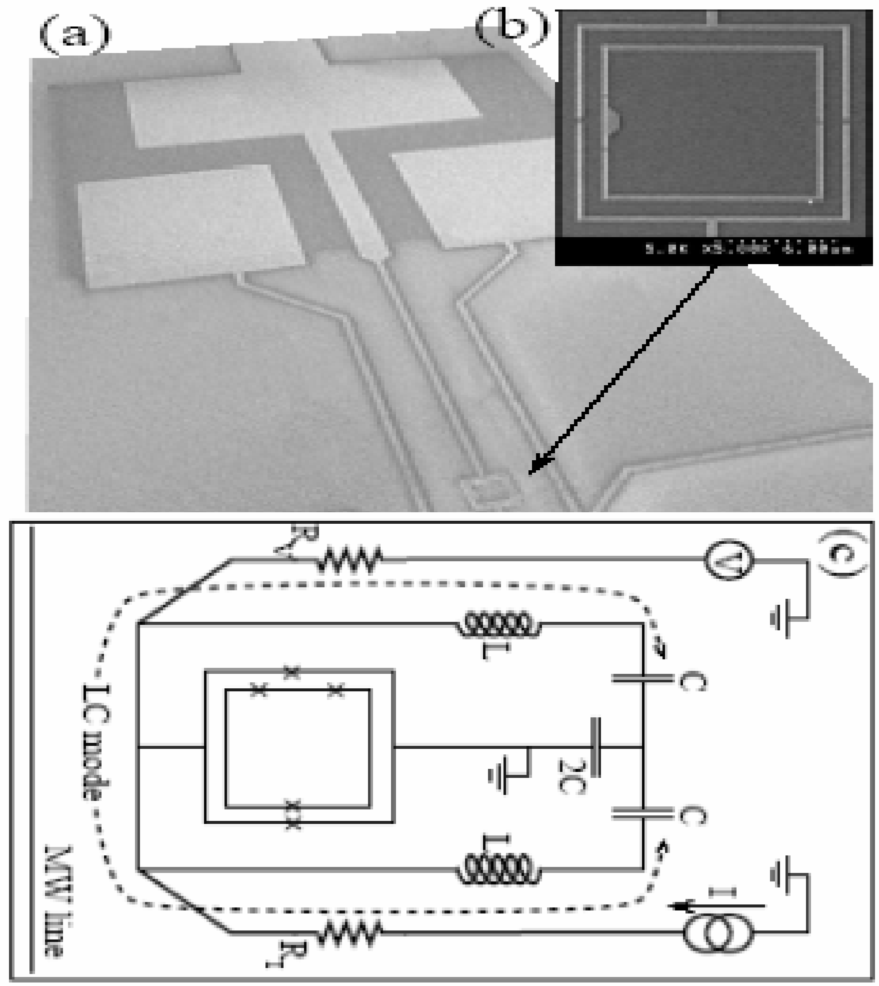

Delft, Nature, 2004
See also: Yale, Nature 2004

NTT, PRL 96, 127006 (2006)

Switchable coupling: data bus

A switchable coupling between the qubit and a data bus could also be realized by changing the magnetic fluxes through the qubit loops.

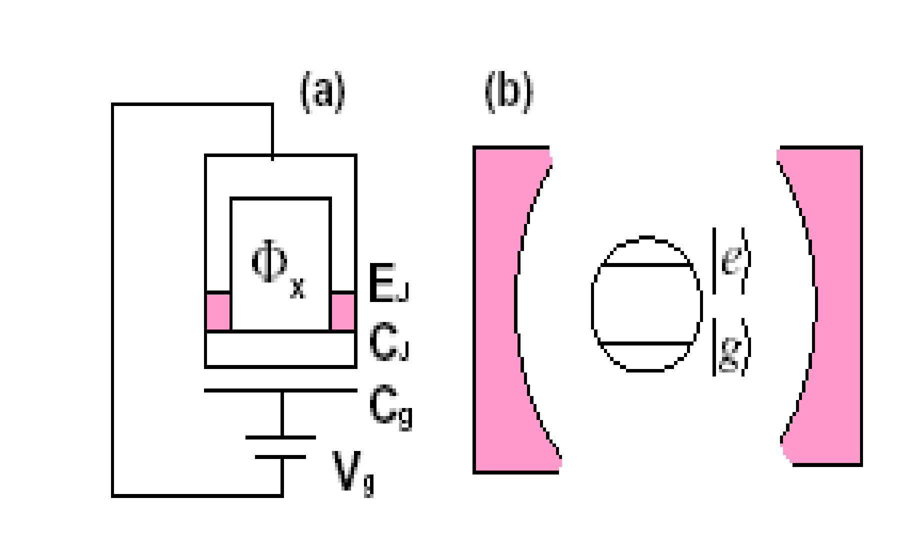

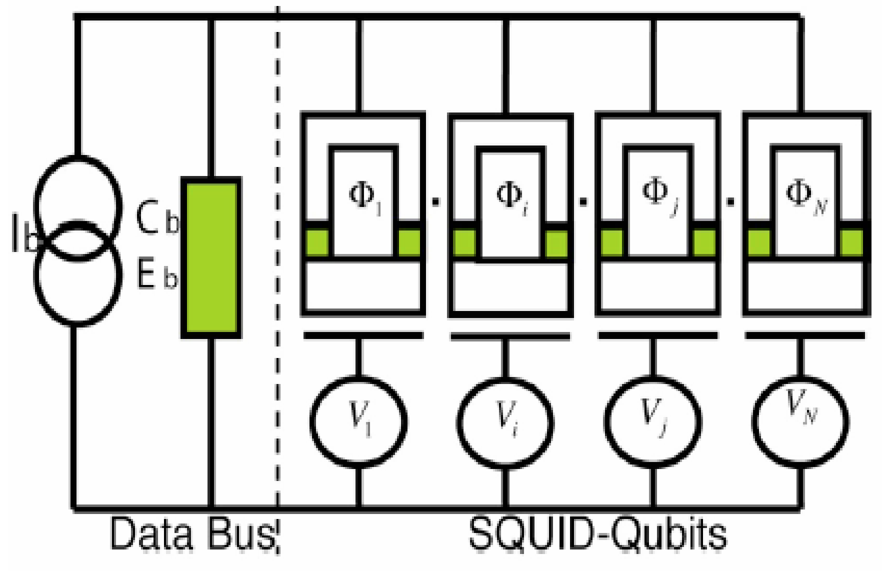

You & Nori (2001, 2003). Also (2004, 2005)

Wei, Liu, Nori, PRB 71, 134506 (2005)

Single-mode cavity field

Current-biased junction

The bus-qubit coupling is proportional to $\cos\left(\pi \frac{\Phi_X}{\Phi_0}\right)$

Superconducting charge qubit inside a cavity

(a brief overview)

QED on a chip   Comparison with atoms

Circuit QED: Superconducting qubit in a cavity	Atom in a cavity
Josephson junction device	Atom
Current and voltage sources	Light sources
Voltmeters and ammeters	Detectors
T = 30 mK	T = 300 K
Electrodynamic environment	Cavity
Strong JJ-environment coupling	Weak atom-field coupling
Dissipation in environment	Photon losses

Scalable circuits

Couple qubits *directly* via a common inductance

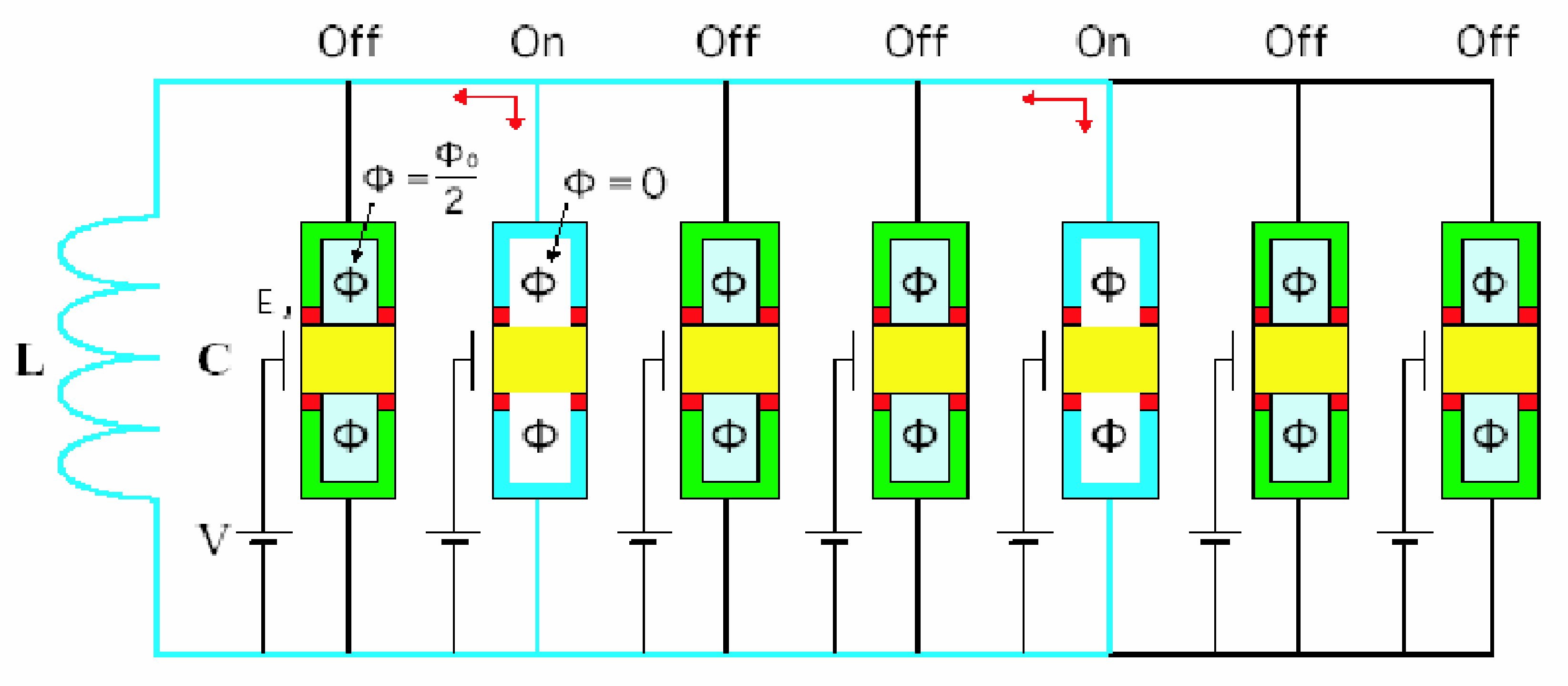

You, Tsai, and Nori, *Phys. Rev. Lett.* 89, 197902 (2002)

Switching on/off the SQUIDs connected to the Cooper-pair boxes, can couple any selected charge qubits by the common inductance (*not* using LC oscillating modes).

Controllable couplings via VFMFs

Applying a Variable-Frequency Magnetic Flux (VFMF)

$$H = H_0 + H(t)$$

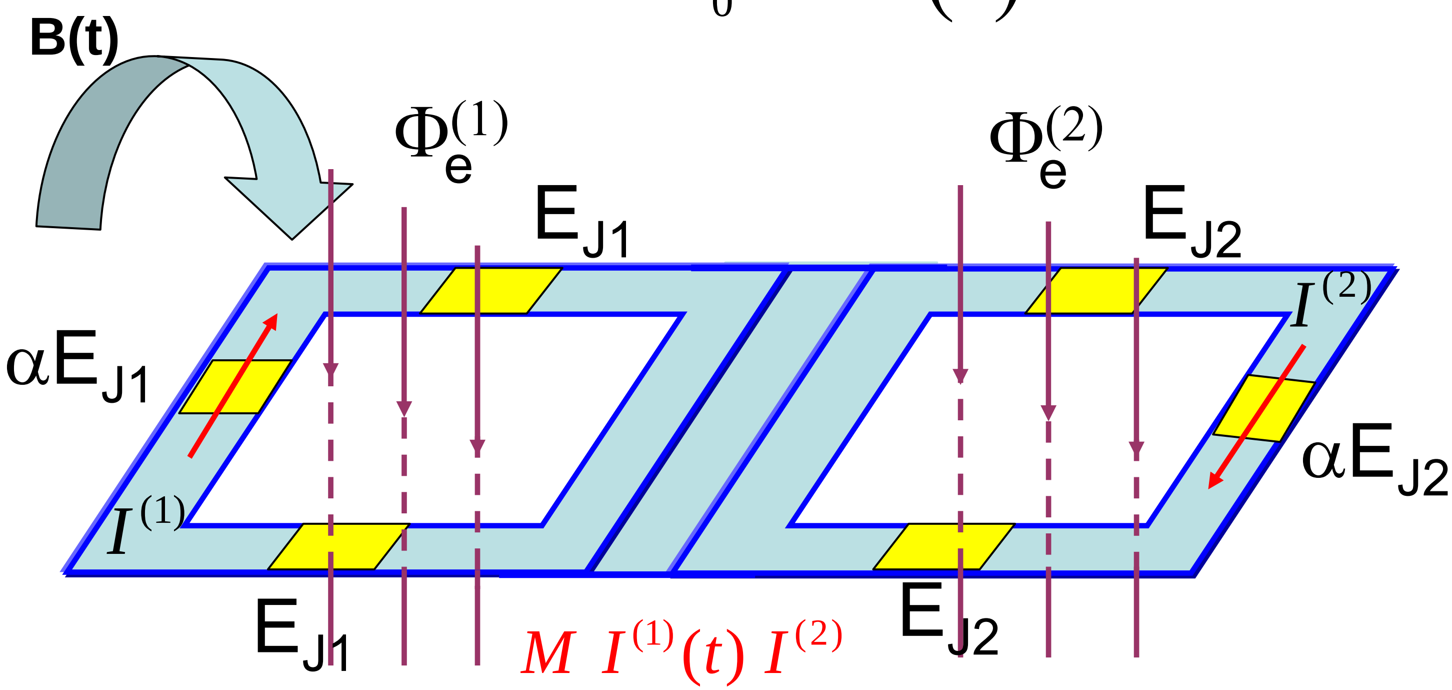

$$I^{(1)}(t) \approx I^{(1)} + \tilde{I}(t)$$

Liu, Wei, Tsai, and Nori, *Phys. Rev. Lett.* 96, 067003 (2006)

Tunable coupling of qubits

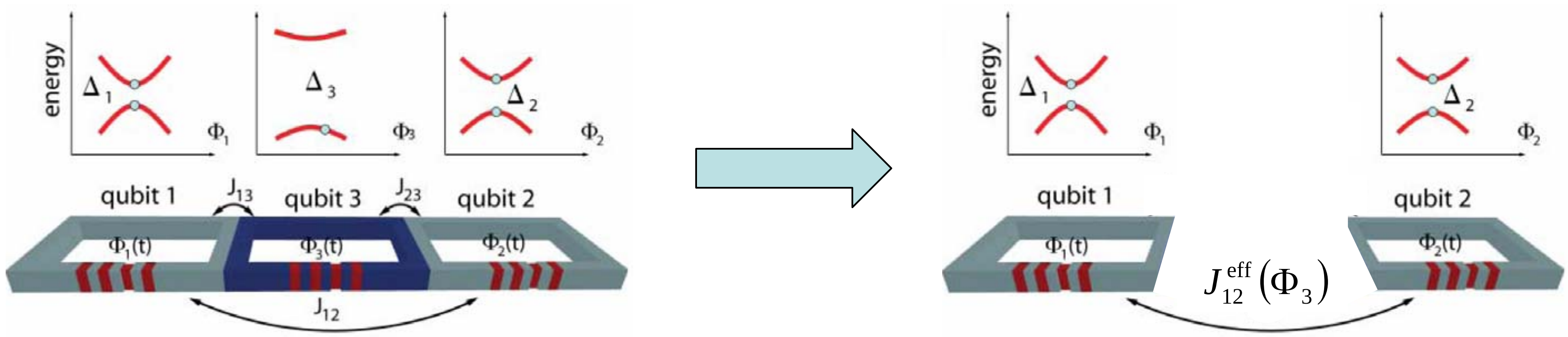

$$\hat{H} = \frac{\Delta_1}{2}\hat{\sigma}_x^{(1)} + \frac{\Delta_2}{2}\hat{\sigma}_x^{(2)} + \left(\frac{\varepsilon_3}{2}\hat{\sigma}_z^{(3)} + \frac{\Delta_3}{2}\hat{\sigma}_x^{(3)}\right) + J_{12}\hat{\sigma}_z^{(1)}\hat{\sigma}_z^{(2)} + J_{13}\hat{\sigma}_z^{(1)}\hat{\sigma}_z^{(3)} + J_{23}\hat{\sigma}_z^{(2)}\hat{\sigma}_z^{(3)}$$

$$\Rightarrow \quad \boxed{\hat{H}_{\text{eff}} = \frac{\Delta_1}{2}\hat{\sigma}_x^{(1)} + \frac{\Delta_2}{2}\hat{\sigma}_x^{(2)} + J_{12}^{\text{eff}}(\Phi_3)\hat{\sigma}_z^{(1)}\hat{\sigma}_z^{(2)}}$$

Niskanen *et al*., Science (2007); Liu, Wei, Tsai, Nori, PRL (2006);
Bertet *et al*., PRB (2006); Niskanen *et al*., PRB (2006);
Grajcar, Liu, Nori, Zagoskin, PRB (2006); Ashhab *et al*., Phys. Rev. B (2008).

Switchable coupling proposals

(without using data buses)

Proposal / Feature →	Weak fields	Optimal point	No additional circuitry
Rigetti et al. (Yale)	No	Yes	Yes
Liu et al. (RIKEN-Michigan)	OK	No	Yes
Bertet et al. (Delft) Niskanen et al. (RIKEN-NEC) Grajnar et al. (RIKEN-Michigan)	OK	Yes	No
Ashhab et al. (RIKEN-Michigan)	OK	Yes	Yes

details

Recent reviews on Superconducting qubits and related topics

- ✓ **Superconducting qubits featured in nine pages in Nature: You & Nori, Nature (June 30, 2011).**
- ✓ **Current status of all qubits for quantum computation: Reports on Progress in Physics (2011).**
- ✓ **Systematic study of quantum interferometry using superconducting qubit circuits: Phys. Reports (2010).**
- ✓ **Quantum Simulators: Buluta & Nori, Science (2009). And long preprint 2011.**
- ✓ **How to quantify entanglement with many qubits: Physics Reports, over 100 pages (2011).**

Recent reviews on Superconducting qubits and related topics

- ✓ **Superconducting qubits featured in nine pages in Nature: You & Nori, Nature (June 30, 2011).**

- ✓ **Current status of all qubits for quantum computation: Reports on Progress in Physics (2011).**

- ✓ **Systematic study of quantum interferometry using superconducting qubit circuits: Phys. Reports (2010).**

- ✓ **Quantum Simulators: Buluta & Nori, Science (2009). And long preprint 2011.**

- ✓ **How to quantify entanglement with many qubits: Physics Reports, over 100 pages (2011).**

30 JUNE 2011 | VOL 474 | NATURE | 589

doi:10.1038/nature10122

Atomic physics and quantum optics using superconducting circuits

J. Q. You[1,2] & Franco Nori[2,3]

Superconducting circuits based on Josephson junctions exhibit macroscopic quantum coherence and can behave like artificial atoms. Recent technological advances have made it possible to implement atomic-physics and quantum-optics experiments on a chip using these artificial atoms. This Review presents a brief overview of the progress achieved so far in this rapidly advancing field. We not only discuss phenomena analogous to those in atomic physics and quantum optics with natural atoms, but also highlight those not occurring in natural atoms. In addition, we summarize several prospective directions in this emerging interdisciplinary field.

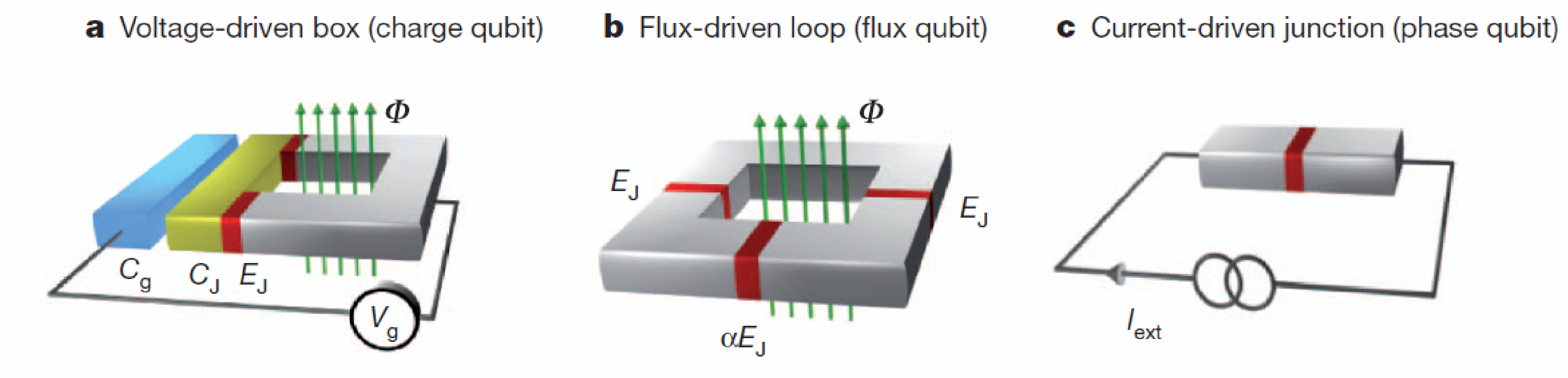

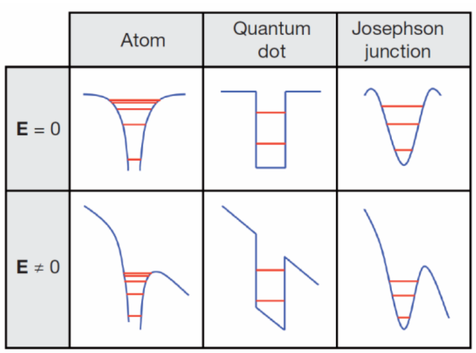

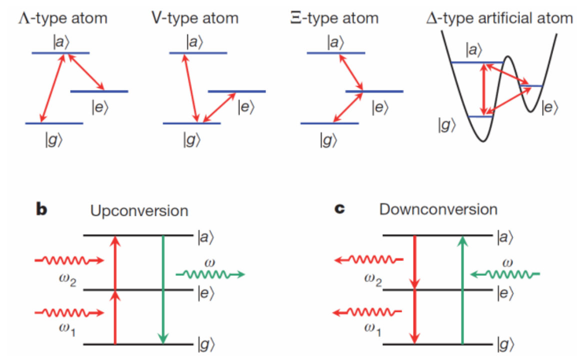

Figure 2 | Three-level atoms and frequency conversions. a, Energy levels of

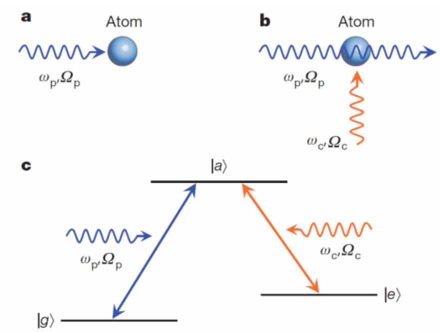

Figure 3 | Electromagnetically induced transparency. a, A probe ligl

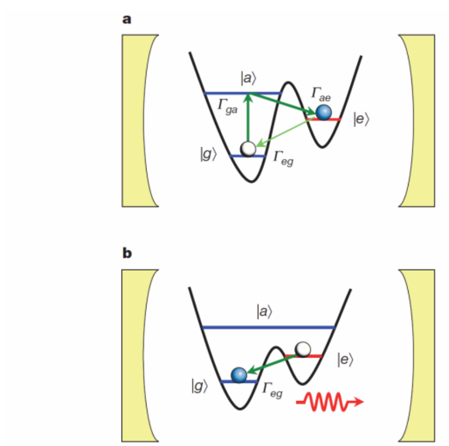

Figure 4 | Lasing. a, State population inversion (for lasing) bet

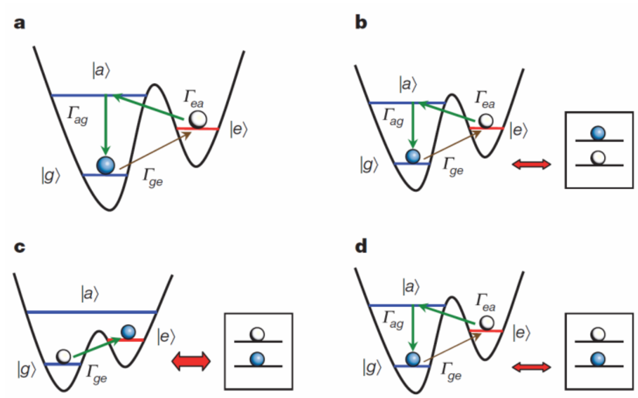

Figure 5 | Cooling a three-level artificial atom and a nearby two-level system. a, Cooling the three-junction loop to its ground state $|g\rangle$. While the

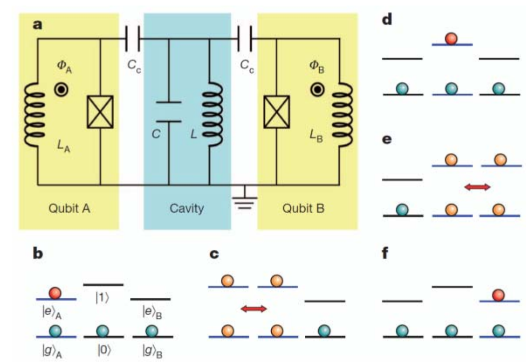

Figure 6 | Transferring quantum information between two stationary qubits via a cavity. a, Schematic diagram of two flux-driven phase qubits capacitively coupled by an on-chip cavity (an *LC* resonator). **b,** Qubit A is

Recent reviews on Superconducting qubits and related topics

- ✓ Superconducting qubits featured in nine pages in Nature: You & Nori, Nature (June 30, 2011).

- ✓ Current status of all qubits for quantum computation: Reports on Progress in Physics (2011).

- ✓ Systematic study of quantum interferometry using superconducting qubit circuits: Phys. Reports (2010).

- ✓ Quantum Simulators: Buluta & Nori, Science (2009). And long preprint 2011.

- ✓ How to quantify entanglement with many qubits: Physics Reports, over 100 pages (2011).

Table 4: Coherence times of superconducting qubits.

Year	**T1**	**T2 (echo)**	**Qubit**	**Ref.**
1999	1 ns	–	Charge	[65]
2002	580 ns	2 ns	Charge	[66]
2002	100 ns	100 ns	Phase	[67]
2002	1.8 μs	500 ns	Hybrid (charge/phase)	[68]
2003	0.9 μs	30 ns	Flux	[69]
2006	1.9 μs	3.5 μs	Flux	[77]
2008	1.87 μs	2.22 μs	Hybrid (charge/phase)	[85]
2009	350 ns	–	Flux	[89]
2010	1.6 μs	1.3 μs	Hybrid (phase/flux)	[96]
2011	12 μs	23 μs	Flux	[98]

Results up to May 2011, when the paper went to press

Table 5: Progress in the implementation of superconducting qubits quantum gates.

Year	Operation	Qubits	Mechanism	Ref.
2003	CNOT gate	2	Direct coupling; gate relies on zz component	[71]
2003	Entangled energy levels	2	Direct xy coupling	[70]
2005	iSWAP; Entanglement	2	Direct xy coupling	[73]
2006	iSWAP; Entanglement	2	Direct xy coupling	[76]
2006	Entangled energy levels	4	Direct coupling	[75]
2006-7	Controllable coupling	2	Coupling mediated by additional circuit element	[74, 78]
2007	CNOT gate	2	Direct coupling; gate relies on zz component	[82]
2007	iSWAP	2	xy coupling to cavity; gate mediated by cavity	[83]
2007	iSWAP	2	xy coupling mediated by cavity	[80]
2007	iSWAP	2	Coupling mediated by additional circuit element; gate relies on xy coupling	[81]
2009	CPhase	2	zz coupling mediated by auxilliary energy levels	[88]
2010	Entanglement	3	xy coupling	[90]
2010	Entanglement	3	zz coupling mediated by auxilliary energy levels	[91]
2011	3-qubit gate	3	Coupling mediated by auxilliary energy levels	[97]

Table 6: Progress in the number of qubits and fidelities for different operations on trapped ions. CZ stands for the Cirac-Zoller scheme [163], and MS for the Mølmer-Sørensen scheme [164].

Year	Operation	Mechanism	Qubits	Fidelity	Ref.
1998	Entanglement	CZ	2	70%	[40]
2000	Entanglement	MS	2	83%	[42]
			4	57%	
2003	CNOT gate	CZ	2	71.3%	[43]
2003	Entanglement	Geometric	2	97%	[45]
2005	Entanglement	CZ	4	>76%	[52]
			5	>60%	
			6	>50%	
2005	Entanglement	CZ	4	85%	[51]
			5	76%	
			6	79%	
			7	76%	
			8	72%	
2006	CNOT gate	CZ	2	92.6%	[53]
2008	Entanglement	MS	2	99.3%	[56]
2009	Toffoli gate	CZ	3	74%	[60]
2010	Entanglement	MS	10	62.9%	[64]
			12	39.6%	
			14	46.3%	

Table A4: Superconducting circuits.

Superconducting circuits	
Qubits	Flux, phase states, charge; also hybrids
Scalability	High potential for scalability
Initialization	Demonstrated for all types of qubits
Long coherence time	$\sim 10\ \mu s$
Universal quantum gates	One-, two-qubit gates
Measurement	Individual measurement possible
Fabrication	
Material	Josephson junctions (Al-Al_xO_y-Al,Nb-Al_xO_yNb)
Well controlled fabrication	yes
Flexible geometry	yes
Distance between qubits	$\sim \mu m$
Operation	
Qubits demonstrated	128 (fabricated) [93], 3 (entangled)
Superposition/Entangled states	yes/yes
One-qubit gates (Fidelity)	yes (99%)
Two-qubit gates (Fidelity)	yes ($> 90\%$) [88]
Operation temperature	mK
Readout	
Readout (Fidelity)	SET, SQUID ($> 95\%$) [84], cavity frequency shift [72]
Single-qubit readout possible	yes
Manipulation	
Controls	Microwave pulses, voltages, currents
Types of operations	One-, two-, three-qubit gates, entanglement
Individual addressing	yes
Decoherence	
Decoherence sources	Electric and magnetic noise, 1/f noise
T_1	$12\ \mu s$ [98]
T_2	$23\ \mu s$ [98]
Q_1	$\sim 10^5$
Q_2	> 100 (gate time 10-50 ns) [88]

Table A2: Trapped ions.

Trapped ions	
Qubits	Internal states (hyperfine or Zeeman sublevels, optical); Motional states (collective oscillations)
Scalability	Ion shuttling, arrays, photon interconnections, long strings
Initialization	Both internal (optical pumping) and motional (laser cooling) states
Long coherence time	Internal: hyperfine > 20 s, optical > 1 s; Motional: ~ 100 ms
Universal quantum gates	One-, two-, three-qubit gates
Measurement	Fluorescence: "quantum jump" technique
Fabrication	
Material	Atomic ions: Ca^+, Be^+, Ba^+, Mg^+, etc
Well controlled fabrication	yes
Flexible geometry	yes
Distance between qubits	A few μm to tens of μm
Operation	
Qubits demonstrated	$10 - 10^3$ (stored), 14 (entangled) [64]
Superposition/Entangled states	yes/yes (2-14 ions, fidelities 99.3%-46%) [64]
One-qubit gates (Fidelity)	yes (99%)
Two-qubit gates (Fidelity)	yes (CNOT $> 99.3\%$ [56]; Toffoli 71.3% [60]; gate time 1.5 ms)
Operation temperature	From μK to mK
Readout	
Readout (Fidelity)	Laser-induced fluorescence (99.9%)
Single-qubit readout possible	yes
Manipulation	
Controls	Optical, microwave, electric/magnetic fields
Types of operations	One-, two-, three-qubit gates, entanglement
Individual addressing	yes
Decoherence	
Decoherence sources	Heating, spontaneous emission, laser, magnetic field fluctuations
T_1	~ 20 s (internal hyperfine); ~ 100 ms (motional)
T_2	1000 s [63] (atomic clocks > 10 min)
Q_1	$\sim 10^{13}$ (single-qubit gate 50 ps) [63]
Q_2	~ 20000 (MS gate 50 μs) [56]; ~ 200 (CZ gate 500 μs) [53]

Table A1: Neutral atoms.

Neutral atoms	
Qubits	Internal states (ground hyperfine states); Motional states (trapping potential eigenstates)
Scalability	Demonstrated in optical lattices; possible in arrays of cavities, atom chips
Initialization	Both internal (optical pumping) and motional (laser cooling) states
Long coherence time	Several seconds [19, 30, 15]
Universal quantum gates	One-, two-qubit gates (several proposals)
Measurement	Fluorescence: "quantum jump" technique
Fabrication	
Material	Trapped neutral atoms: Rb, Li, K, Cs, etc
Well controlled fabrication	yes
Flexible geometry	yes (especially in optical lattices)
Distance between qubits	A few hundred nm to a few μm [1]
Operation	
Qubits demonstrated	$> 10^6$ (stored), 2 (entangled)
Superposition/Entangled states	yes/yes
One-qubit gates (Fidelity)	yes (99.98 %)
Two-qubit gates (Fidelity)	yes (SWAP >64% [20]); CNOT (73% [33])
Operation temperature	From nK toμK
Readout	
Readout (Fidelity)	Laser-induced fluorescence (99.9%)
Single-qubit readout possible	yes
Manipulation	
Controls	Optical fields, microwave
Types of operations	One-, two-qubit gates, entanglement
Individual addressing	To be demonstrated [24, 29, 35, 32, 31]
Decoherence	
Decoherence sources	Photon scattering, heating, stray fields, laser fluctuations
T_1	$\sim$ s
T_2	$\sim$ 40 ms
Q_1	$\sim 10^4$
Q_2	$\sim$ 40000

Table A3: Nuclear spins manipulated by Nuclear Magnetic Resonance (NMR).

NMR	
Qubits	Nuclear spin
Scalability	Not available in liquid-state NMR; possible for solid-state NMR
Initialization	Demonstrated
Long coherence time	> 1 s
Universal quantum gates	One-, two-, three-qubit gates
Measurement	Single-qubit measurement not available
Fabrication	
Material	Organic molecules (alanine, chloroform, cytosine)
Well controlled fabrication	yes
Flexible geometry	no
Distance between qubits	$\sim$ Å
Operation	
Qubits demonstrated	7, 12 (entangled) liquid-state [140]; >100 (correlated) solid-state
Superposition/Entangled states	yes/yes
One-qubit gates (Fidelity)	yes ($> 98\%$)
Two-qubit gates (Fidelity)	yes ($> 98\%$ CNOT and SWAP)
Operation temperature	Room temperature
Readout	
Readout (Fidelity)	Voltage in neighboring coil induced by precessing spins, 99.9%
Single-qubit readout possible	no
Manipulation	
Controls	RF pulses
Types of operations	One-, two-, three-qubit gates
Individual addressing	no
Decoherence	
Decoherence sources	Coupling errors
T_1	> 1 s (liquid-state); > 1 min (solid-state)
T_2	~ 1 s (liquid-state); > 1 s (solid-state)
Q_1	
Q_2	100 (gate time 10 ms)

Table A5: Spins in solids. Here, QDs stand for quantum dots, NV centers for nitrogen-vacancy centers in diamond and P:Si for phosphorous on silicon. The asterisk $*$ refers to room temperature.

Spins in solids	
Qubits	Electron spin; Electron and nuclear spins in NV centers in diamond, P:Si
Scalability	High potential for scalability
Initialization	Demonstrated
Long coherence time	> 1 s (QDs); $\sim$ s (NV centers), ~ 100 s (P:Si)
Universal quantum gates	One-qubit gates
Measurement	Electrical, optical
Fabrication	
Material	GaAs, InGaAs (QDs), NV centers in diamond, P:Si
Well controlled fabrication	yes
Flexible geometry	yes
Distance between qubits	100-300 nm(QDs); ~ 10 nm (NV centers)
Operation	
Qubits demonstrated	1 (QDs), 3 (NV centers) [123]
Superposition	yes
One-qubit gates (Fidelity)	yes ($> 73\%$ QDs [112]; $> 99\%$ NV centers [130])
Two-qubit gates (Fidelity)	yes (90% NV centers [108])
Operation temperature	From mK to a few K (QDs); room temperature (NV centers)
Readout	
Readout (Fidelity)	electrical, optical (90-92%)
Single-qubit readout possible	yes
Manipulation	
Controls	RF, optical pulses, electrical
Types of operations	One-qubit gates (>73% gate time 25 ns)
Individual addressing	yes
Decoherence	
Decoherence sources	Co-tunneling, charge noise, coupling with nuclear spins
T_1	> 1 s (QDs) [119]; > 5 ms * (NV centers) [123]; 6 s [133] (P:Si); 100 s [134] (P:Si)
T_2	~ 270 μs [129, 128]; ~ 1.8 ms (NV centers) [124]; ~ 60 ms [106] (P:Si); 2 s [9] (P:Si)
Q_1	$\sim 10^3$ (gate time 180 ps); $\sim 10^4$ (gate time 30 ps) [120]; $> 10^6$ (gate time ~ 1 ns)
Q_2	tbd

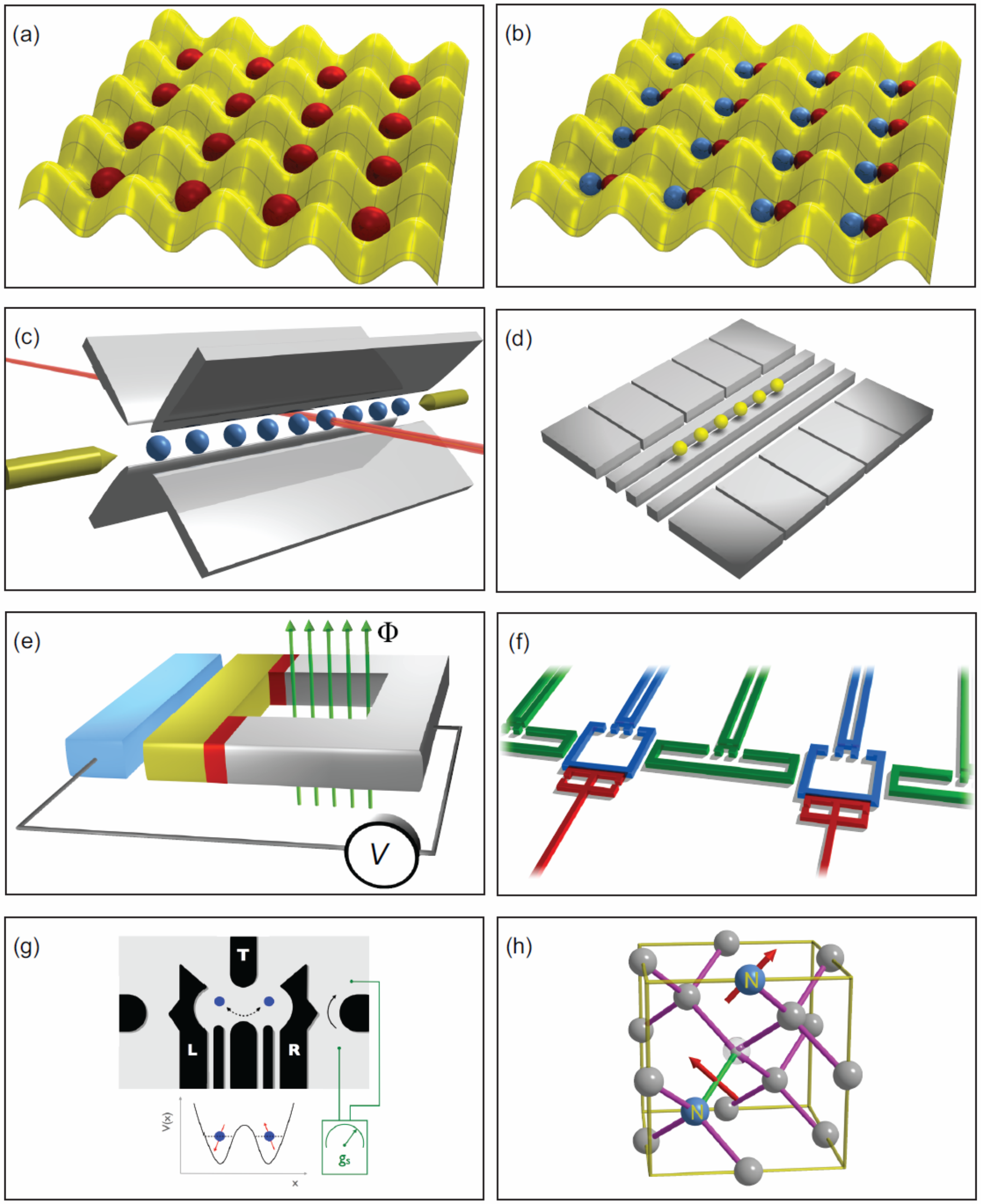
(a)
(b)
(c)
(d)
(e)
Φ
V
(f)
(g)
T
L
R
V(x)
x
g_s
(h)
N
N

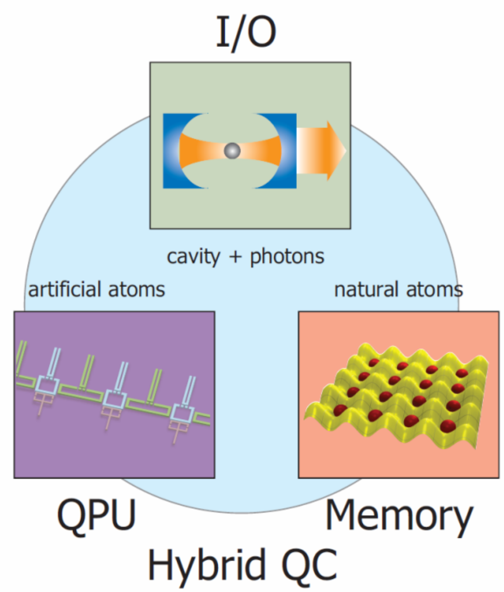
I/O
cavity + photons
artificial atoms
natural atoms
QPU
Memory
Hybrid QC

Table 1: Comparison between natural and artificial atoms.Note: [(a)] distance between qubits for NV centers and [(b)] typical distances between quantum dots.

	Natural atoms		**Artificial atoms**	
	Neutral atoms	Trapped ions	Supercond. circuits	Spins in solids
Energy gap	GHz (hyperfine), 10^{14} Hz (optical)	GHz (hyperfine), 10^{14} Hz (optical)	$1-10$ GHz	GHz, 10^{13} Hz
Photon	Optical, MW	Optical, MW	MW	Optical, MW, infrared
Dimension	~ 2 Å	~ 2 Å	$\sim \mu$m	$\sim$ nm
Distance between qubits	< 1 μm	~ 5 μm	$\sim \mu$m	~ 10 nm [(a)], ~ 100 nm [(b)]
Operating temperature	nK$-$ μK	μK $-$ mK	$\sim$ mK	mK $-$ 300 K
Qubit interactions	Collisions, exchange	Coulomb	Capacitive, inductive	Coulomb, exchange, dipolar
Cooling	Doppler, Sisyphus, evaporative	Doppler, sideband	Cryogenic	Cryogenic
Cavity	Optical, MW	Optical, vib. modes	Transmission line, LC circuit	Optical, MW

Natural and artificial atoms for quantum computation

	Natural atoms		**Artificial atoms**	
	Neutral atoms	Trapped ions	Supercond. circuits	Spins in solids
# entangled qubits	2 [a]	14	3 (4 [b])	1 (3 [c])
One-qubit gates fidelity	99%	99%	99%	$> 73\%$ ($> 99\%$ [c])
Two-qubit gates fidelity	$> 64\%$	99.3%	$> 90\%$	90% [c]
Entangled states	Bell	Bell, GHZ, W, cat	Bell, GHZ [i] W, cat	GHZ [c]
Measurement efficiency	99.9%	99.9%	$> 95\%$	99%
T_1	$\sim$ s	~ 100 ms [d] > 20 ms [e]	10 μs	~ 1 s [f]
T_2	~ 40 ms	1000 s [g]	20 μs	200 μs [f]
Q_1	$\sim 10^4$	$\sim 10^{13}$	$\sim 10^5$	$\sim 10^3 - 10^4$ (10^6 [c])
Q_2	$\sim 4 \times 10^4$	$2 \times 10^2 - 2 \times 10^3$ $\sim 2 \times 10^4$	> 100	tbd
Interfaceable with	photons, SC circuits	photons, SC circuits	photons, atoms, ions	photons

Recent reviews on Superconducting qubits and related topics

- ✓ Superconducting qubits featured in nine pages in Nature: You & Nori, Nature (June 30, 2011).

- ✓ Current status of all qubits for quantum computation: Reports on Progress in Physics (2011).

- ✓ Systematic study of quantum interferometry using superconducting qubit circuits: Phys. Reports (2010).

- ✓ Quantum Simulators: Buluta & Nori, Science (2009). And long preprint 2011.

- ✓ How to quantify entanglement with many qubits: Physics Reports, over 100 pages (2011).

2 OCTOBER 2009 VOL 326 SCIENCE www.sciencemag.org

Quantum Simulators

Iulia Buluta[1] and Franco Nori[1,2*]

Quantum simulators are controllable quantum systems that can be used to simulate other quantum systems. Being able to tackle problems that are intractable on classical computers, quantum simulators would provide a means of exploring new physical phenomena. We present an overview of how quantum simulators may become a reality in the near future as the required technologies are now within reach. Quantum simulators, relying on the coherent control of neutral atoms, ions, photons, or electrons, would allow studying problems in various fields including condensed-matter physics, high-energy physics, cosmology, atomic physics, and quantum chemistry.

I. Georgescu and F. Nori, long preprint (2011)

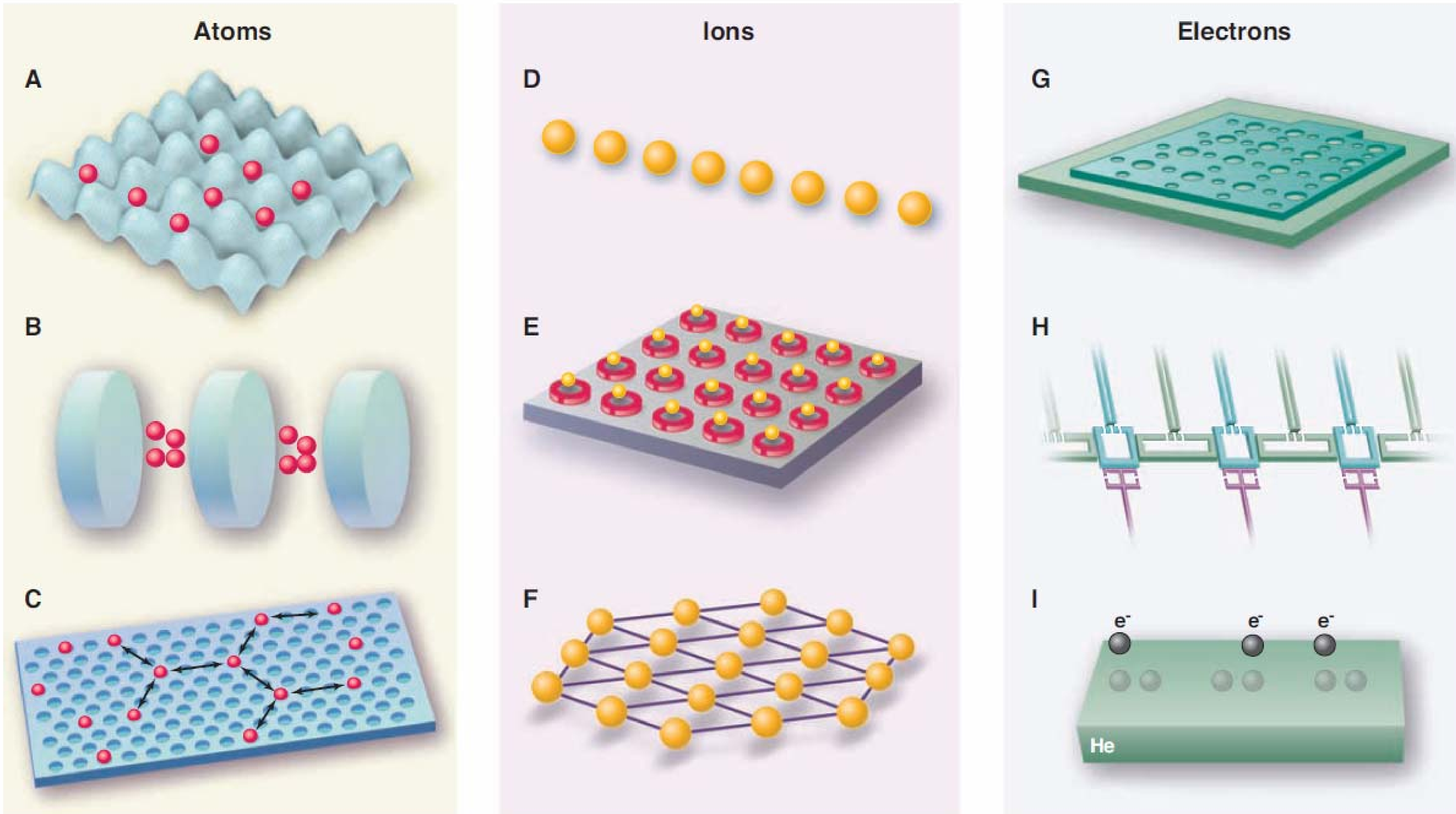

Buluta and Nori, Science (2009); Georgescu and Nori, long preprint (2011).

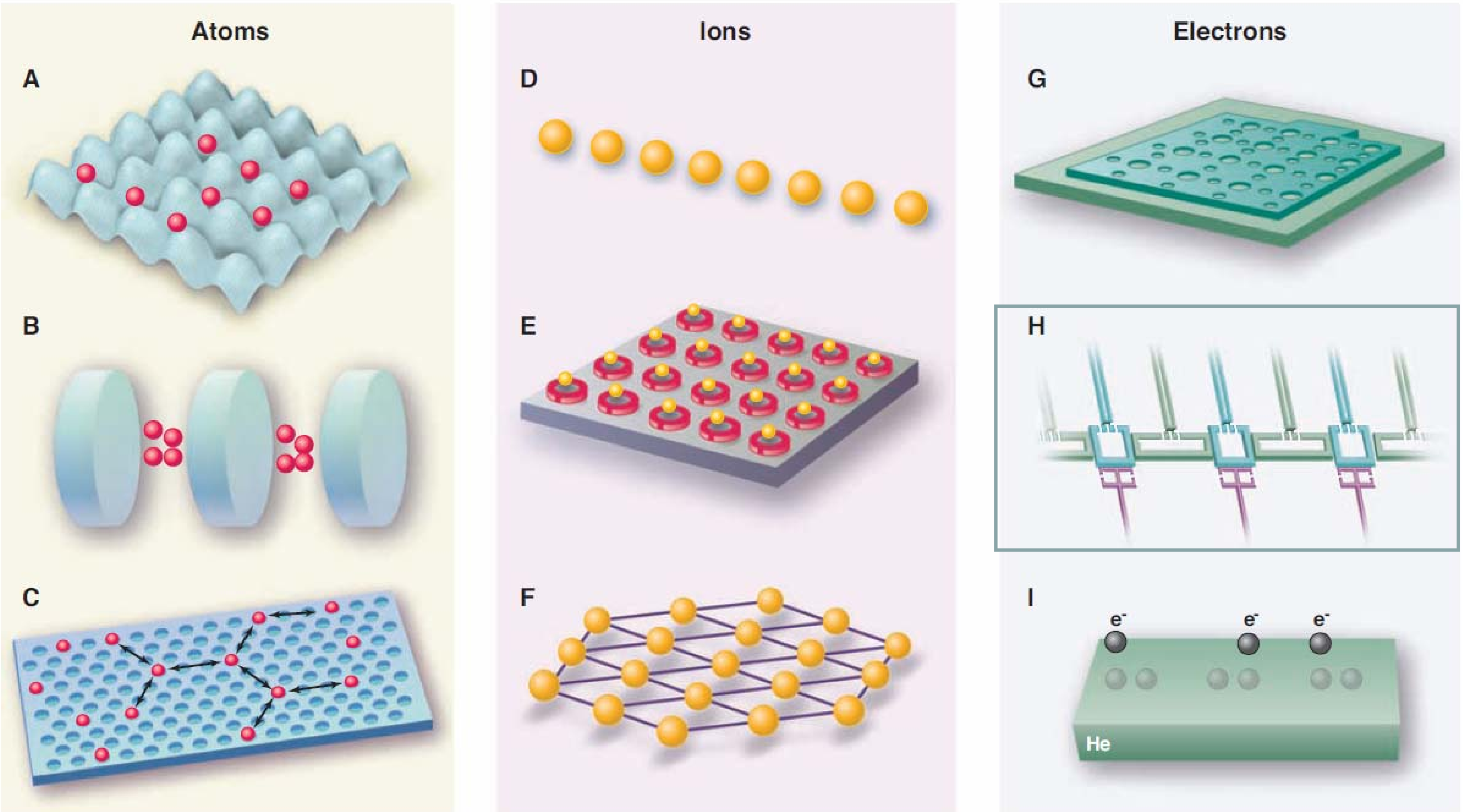

Buluta and Nori, Science (2009); Georgescu and Nori, long preprint (2011).

You, Shi, Nori,
Topological states and braiding statistics using quantum circuits**,**
arXiv:0809.0051v1 (2008).

Shi, Yu, You, Nori,
Topological quantum phase transition in an extended Kitaev spin model,
Phys. Rev. B 79, 134431 (2009).

You, Shi, Hu, Nori,
Quantum emulation of a spin system with topologically protected ground states using superconducting quantum circuits,
Phys. Rev. A 81, 063823 (2010).

PHYSICAL REVIEW B **81**, 014505 (2010)

Quantum emulation of a spin system with topologically protected ground states using superconducting quantum circuits

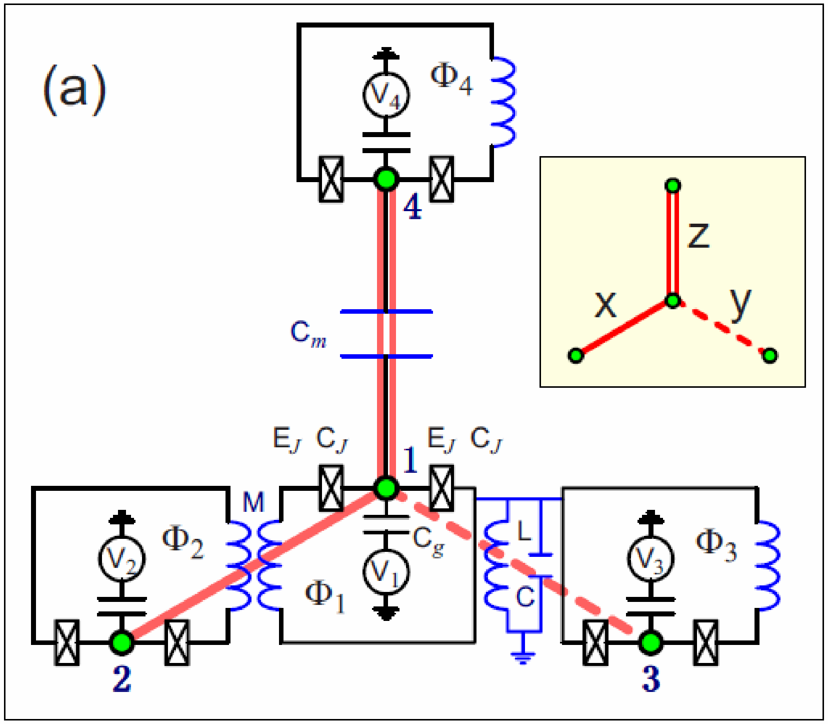

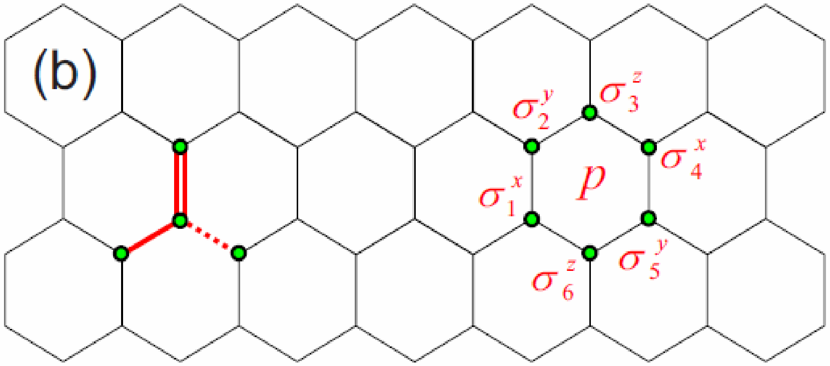

F. Nori, *Quantum football*, Science **325**, 689 (2009).

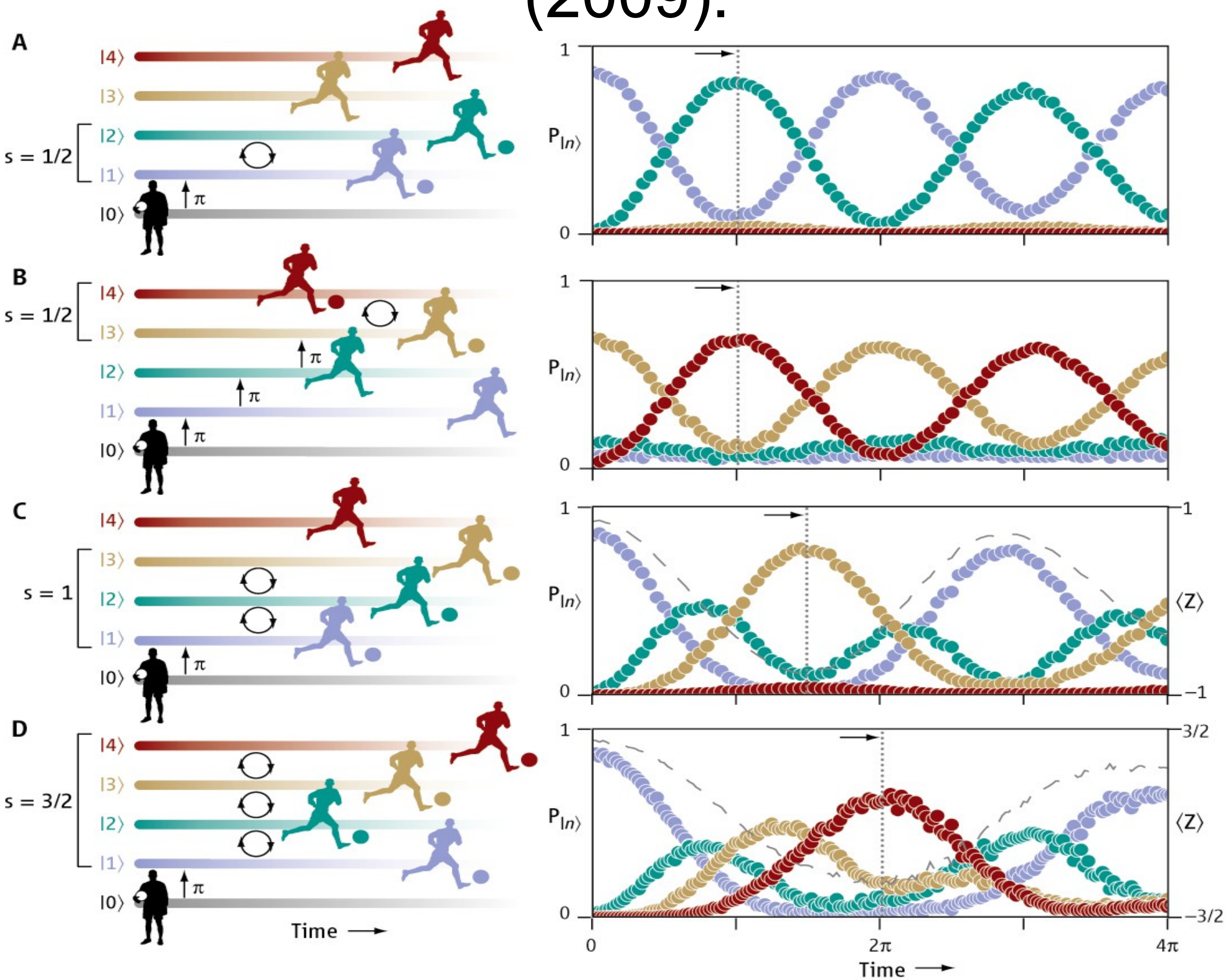

Recent reviews on Superconducting qubits and related topics

- ✓ **Superconducting qubits featured in nine pages in Nature: You & Nori, Nature (June 30, 2011).**

- ✓ **Current status of all qubits for quantum computation: Reports on Progress in Physics (2011).**

- ✓ **Systematic study of quantum interferometry using superconducting qubit circuits: Phys. Reports (2010).**

- ✓ **Quantum Simulators: Buluta & Nori, Science (2009). And long preprint 2011.**

- ✓ **How to quantify entanglement with many qubits: Physics Reports, over 100 pages (2011).**

Model
(driven two-level system)

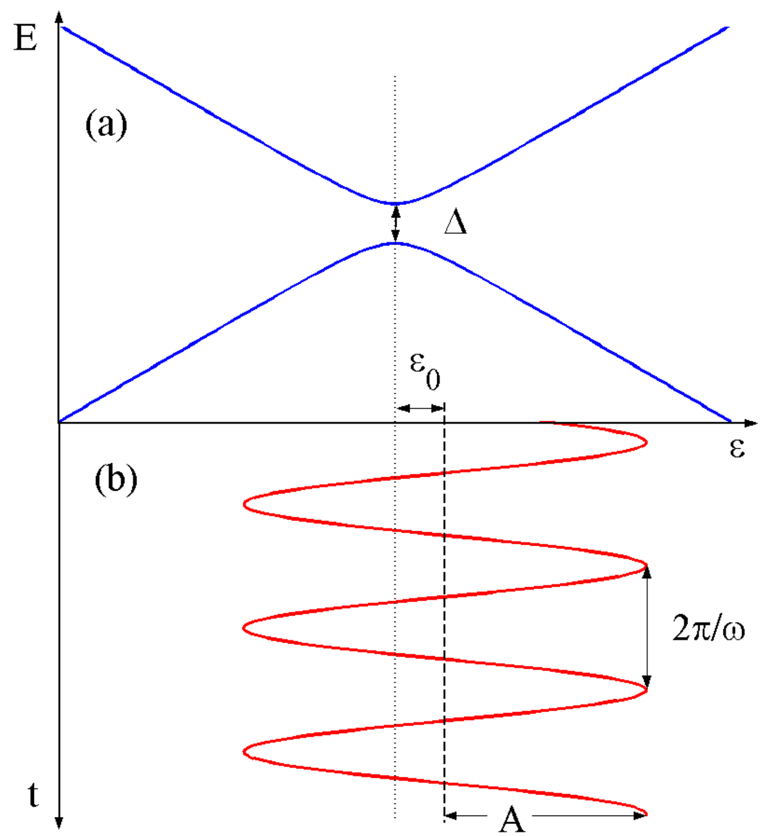

$$\hat{H} = -\frac{\Delta}{2}\hat{\sigma}_x - \frac{\varepsilon_0 + A\cos(\omega t + \phi)}{2}\hat{\sigma}_z$$

Model
(driven two-level system)

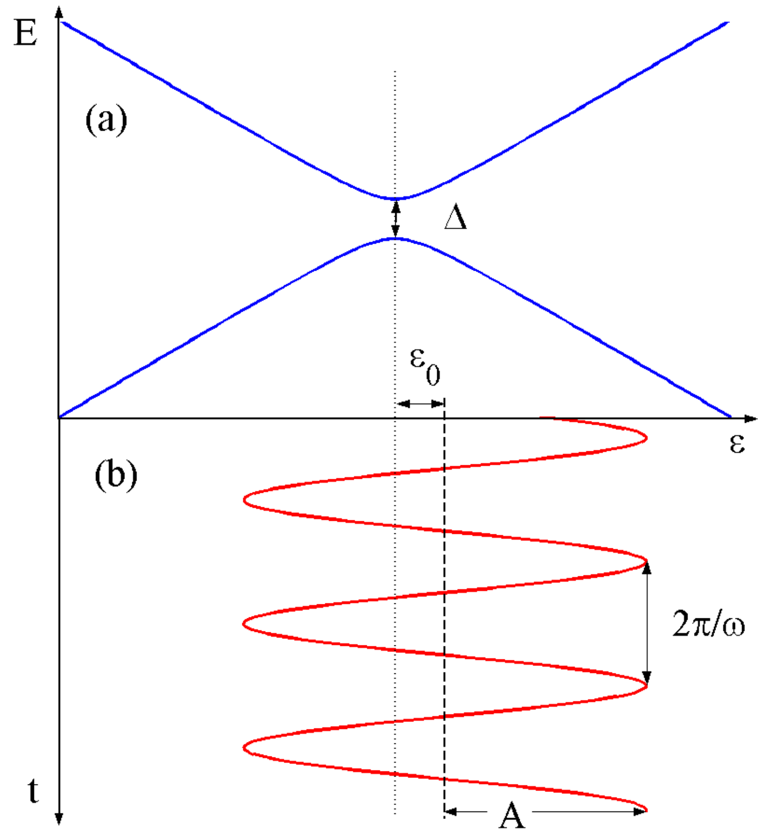

Treat as variable parameters.

$$\hat{H} = -\frac{\Delta}{2}\hat{\sigma}_x - \frac{\varepsilon_0 + A\cos(\omega t + \phi)}{2}\hat{\sigma}_z$$

Recent experiments

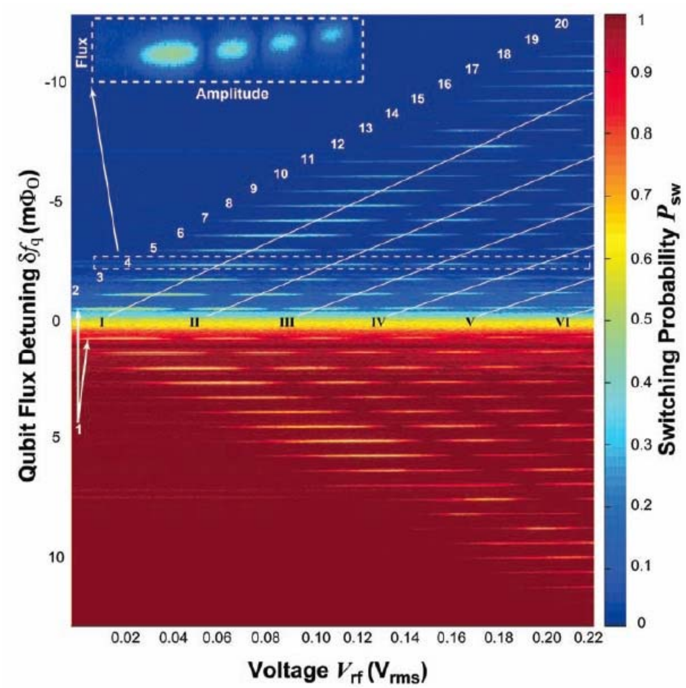

Oliver *et al.*, Science (2005)

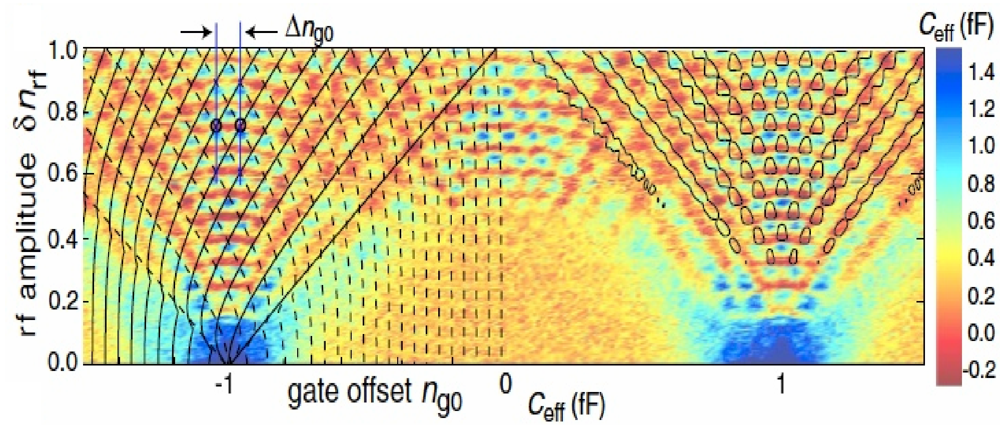

Sillanpää *et al.*, PRL (2006)

Izmalkov *et al.*,
PRL (2008)

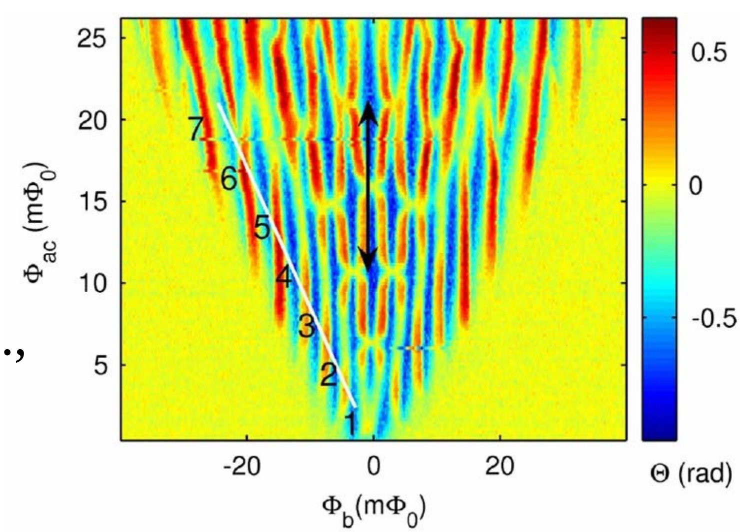

Interference in a single cycle: constructive or destructive

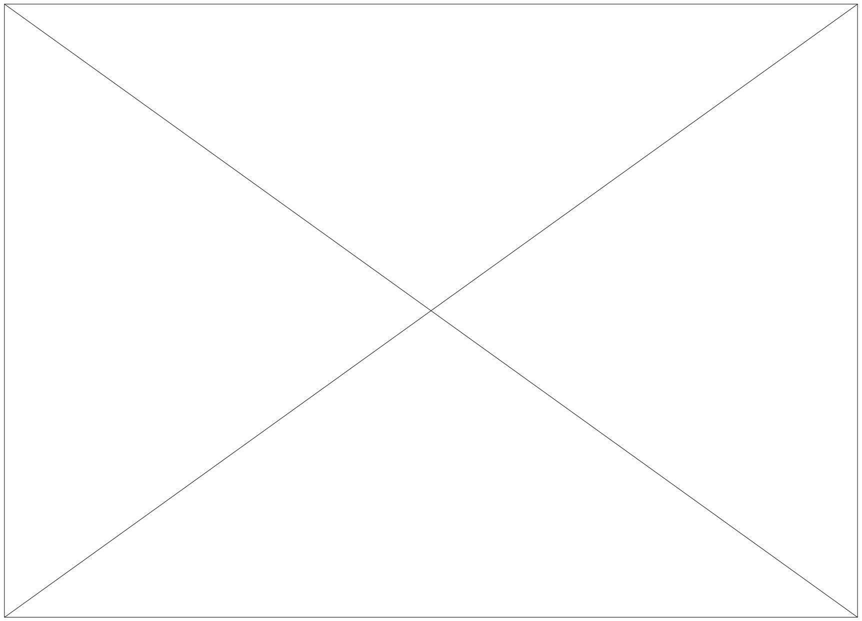

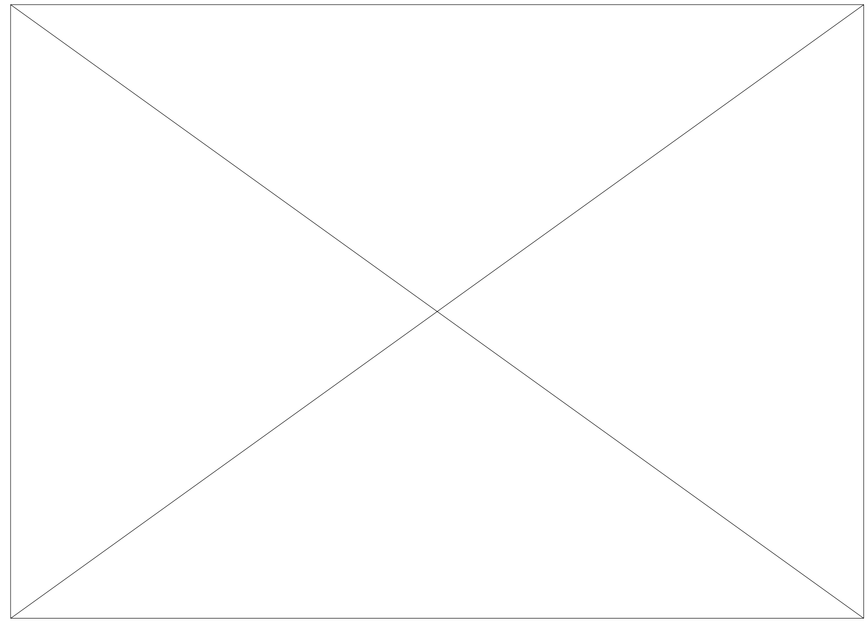

Constructive interference between successive LZ crossings (within one driving period).

Full oscillations

Destructive interference between successive LZ crossings (within one driving period).

No oscillations

Interference between LZ crossings:
constructive or destructive

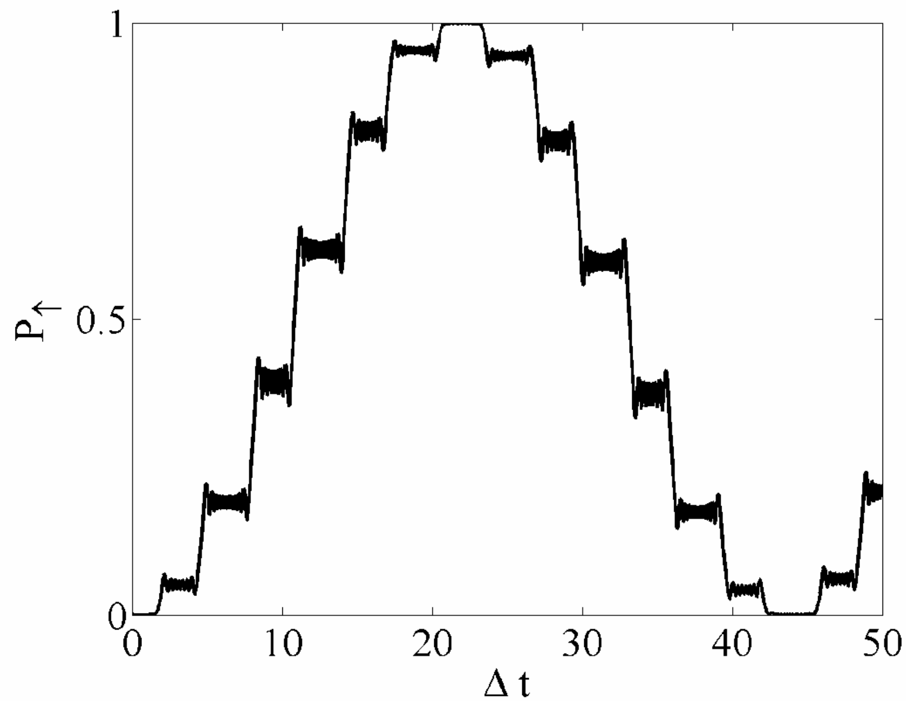

Successive LZ crossings add up coherently and constructively.

⇨ Nice oscillations

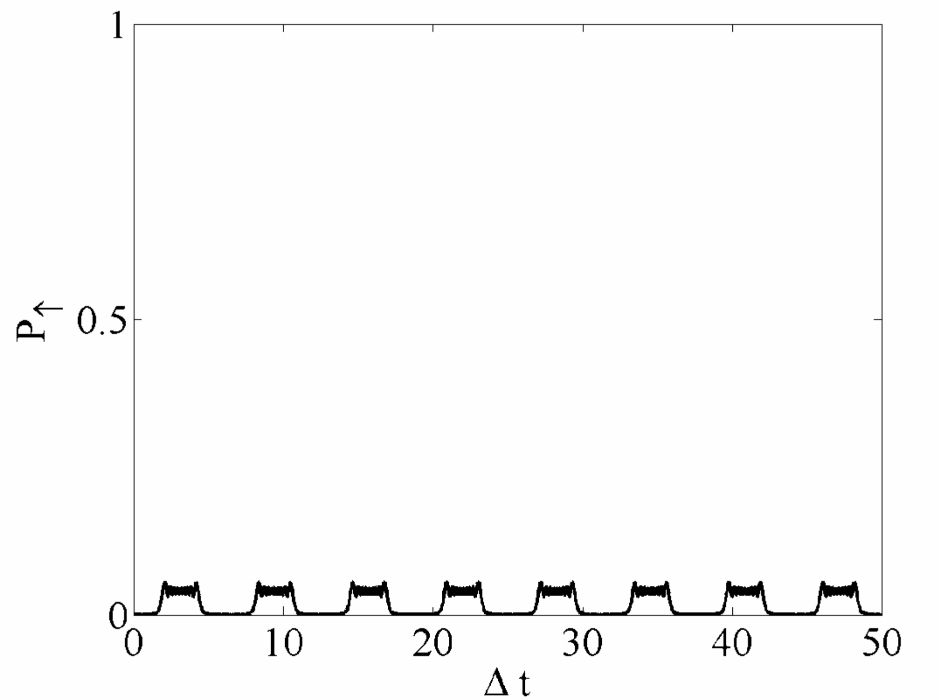

Successive LZ crossings in a single cycle cancel each other.

⇨ No oscillations

LANDAU-ZENER-STUCKELBERG INTERFEROMETRY

Dependence of the tank voltage phase shift on the *dc* flux bias Φ_{dc} and the *ac* flux amplitude Φ_{ac} (the microwave amplitude)

theory

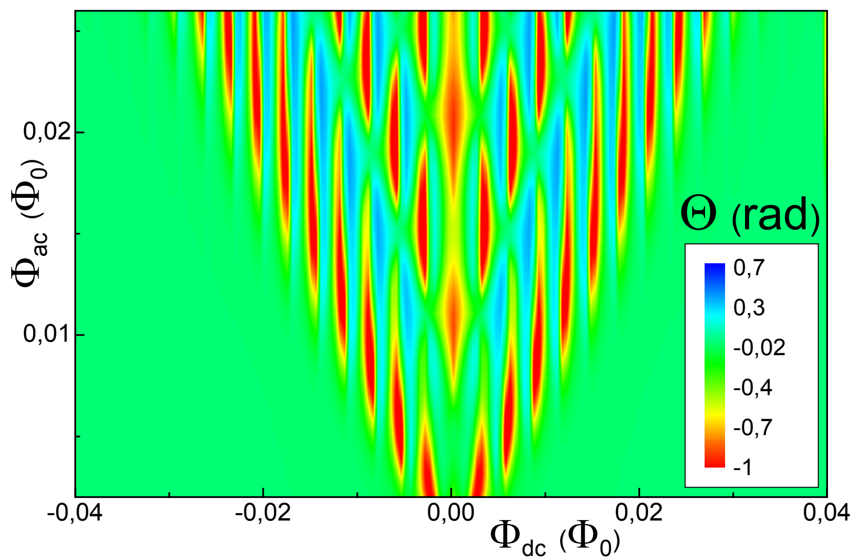

experiment

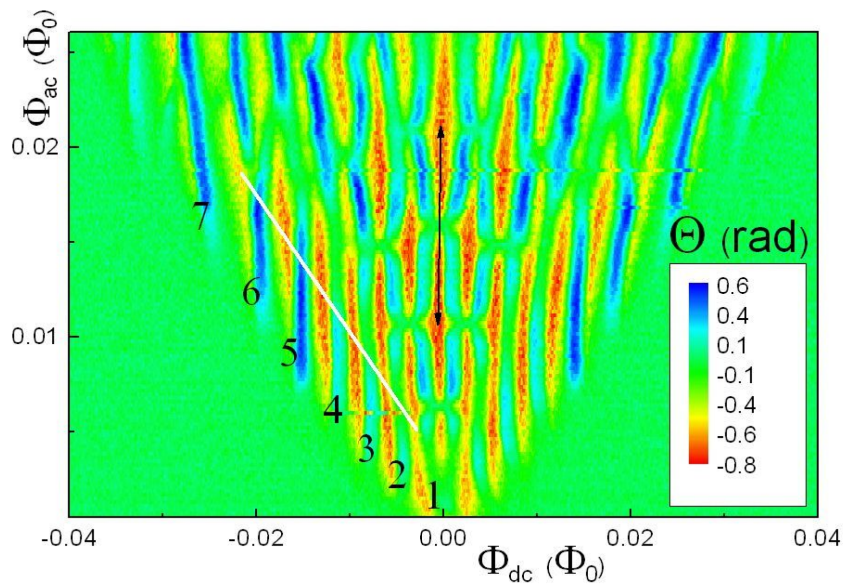

Izmalkov et al., PRL **101**, 017003 (2008)

- multiphoton resonances: $\Delta E(\Phi_{dc}) \approx n \cdot \hbar\omega$
- Stückelberg oscillations
- calibration of the driving power

MACH-ZEHNDER INTERFEROMETRY IN A FLUX QUBIT

[Oliver, Yu, Lee, Berggren, Levitov, Orlando, Science **310**, 1653 (2005)]

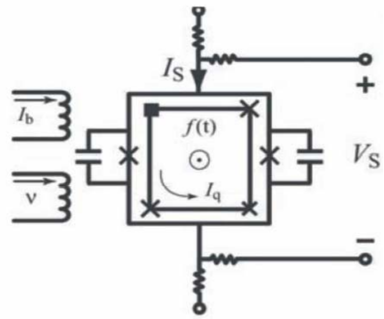

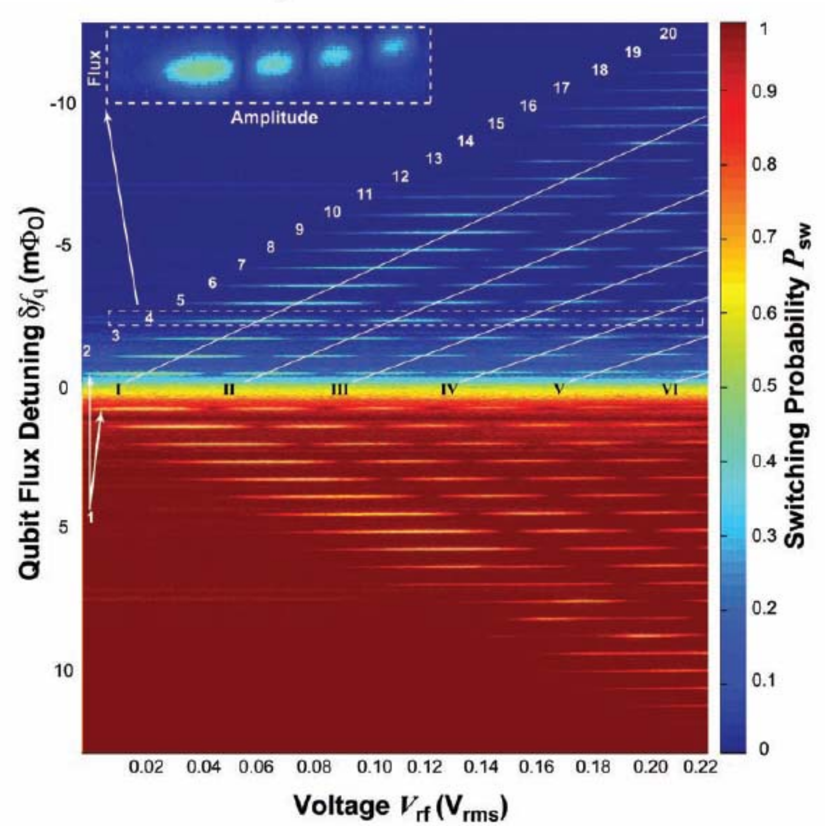

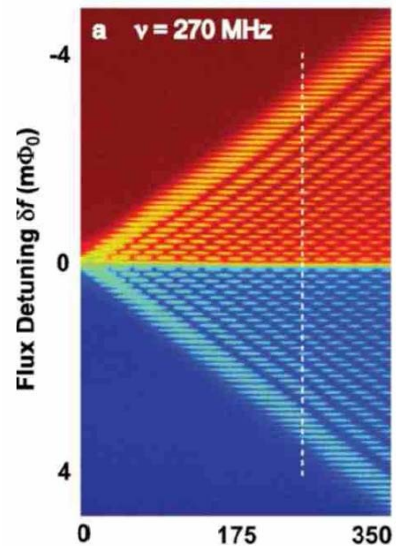

n=45

PRL **97**, 150502 (2006)

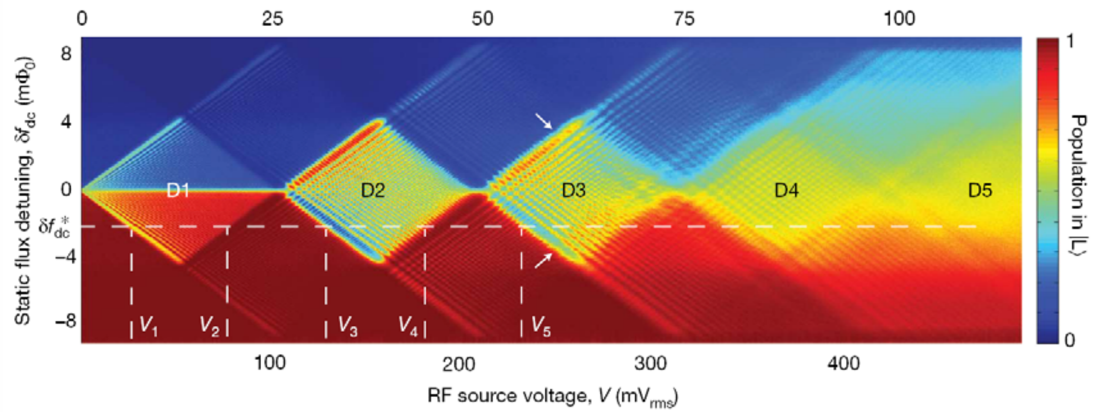

Nature **455**, 51 (2008)

driving amplitude

LZ INTERFERENCE IN A COOPER-PAIR BOX

[Sillanpaa, Lehtinen, Paila, Makhlin, Hakonen, PRL **96** 187002 (2006)]

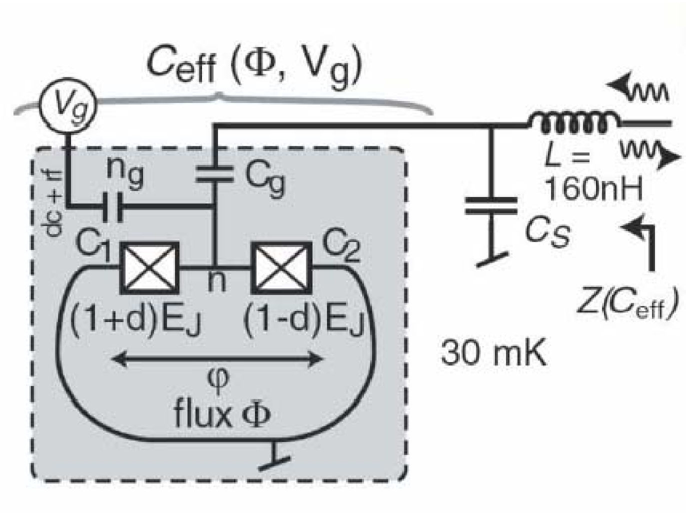

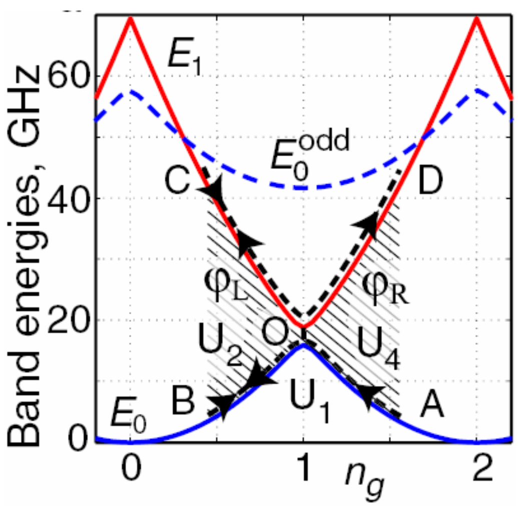

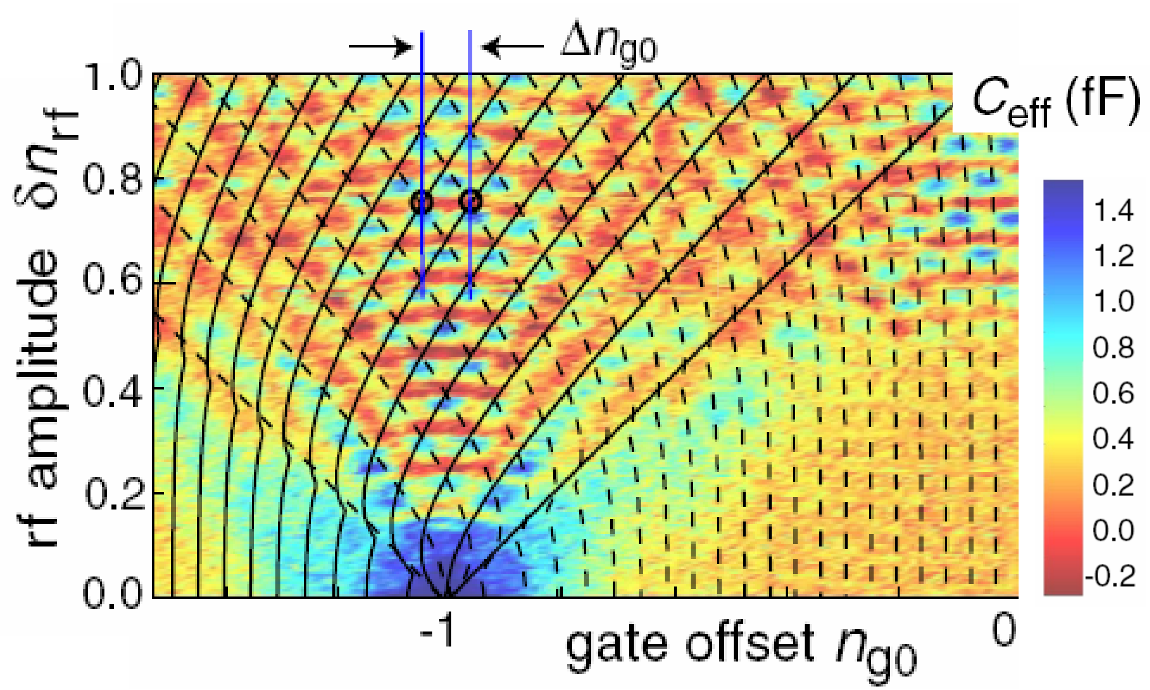

COHERENCE TIMES OF DRESSED STATES OF A SUPERCONDUCTING QUBIT UNDER EXTREME DRIVING

[Wilson, Duty, Persson, Sandberg, Johansson, and Delsing, PRL **98**, 257003 (2007)]

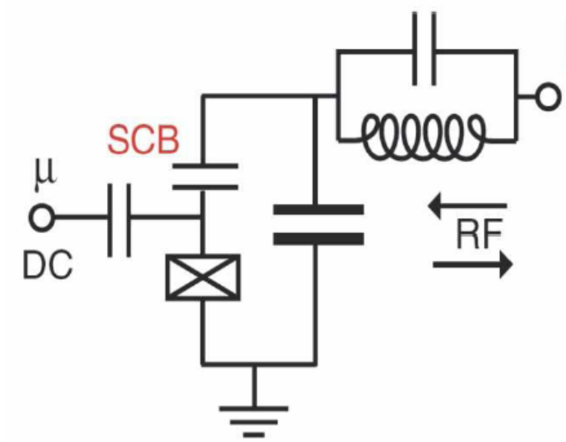

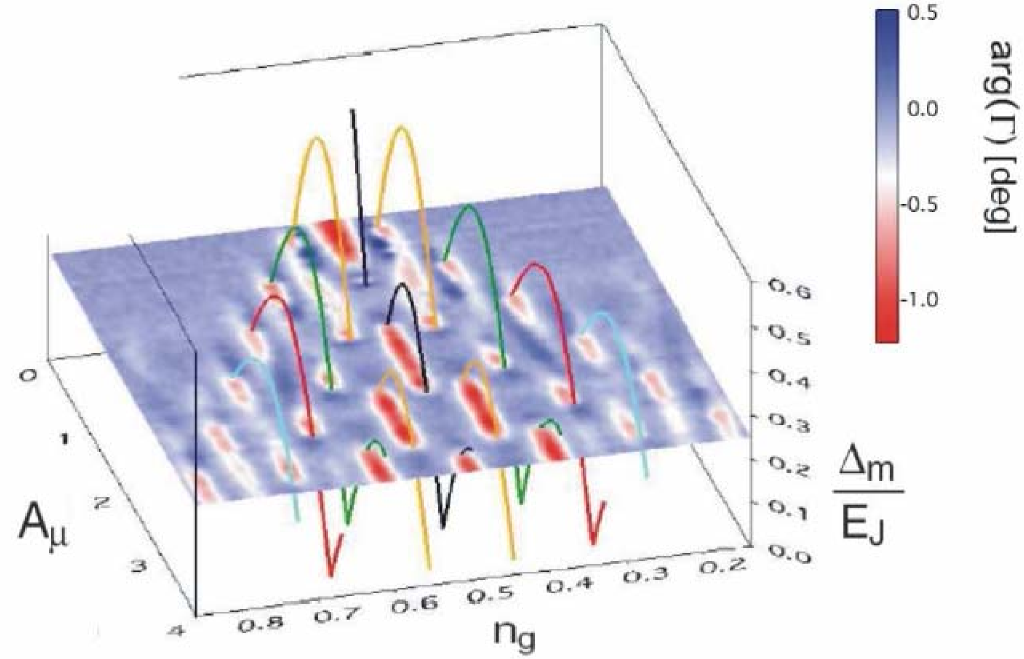

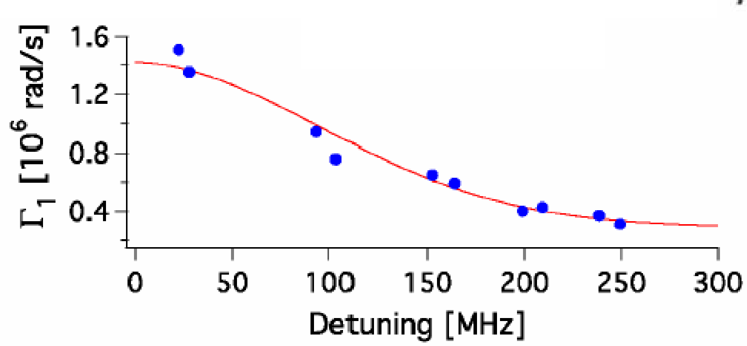

APPLIED PHYSICS LETTERS 94, 102502 (2009)

Population inversion induced by Landau–Zener transition in a strongly driven rf superconducting quantum interference device

Guozhu Sun,[1,a)] Xueda Wen,[2] Yiwen Wang,[2] Shanhua Cong,[1] Jian Chen,[1] Lin Kang,[1] Weiwei Xu,[1] Yang Yu,[2,b)] Siyuan Han,[1,3] and Peiheng Wu[1]
[1]*Department of Electronic Science and Engineering, Research Institute of Superconductor Electronics, Nanjing University, Nanjing 210093, People's Republic of China*
[2]*Department of Physics, National Laboratory of Solid State Microstructures, Nanjing University, Nanjing 210093, People's Republic of China*
[3]*Department of Physics and Astronomy, University of Kansas, Lawrence, Kansas 66045, USA*

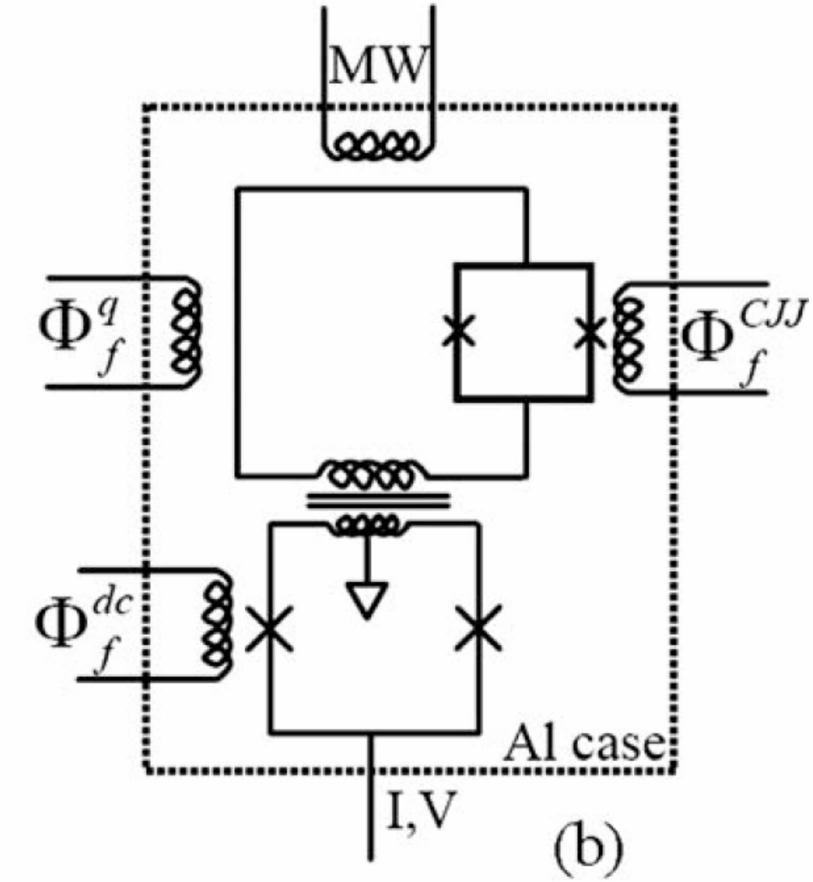

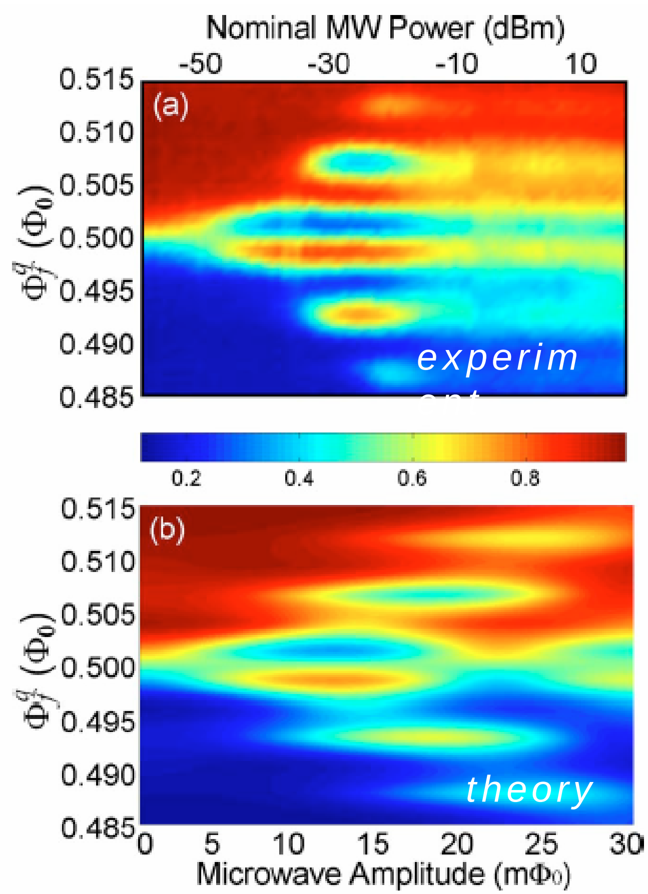

"Gigahertz Dynamics of a Strongly Driven Single Quantum Spin",
G. D. Fuchs, V. V. Dobrovitski, D. M. Toyli, F. J. Heremans, and D. D. Awschalom,
Science 326, 1520 (2009).

Related article: "A Strongly Driven Spin", Science 326, 1489 (2009)

The counterrotating field has negligible impact on the spin dynamics provided that it is small compared with [the Larmor field] H_0 because the direction of the torque it applies on the spin varies rapidly in time and therefore averages out.

This argument forms the basis of the rotating wave approximation (15) and is the cornerstone of both theory and experiment for nearly all two-level resonance phenomena.

In the “strong-driving” regime, where the rotating fields have amplitudes roughly equal to H_0, the spin dynamics are predicted (16, 17) to become highly anharmonic as the co- and counter-rotating fields generate dynamics on the same time scale as the Larmor precession.

These dynamics are not chaotic, but they are also not a small modulation of sinusoidal Rabi oscillations seen in classical systems (18).

We experimentally examined these dynamics in a single quantum spin at room temperature by using an NV center in diamond driven by an oscillating field through an on-chip waveguide.

This regime has been of strong theoretical interest on fundamental grounds (16, 17) and in the context of optimal control theory (19–21).

Rather than avoiding the effects of the counter-rotating field, we studied its influence on a single spin where the dynamics can be transparently interpreted.

"Gigahertz Dynamics of a Strongly Driven Single Quantum Spin",
G. D. Fuchs, V. V. Dobrovitski, D. M. Toyli, F. J. Heremans, and D. D. Awschalom,
Science 326, 1520 (2009).

Related article: "A Strongly Driven Spin", Science 326, 1489 (2009)

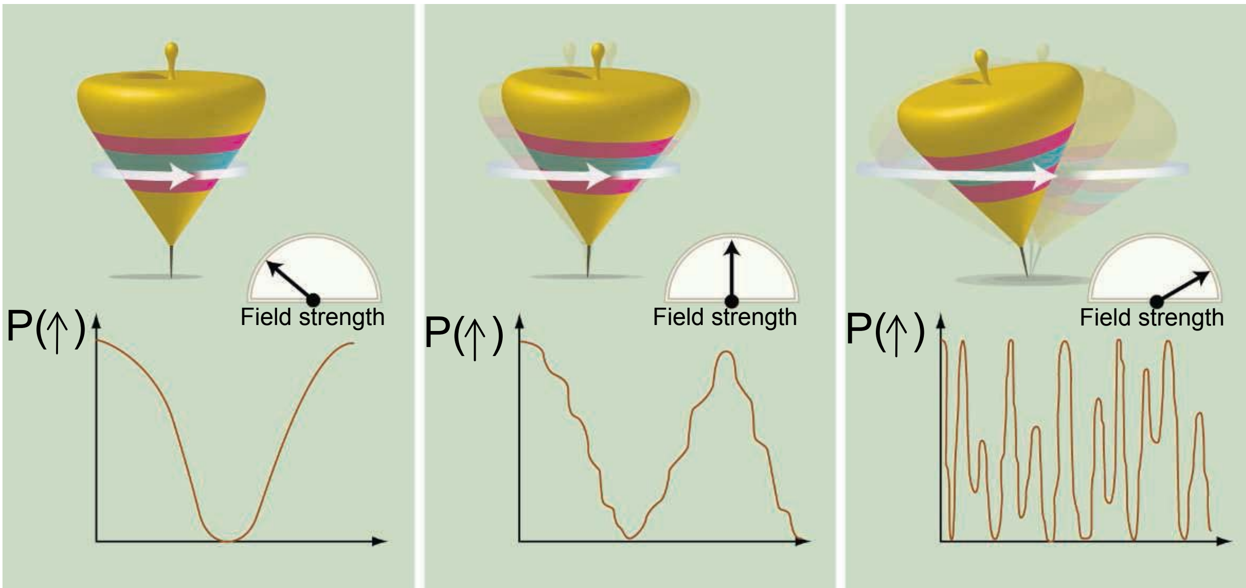

Ashhab et al *PRA* (2004) and Shevchenko et al *Phys. Reports* (2010)

Dynamics of spinning tops and resonantly driven electrons.

(A and B) Most studies involving two-level system manipulation are performed with driving field strengths H_1 that are much weaker relative to the energy difference between the levels.

In this regime, the two-level dynamics correspond to that of a fictitious spinning top, whose rotation frequency is proportional to H_1. For an electron spin in an external magnetic field, the spin population [expressed as the population of spin up, P(↑)], either varies smoothly (A) or exhibits small variations corresponding to the top slightly wobbling (B).

(C) Fuchs et al. explored the regime of an electron spin where H_1 is comparable to the energy difference of the spin states. The complex dynamics correspond to a highly unstable spinning top.

However, the inherently faster spin dynamics potentially allow much faster control. In their experiment, the spin could be controllably flipped in less than 1 ns.

COHERENT BEAM SPLITTER FOR ELECTRONIC SPIN STATES

[Petta, Lu, Gossard, Science **327**, 669 (2010), Burkard, *ibid.*, **327**, 650 (2010)]

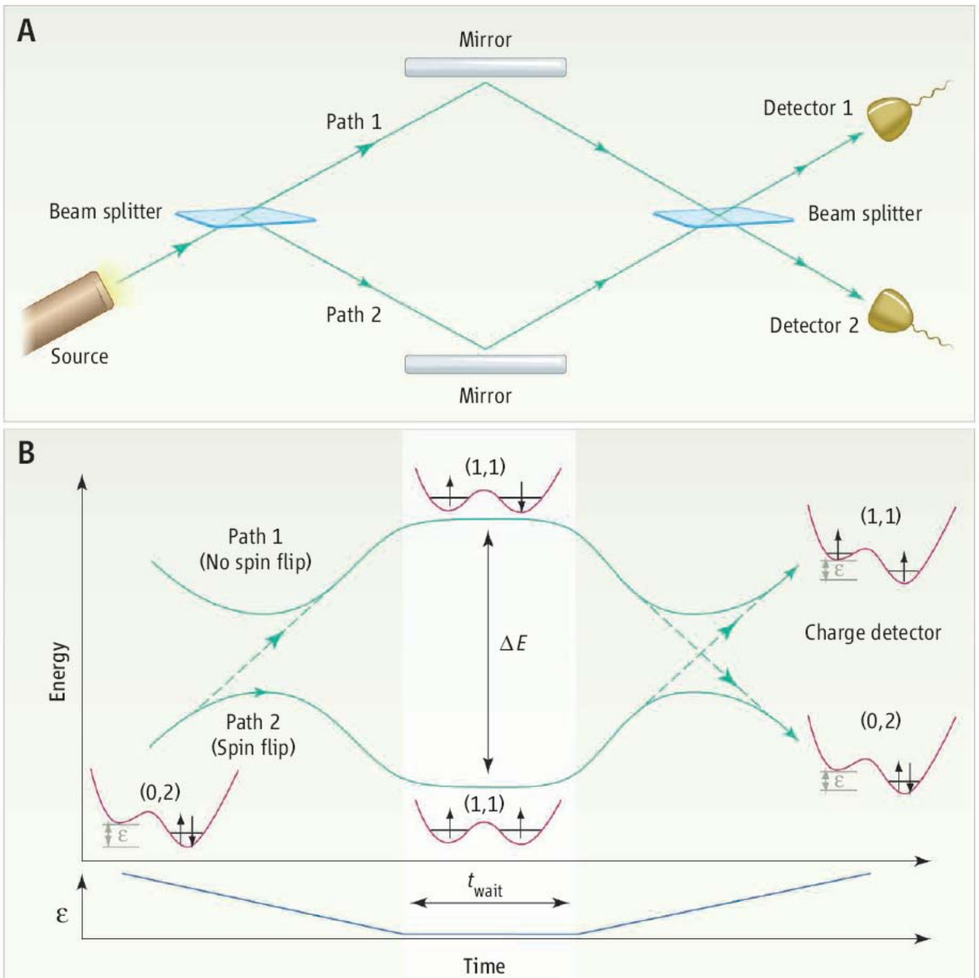

optical (Mach-Zehnder) interferometer

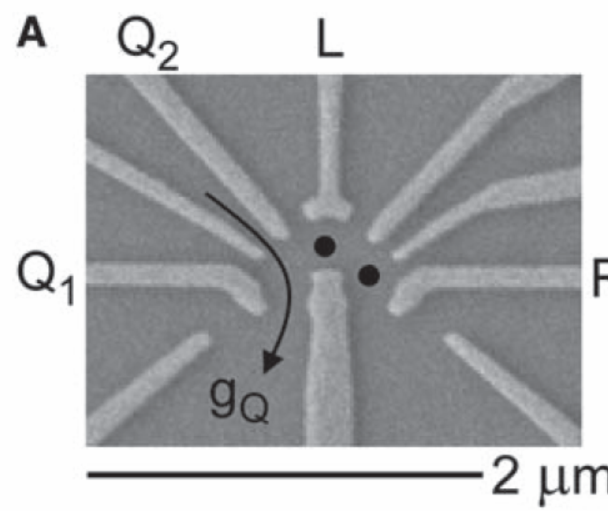

Electronic spin state (Landau-Zener-Stuckelberg) interferometer

NANOMECHANICAL MEASUREMENTS OF A SUPERCONDUCTING QUBIT

[LaHaye, Suh, Echternach, Schwab & Roukes, Nature **459**, 960 (2009)]

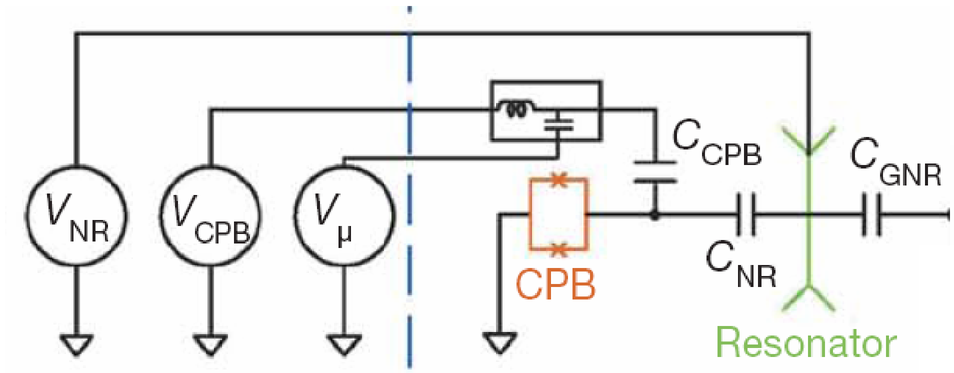

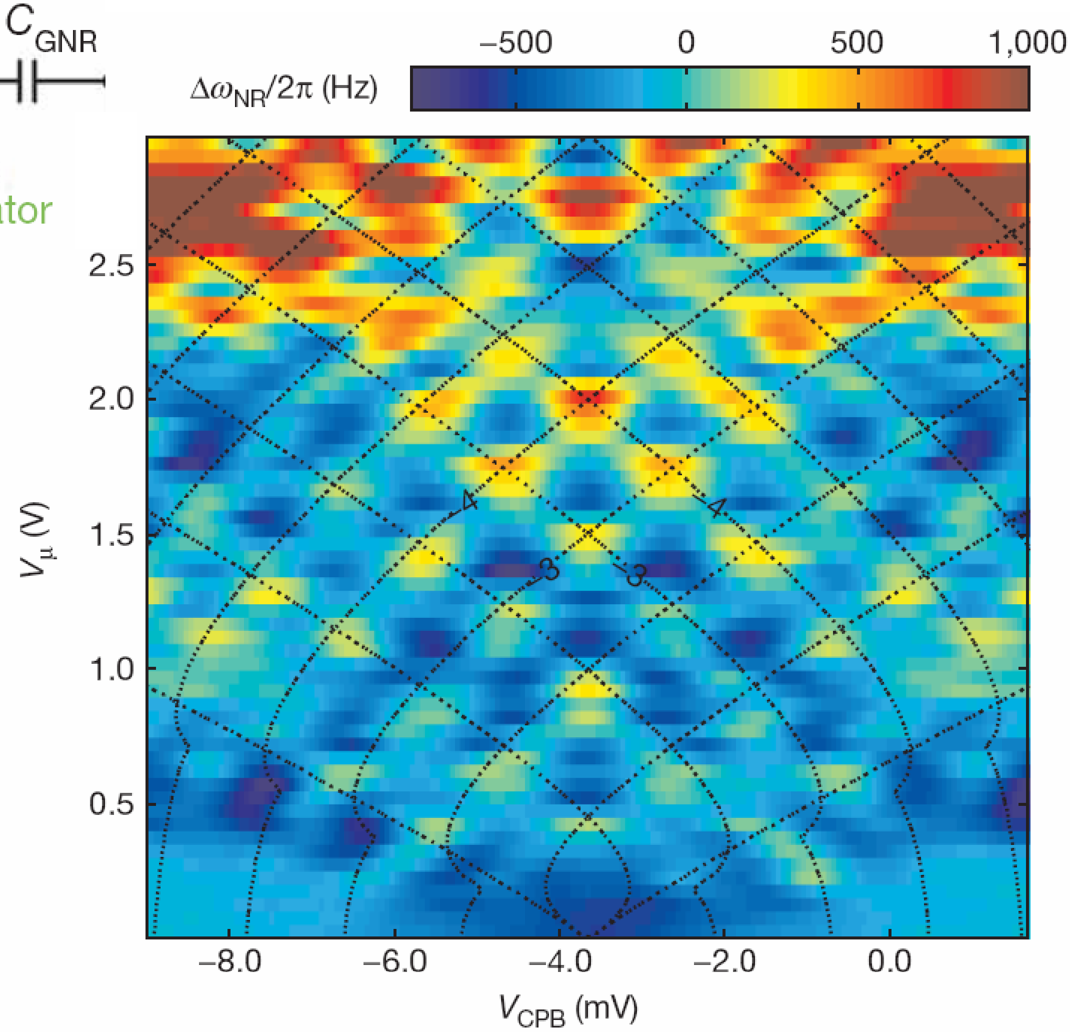

STRONGLY-DRIVEN REGIME: QUALITATIVE DESCRIPTION

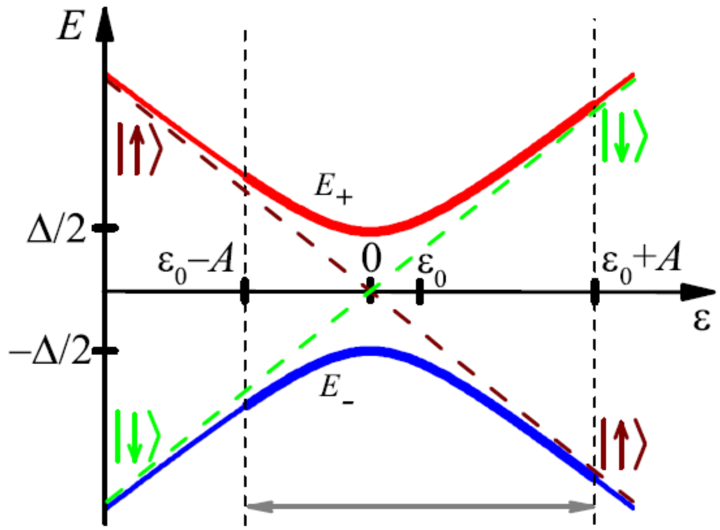

$$H = -\frac{\Delta}{2}\sigma_x - \frac{\varepsilon(t)}{2}\sigma_z$$

$$\varepsilon(t) = \varepsilon_0 + A\sin\omega t$$

$$\Delta\theta = \oint \left(E_\uparrow(t) - E_\downarrow(t)\right) dt = \int_0^{2\pi/\omega} \varepsilon(t) dt = \varepsilon_0 \frac{2\pi}{\omega} = 2\pi k$$

$$\Delta_k \ = \ \Delta J_k\left(\frac{A}{\omega}\right)$$

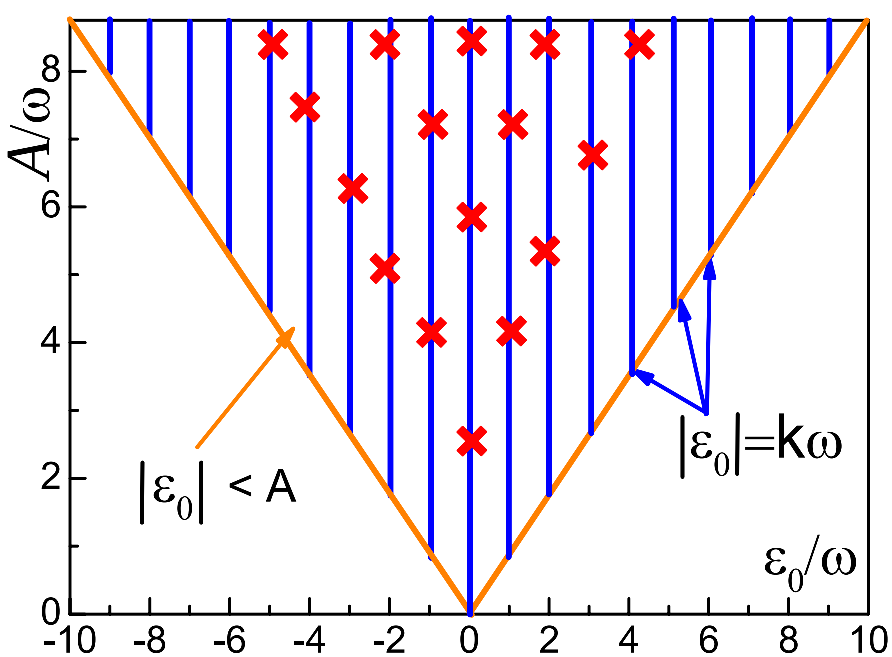

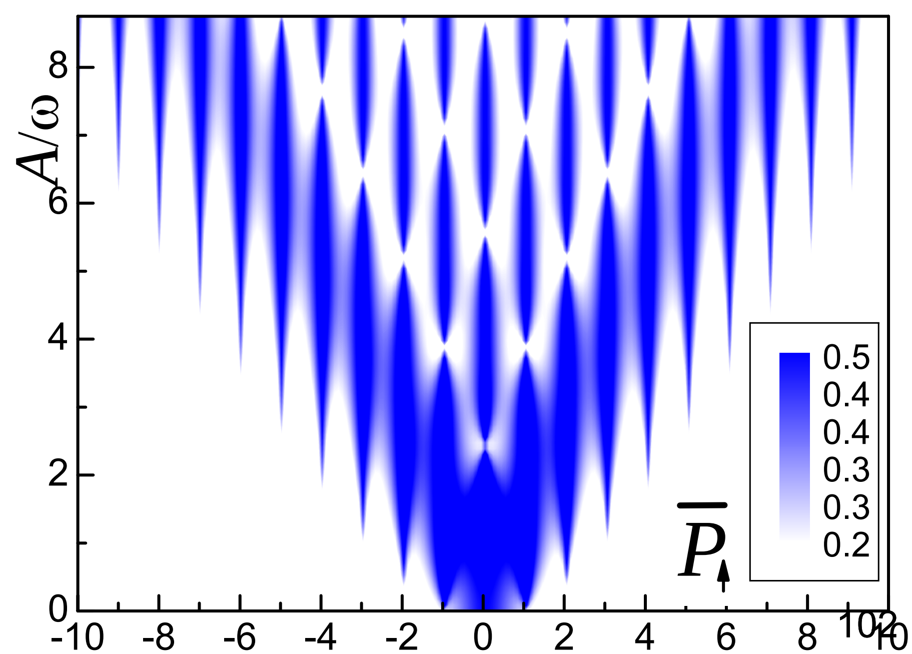

Table 1

Parameters used in different experiments studying LZS interferometry: tunneling amplitude Δ, maximal driving amplitude $A^{\max}$, and driving frequency ω in the units $\mathrm{GHz}\times 2\pi$, minimal adiabaticity parameter $\delta^{\min} = \Delta^2/(4\omega A^{\max})$, and maximal LZ probability $P_{\mathrm{LZ}}^{\max} = \exp(-2\pi\delta^{\min})$.

	Δ	$A^{\max}$	ω	$\delta^{\min}$	$P_{\mathrm{LZ}}^{\max}$
(Oliver et al., 2005)	0.004	24	1.2	10^{-7}	1
(Sillanpää et al., 2006)	12.5	95	4	0.1	0.5
(Wilson et al., 2007)	2.6	62	7	0.004	0.98
(Izmalkov et al., 2008)	3.5	40	4	0.02	0.9

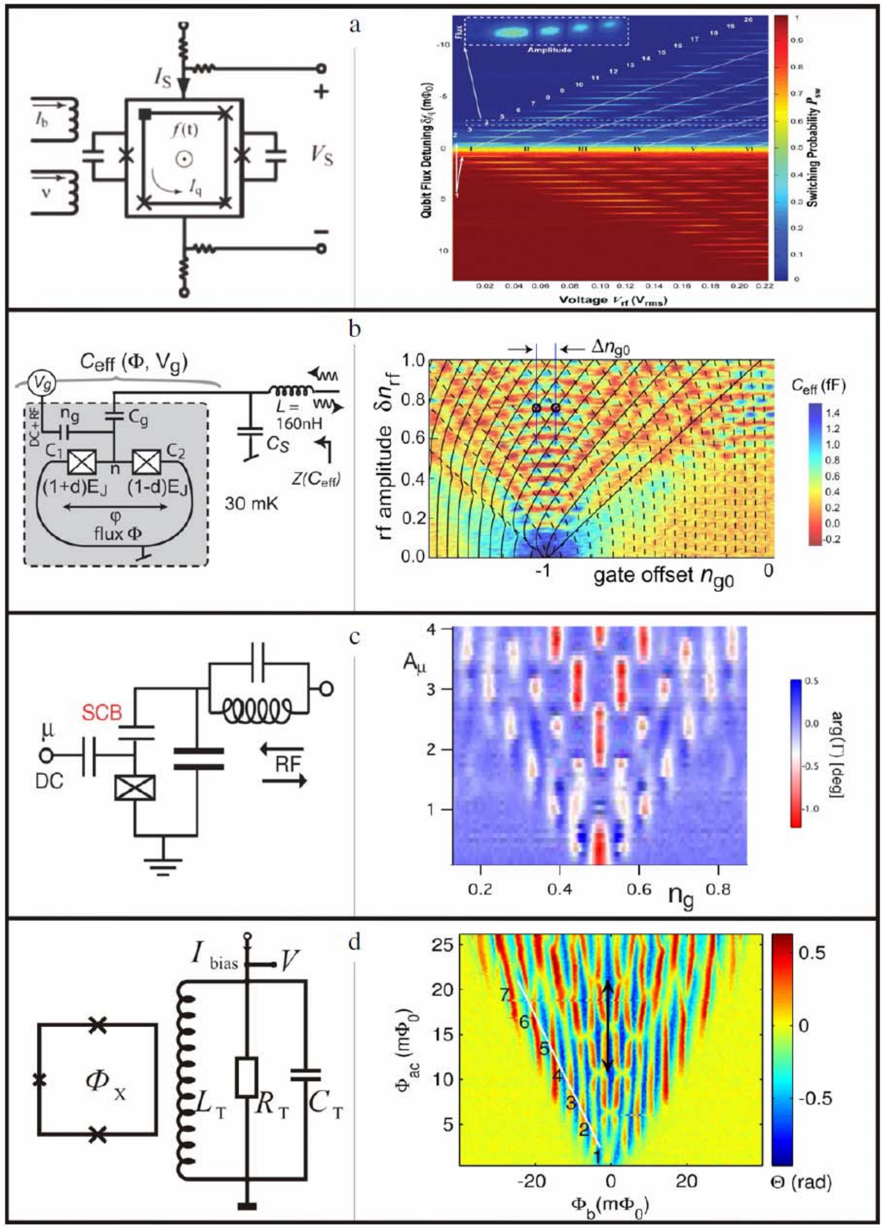

Fig. 11. (Color online) Experimentally realized Landau–Zener–Stückelberg (LZS) interferometry. The panels from top to bottom present the results of the following articles: (a) Oliver et al. (2005), (b) Sillanpää et al. (2006), (c) Wilson et al. (2007), (d) Izmalkov et al. (2008). Schematic diagrams of the circuits used are shown to the left, while results for the LZS interferometry are presented to the right. A more detailed description of the experiments can be found in the main text and, of course, in the respective original articles. Figure (a) is reprinted from Oliver et al. (2005) with permission from AAAS. Figure (b) is reprinted from Sillanpää et al. (2006) with permission; copyright (2006) by APS. Figure (c) is reprinted from Wilson et al. (2007) with permission; copyright (2007) by APS. Figure (d) is reprinted from Izmalkov et al. (2008) with permission; copyright (2008) by APS.

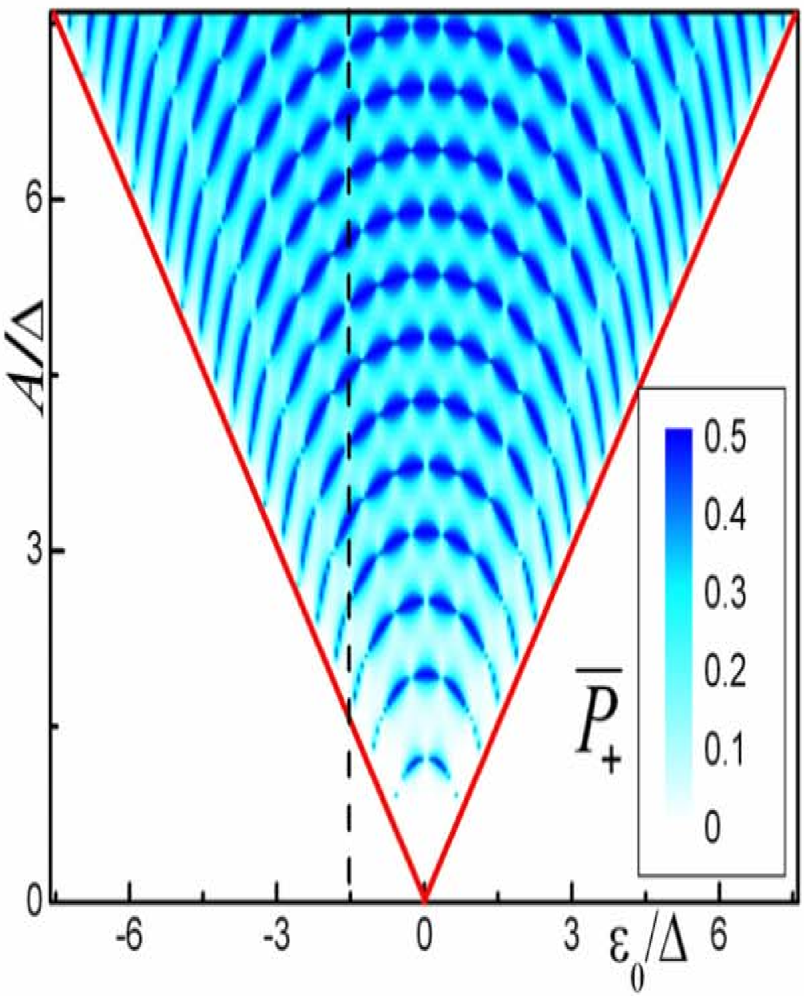

Fig. 6. (Color online) Slow-driving LZS interferometry for $A\omega \lesssim \Delta^2$. The time averaged upper level occupation probability $\overline{P_+}$ as a function of the energy bias ε_0 and the driving amplitude A. The graph is calculated with Eq. (38) for $\omega/\Delta = 0.32 < 1$. The inclined red lines mark the region of the validity of the theory: $\varepsilon_0 < A$, which means that the system experiences avoided level crossings. Outside of this region the excitation probability is negligibly small. The vertical dashed line shows the alteration of the excitation maxima and minima.

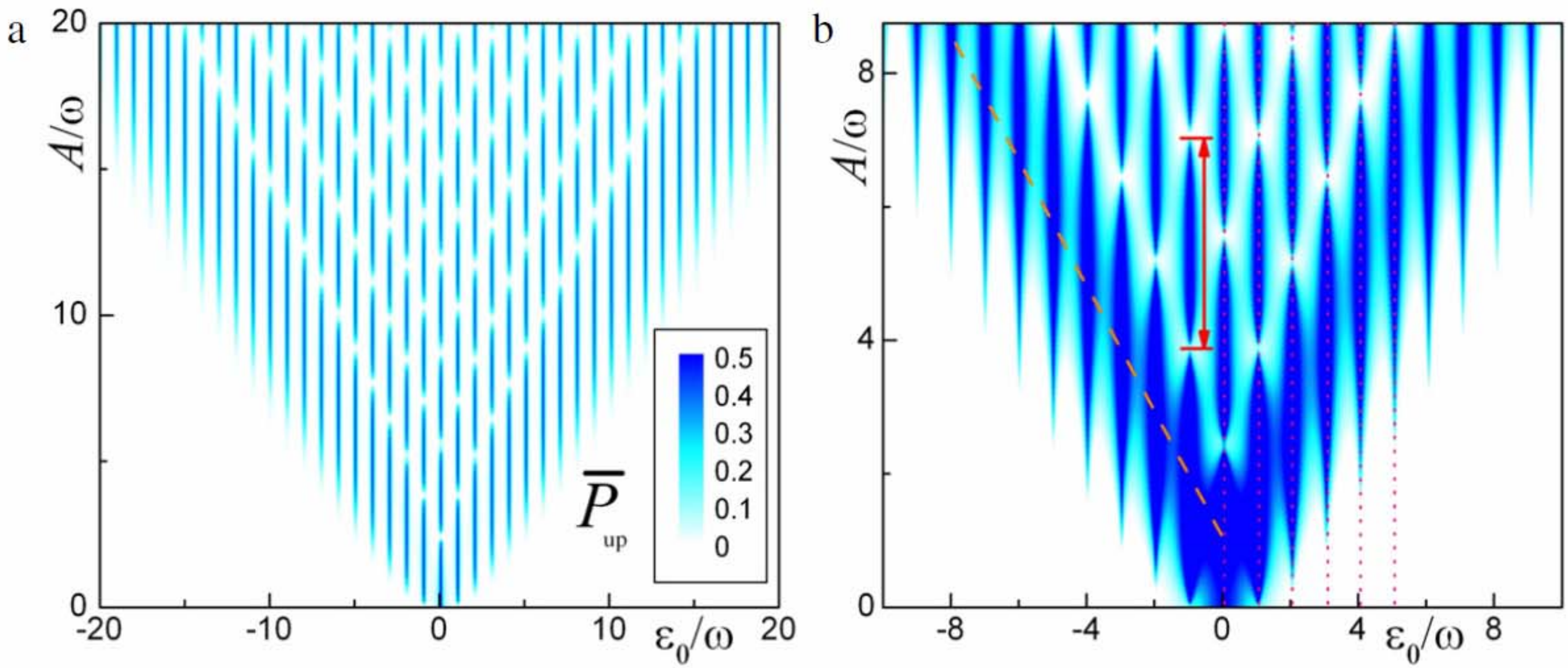

Fig. 7. (Color online) Fast-driving LZS interferometry for $A\omega \gg \Delta^2$: dependence of the time-averaged upper diabatic state occupation probability $\overline{P}_{up}$ on ε_0/ω and A/ω. The graphs are plotted using Eq. (57) for $\omega/\Delta = 300 \gg 1$, $\omega T_1/(2\pi) = 2.4 \times 10^4$ and $\omega T_2/(2\pi) = 24$ (a) and $\omega/\Delta = 1.14 > 1$, $\omega T_1/(2\pi) = \omega T_2/(2\pi) = 6$ (b). Several multiphoton resonances are shown by the vertical pink dotted lines at $\varepsilon_0 = k\omega$ (for $k = 0, 1, 2, \ldots, 5$, only) modulated by Bessel functions. The vertical red double-arrow in (b) shows the distance between two consecutive zeros of the Bessel function.

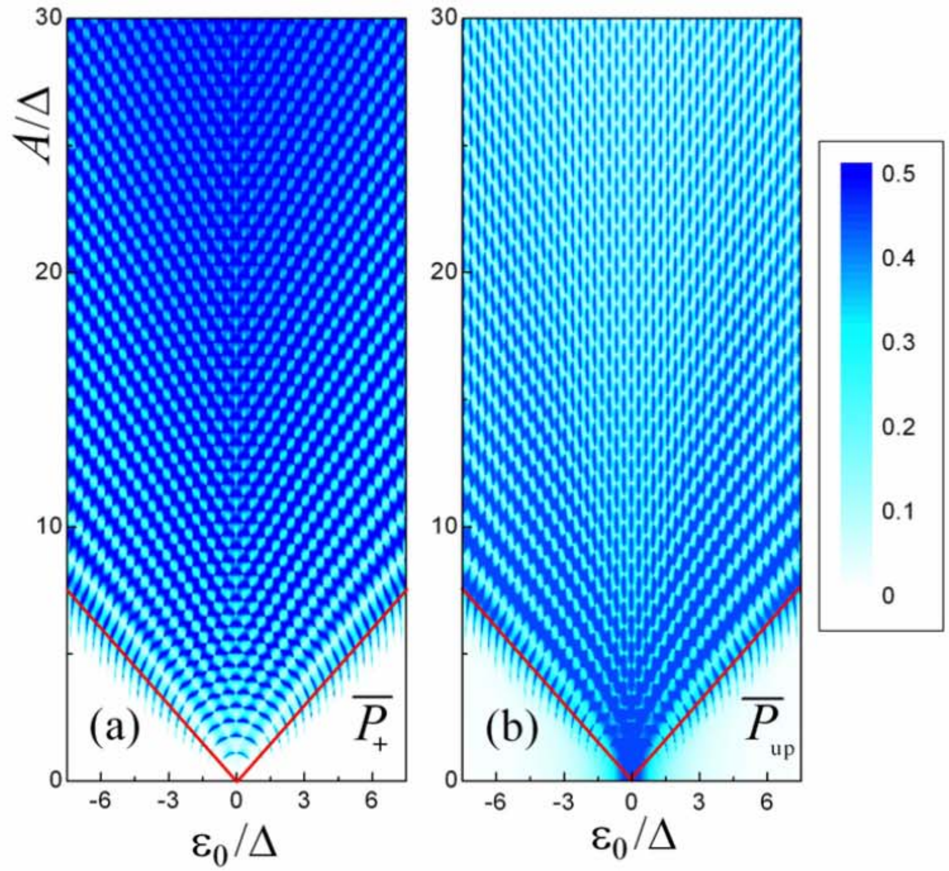

Fig. 8. (Color online) Crossover from the slow-passage limit (bottom part of the figure) to the fast-passage limit (top part of the figure) as the driving amplitude A is increased. On the left the steady-state probability $\overline{P}_+$ of the *adiabatic* excited state is plotted as a function of bias offset ε_0 and driving amplitude A. On the right the probability $\overline{P}_{\mathrm{up}}$ of the upper *diabatic* state is plotted. One can see that the resonance features are clearest in the adiabatic basis for slow passage and in the diabatic basis for fast passage. The ratio ω/Δ is equal to 0.32, and there is no decoherence. Note that panel (a) differs from Fig. 6 because that figure was generated using Eq. (38), whereas in this figure we numerically solve the Bloch equations.

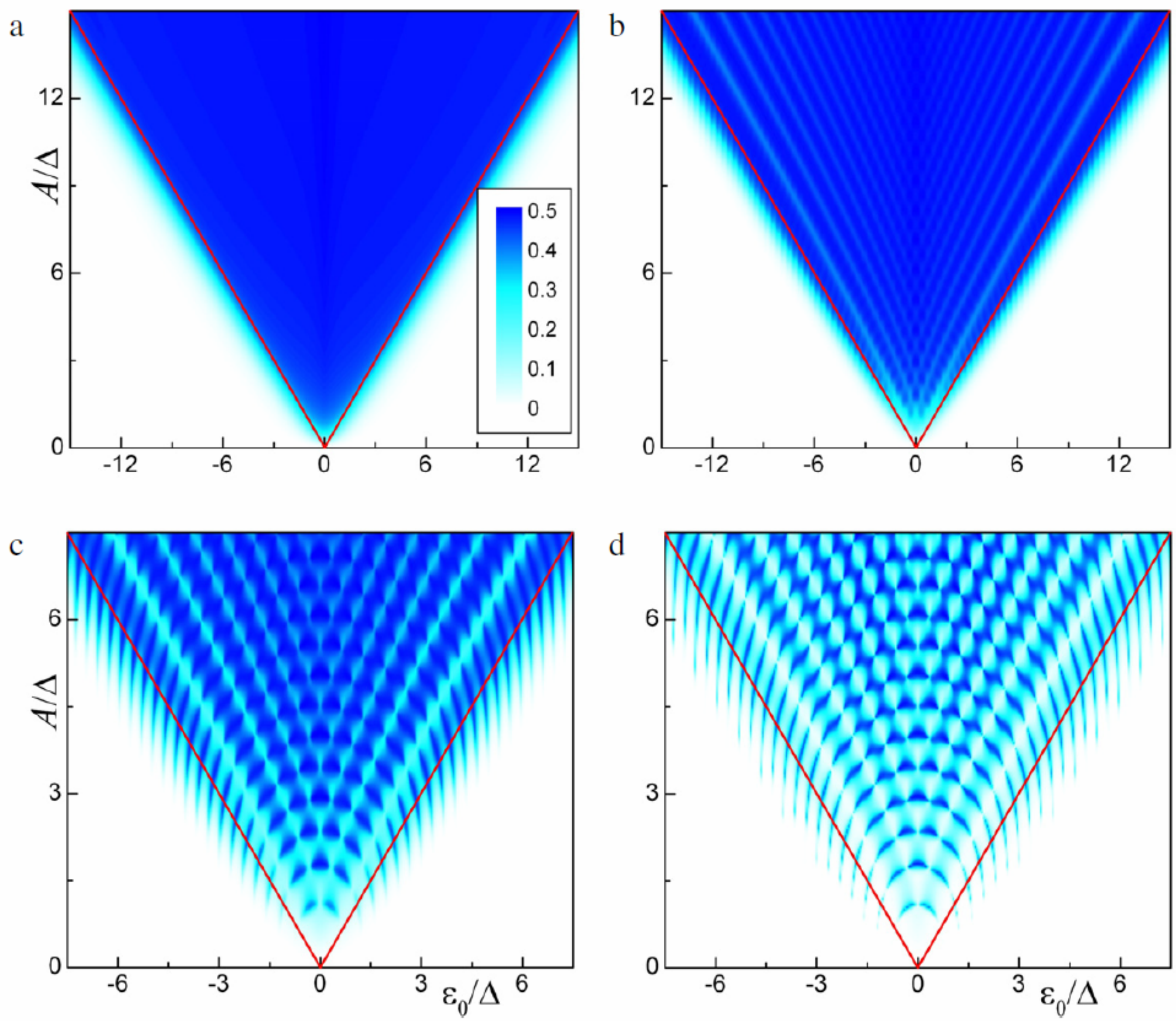

Fig. 9. (Color online) Same as in Fig. 6 (i.e. LZS interferometry with low-frequency driving), but including the effects of decoherence. The time averaged upper level occupation probability $\overline{P_+}$ was obtained numerically from the Bloch equations with the Hamiltonian (1). The dephasing time T_2 is given by $\omega T_2/(2\pi) = 0.1$ in (a), 1 in (b), 5 in (c) and $T_2 = 2T_1$ in (d). The relaxation time is given by $\omega T_1/(2\pi) = 10$.

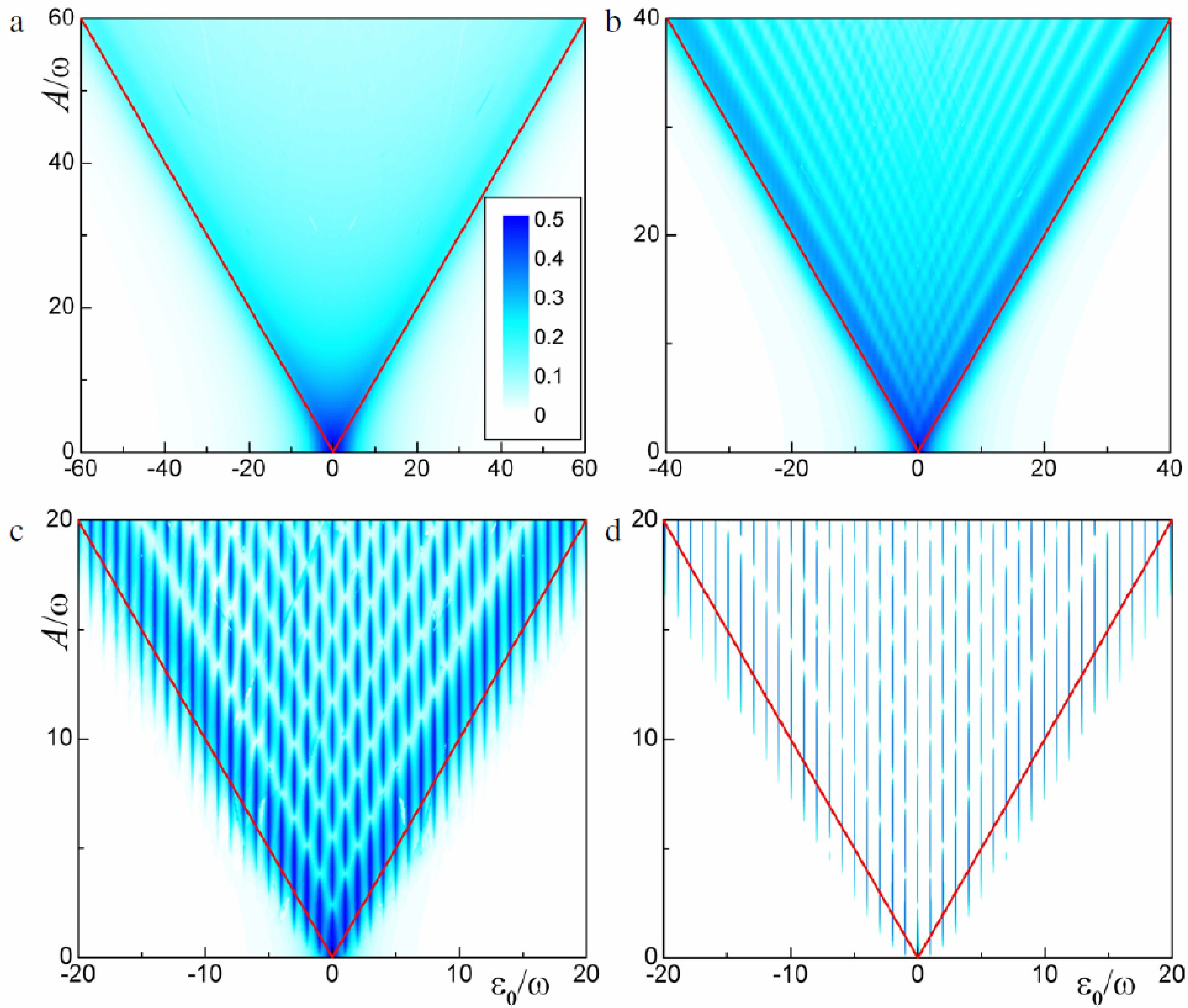

Fig. 10. (Color online) Same as in Fig. 7 (i.e. LZS interferometry with high-frequency driving), but including the effects of decoherence. The time-averaged upper diabatic state occupation probability $\overline{P}_{\rm up}$ is obtained numerically by solving the Bloch equations with the Hamiltonian (1). The dephasing time T_2 is given by $\omega T_2/(2\pi) = 0.1$ in (a), 0.5 in (b), 1 in (c) and $T_2 = 2T_1$ in (d). The relaxation time is given by $\omega T_1/(2\pi) = 10^3$.

Physics Reports 492 (2010) 1–30

Contents lists available at ScienceDirect

Physics Reports

journal homepage: www.elsevier.com/locate/physrep

Landau–Zener–Stückelberg interferometry

S.N. Shevchenko [a,b,*], S. Ashhab [b,c], Franco Nori [b,c]

[a] B.Verkin Institute for Low Temperature Physics and Engineering, Kharkov, Ukraine
[b] RIKEN Advanced Science Institute, Wako-shi, Saitama, Japan
[c] Department of Physics, The University of Michigan, Ann Arbor, MI, USA

A R T I C L E I N F O

Article history:
Accepted 26 February 2010
Available online 24 March 2010
editor: S.N. Coppersmith

Keywords:
Landau–Zener transition
Stückelberg oscillations
Superconducting qubits
Multiphoton excitations
Spectroscopy
Interferometry

A B S T R A C T

A transition between energy levels at an avoided crossing is known as a Landau–Zener transition. When a two-level system (TLS) is subject to periodic driving with sufficiently large amplitude, a sequence of transitions occurs. The phase accumulated between transitions (commonly known as the Stückelberg phase) may result in constructive or destructive interference. Accordingly, the physical observables of the system exhibit periodic dependence on the various system parameters. This phenomenon is often referred to as Landau–Zener–Stückelberg (LZS) interferometry. Phenomena related to LZS interferometry occur in a variety of physical systems. In particular, recent experiments on LZS interferometry in superconducting TLSs (qubits) have demonstrated the potential for using this kind of interferometry as an effective tool for obtaining the parameters characterizing the TLS as well as its interaction with the control fields and with the environment. Furthermore, strong driving could allow for fast and reliable control of the quantum system. Here we review recent experimental results on LZS interferometry, and we present related theory.

Contents

Contents

-Recent progress (2010-2011):

- ✓ Superconducting qubits featured in nine pages in Nature: You & Nori, Nature (June 30, 2011).

- ✓ Current status of all qubits for quantum computation: Reports on Progress in Physics (2011).

- ✓ Systematic study of quantum interferometry using superconducting qubit circuits: Phys. Reports (2010).

- ✓ Quantum Simulators: Buluta & Nori, Science (2009). And long preprint 2011.

- ✓ How to quantify entanglement with many qubits: Physics Reports, over 100 pages (2011).

Interdisciplinary research at the intersection of
nanoscience, atomic physics, quantum optics, condensed matter, quantum devices, and computer science,
that apply quantum mechanics to quantum circuits.

Nanoscience

Quantum Physics

Quantum Devices

Quantum Circuits

Computing

Quantum Nano-Electro-Mechanics
Quantum Nano-Opto-Electronics

Controlling the quantum mechanical state of micron-scale circuits (= artificial atoms).

Coupling artificial atoms in circuits with either electro-magnetic or mechanical resonators, etc.

Artificial atom lasing, on-demand photons, phonon quantization, resonator cooling.

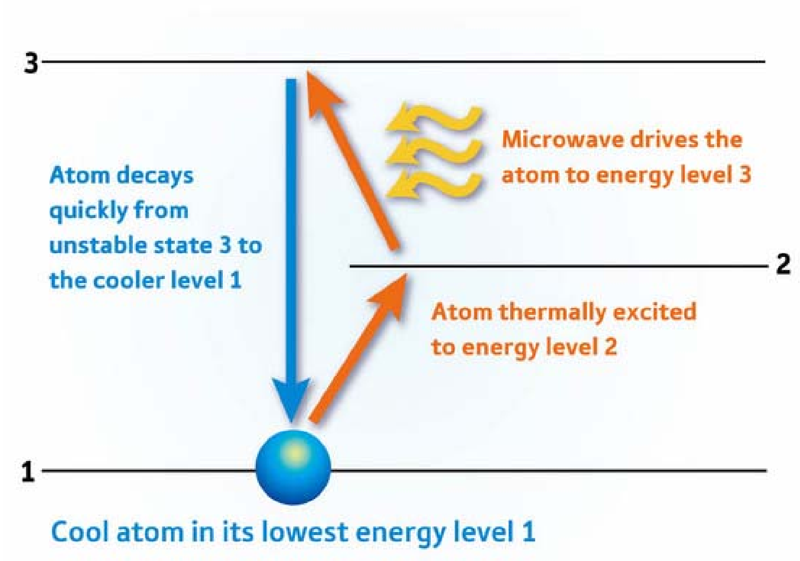

The talk ends here

Additional slides
(in case there is
time at the end)

An LC circuit as a data bus coupling qubits

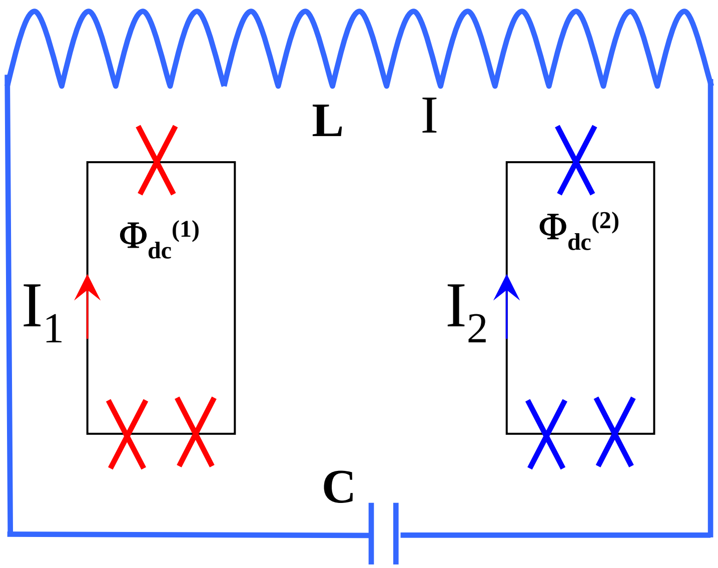

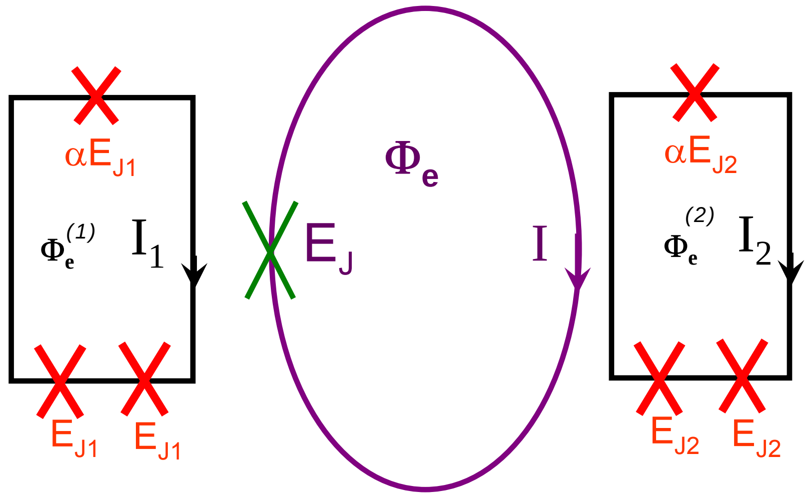

A data bus could couple several qubits.

Liu, Wei, Tsai, Nori, *PRL* (2006)

Analogies between natural atoms and artificial atoms made of superconducting qubits.

Both have discrete energy levels and exhibit coherent quantum oscillations between those levels.

However, whereas natural atoms are controlled using visible or microwave photons that excite electrons from one state to another, the artificial atoms (qubits) in the circuits are driven by currents, voltages and microwave photons.

Differences between quantum circuits and natural atoms include:

- how strongly each system couples to its environment (the coupling is weak for atoms and strong for circuits), and
- the energy scales of the two systems differ.
- In contrast to naturally occurring atoms, artificial atoms can be lithographically designed to have specific characteristics, such as a large dipole moment or particular transition frequencies.
- With a view to applications, this degree of tunability is an important advantage over natural atoms.

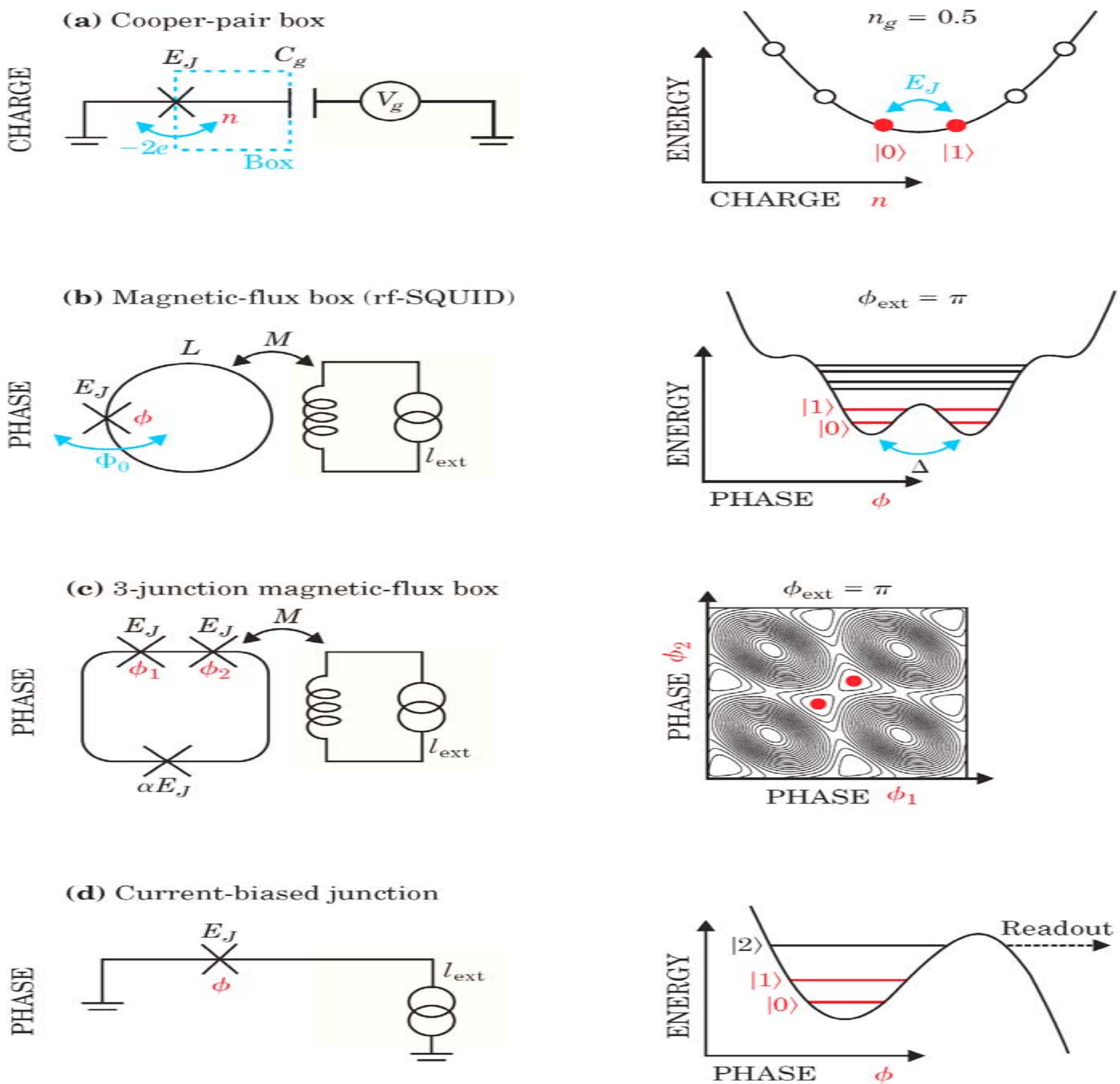

Figures from: You and Nori, *Physics Today* (November 2005)

superconducting qubits

Typical parameters

	Charge	Charge-flux	Flux	Phase
E_J/E_C	0.1	1	10--100	10^6
T_1 (μs)	1--10	1--10	1--20	1
T_2 (μs)	0.1--1	0.1--1	1--10	0.1--1
ν_{01} (GHz)	10	10	20	10

You and Nori, Phys. Today 58 (11), 42 (2005)

Comparison between SC qubits and trapped ions

Qubits	Trapped ions	Superconducting qubits
Quantized bosonic mode	Vibration mode	LC circuit
Classical fields	Lasers	Magnetic fluxes

A data bus using TDMF to couple several qubits

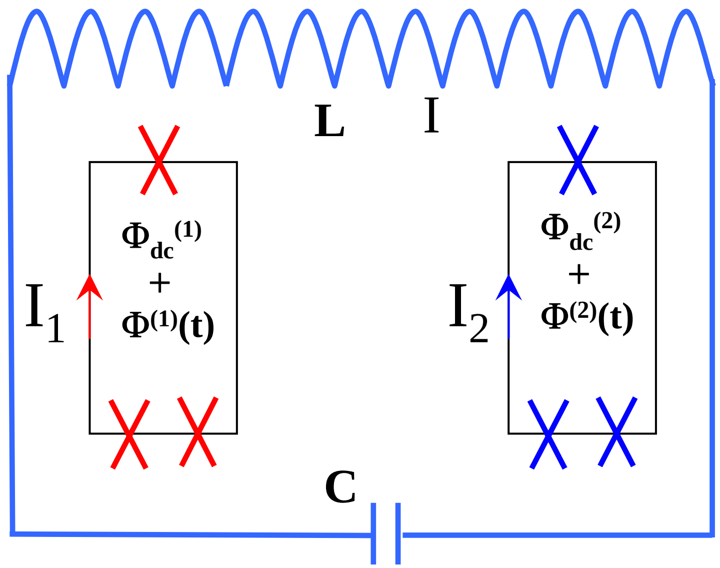

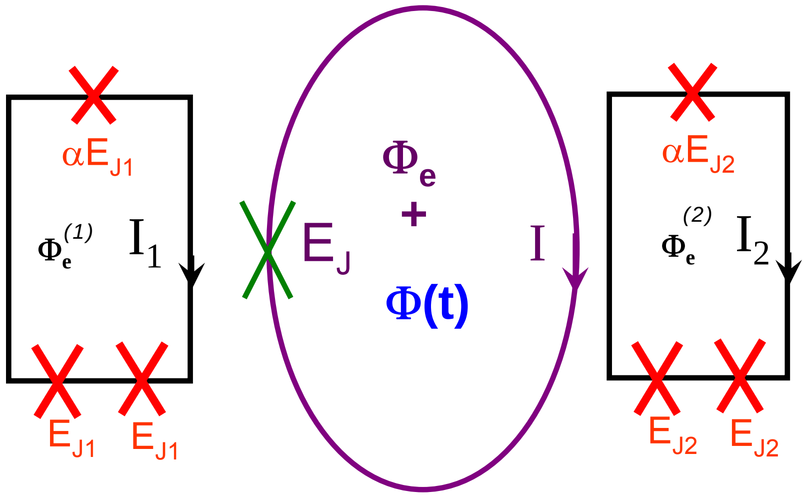

A data bus could couple several tens of qubits.

The TDMF introduces a nonlinear coupling between the qubit, the LC circuit, and the TDMF.

Liu, Wei, Tsai, Nori, *PRL* (2006)

Comparison of our proposal with a micromaser

Carrier process: thermal excitation for micromaser

First red sideband excitation: the excited atoms enter the cavity, decay, and emit photons

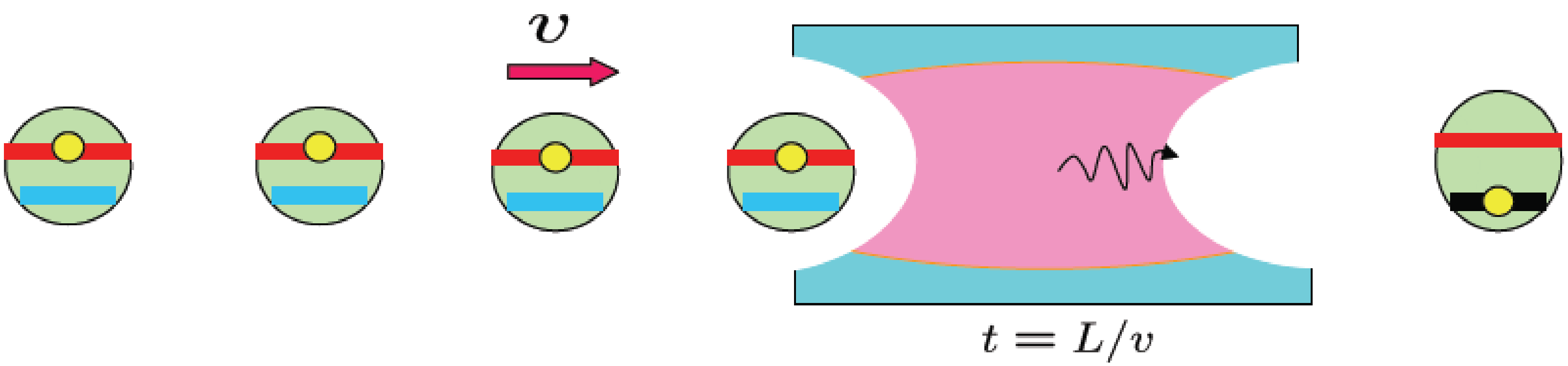

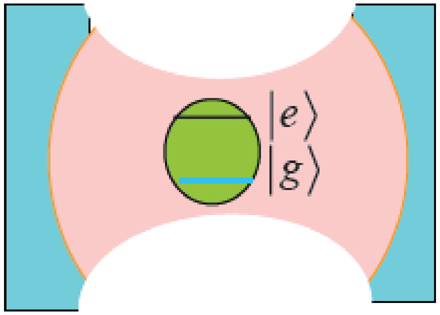

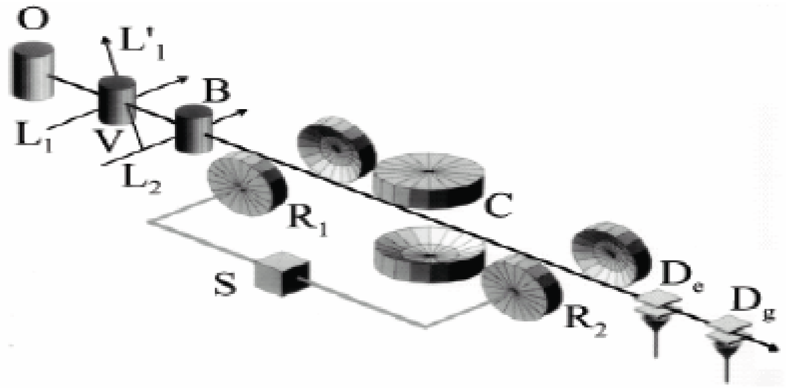

X. Maitre, et al., PRL 79, 769 (1997)

Comparison of our proposal with a micromaser

	JJ qubit photon generator	Micromaser
Before	JJ qubit in its ground state then excited via $n_g = 1/2, \;\; \Phi_C = \Phi_0$	Atom is thermally excited in oven
Interaction with microcavity	JJ qubit interacts with field via $n_g = 1, \;\; \Phi_C = \Phi_0/2$	Flying atoms interact with the cavity field
After	Excited JJ qubit decays and emits photons	Excited atom leaves the cavity, decays to its ground state providing photons in the cavity.

Liu, Wei, Nori, *EPL* (2004); *PRA* (2005); *PRA* (2005)

Units

Three units: K, eV, Hz $\varepsilon = k_B T/2$; $\varepsilon = h\nu$; $\varepsilon =$ eV

$k_B = 1.38 \text{ X } 10^{-23}$ $J\,K^{-1}$; $h = 6.62 \text{ X } 10^{-34}$ Js; $eV = 1.602 \text{ X } 10^{-19}$ J

1	K	eV	Hz
K	1	8.6 X10^2 μeV	21 GHz
eV	1.16 X 10^4 K	1	2.42 X 10^5 GHz
Hz	4.8 X 10^{-11} K	4.13 X 10^{-15} eV	1

Hamiltonian

The Cooper pair number *n* is the quantum mechanical conjugate of the phase φ, that is,

$$\hat{n} = -i\frac{\partial}{\partial\varphi} \quad \text{and} \quad [\varphi, \ \hat{n}\ ] = i$$

In the charge (or Cooper-pair-number) basis:

$$\hat{n} = \sum_{n=0} n|n\rangle\langle n| \ , \qquad \cos\varphi = \frac{1}{2}\sum\left(|n\rangle\langle n+1| + |n+1\rangle\langle n|\right)$$

Thus, in the charge basis, the Hamiltonian

$$H = 4E_c(n - C_g V_g/2e)^2 - E_J\cos\varphi$$

is replaced by

$$H = \sum 4E_c(n-n_g)^2|n\rangle\langle n| - \frac{1}{2}\mathrm{E_J}\sum\left(|n+1\rangle\langle n| + |n\rangle\langle n+1|\right),$$

with the gate-induced charge $n_g = C_g V_g / 2e$

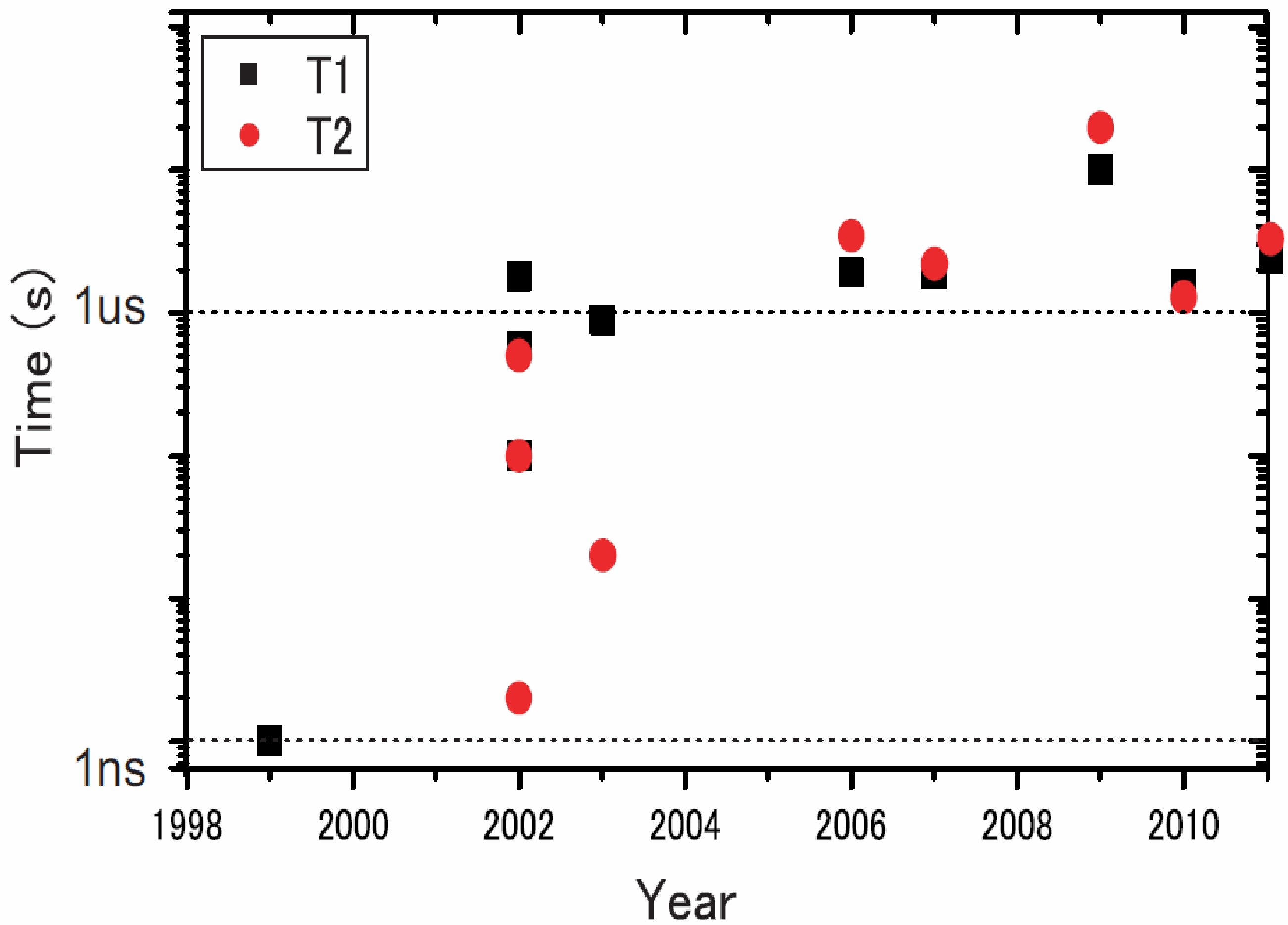

Figure 2: An example of the progress that has been achieved for superconducting circuits in the last decade. The decoherence time kept increasing, and the current trend promises decoherence times of the order of ms in the next couple of years. Visibility also increased and now it is larger than 95%. The black squares show T_1 and the red dots T_2.

Interdisciplinary research at the intersection of
nanoscience, atomic physics, quantum optics, condensed matter, quantum devices, and computer science,
that apply quantum mechanics to quantum circuits.

Nanoscience

Quantum Physics

Quantum Devices

Quantum Circuits

Computing

Quantum Nano-Electro-Mechanics
Quantum Nano-Opto-Electronics

Controlling the quantum mechanical state of micron-scale circuits (= artificial atoms).

Coupling artificial atoms in circuits with either electro-magnetic or mechanical resonators, etc.

Artificial atom lasing, on-demand photons, phonon quantization, resonator cooling.